The Thesis Committee for Cesar Mattos de Salles Soares
Certifies that this is the approved version of the following thesis:

Development and Applications of a New System to Analyze Field Data and Compare Rate of Penetration (ROP) Models

APPROVED BY
SUPERVISING COMMITTEE:

Supervisor:

Kenneth E. Gray

Hugh C. Daigle

Development and Applications of a New System to Analyze Field Data and Compare Rate of Penetration (ROP) Models

by

Cesar Mattos de Salles Soares, B.S.M.E.

Thesis

Presented to the Faculty of the Graduate School of

The University of Texas at Austin

in Partial Fulfillment

of the Requirements

for the Degree of

Master of Science in Engineering

The University of Texas at Austin

August 2015

Dedication

To my parents, Deborah and Jair, and to my brother, Dante.

Acknowledgements

First, I would like to express my gratitude to Dr. Kenneth E. Gray for the opportunity to work with the Wider Windows Industrial Affiliate Program and for invaluable expertise, vital to my education as a graduate student at The University of Texas at Austin. I would also like to thank Dr. Hugh C. Daigle and Dr. Evgeny Podnos for guidance and fruitful recommendations in completing this project.

I would like to acknowledge Wider Windows sponsor companies and their representatives for constructive criticism during our bi-annual meetings. Special thanks to Marathon and NOV for providing the field data utilized in this thesis.

Without the support of all my family and friends, this work would not have been successful. In particular, I would like to recognize my family members in Rio de Janeiro and Sao Paulo, especially my grandmothers Leda and Edy; my girlfriend Elifnaz and her immense patience and endless support; all my friends in Rio de Janeiro and Los Angeles; my close friends in Austin: Max, Bernardo, Matheus, Joao, Luis and George; and current and graduated Wider Windows and PGE colleagues that have assisted me throughout my graduate studies at UT.

Abstract

Development and Applications of a New System to Analyze Field Data and Compare Rate of Penetration (ROP) Models

Cesar Mattos de Salles Soares, M.S.E.

The University of Texas at Austin, 2015

Supervisor: Kenneth E. Gray

Improvements in data acquisition technology have enhanced rate of penetration (ROP) modeling capabilities. Modern logging tools are able to record more complete drilling datasets at a higher frequency, allowing for better understanding of the many variables that affect the drilling process. ROP models published in literature simplify drilling rate formulations by combining complex drilling factors into model coefficients. The lithology dependence of ROP model coefficients, as well as the model's performance evaluated based on different types of rocks, is a topic explored throughout this project. A data analysis software developed in Microsoft Excel VBA, named ROPPlotter, provides ROP field data visualization and comparison of different ROP models. Userforms offer great flexibility in selecting different sections of the well and in highlighting lithology changes. The program accomplishes data filtering by detecting data outliers in the original dataset and excluding them for a more meaningful analysis. Then, VBA coding is applied in order to produce neat-looking plots automatically, overcoming Excel's poor standard plot formatting. Excel Solver is employed in determining coefficients of six ROP models:

Bingham (1964), Bourgoyne & Young (1974), Winters-Warren-Onyia Roller Bit (1987), Hareland Drag Bit (1994), Hareland Roller Bit (2010) and Motahhari PDC Bit (2010). By studying how these coefficients change with varying rock formations, valuable information about each model's behavior is obtained. Plots containing field data and ROP models, in addition to parsed data utilized in model calculations, can be saved for future analysis with the click of a button. ROPPlotter is useful in conducting case studies for industry, such as slow ROP in a section of the well or slide drilling. Furthermore, it provides a systematic way to assess ROP model performance and aims to quantify the lithology dependence of ROP models and their coefficients. This exercise provides a means of determining which ROP model works best for a specific field application. Later, by using an average value of model coefficients calculated for a certain field, optimal values of parameters controlled at the rig floor (weight-on-bit, rotary speed, flow rate) are determined for a future well to be drilled on the same pad.

Table of Contents

List of Tables

List of Figures

Chapter 1: Introduction

1.1 Motivation

Drilling accounts for a substantial part of the cost of constructing a well to extract hydrocarbons from downhole reservoirs. For many years, the oil and gas industry has committed numerous resources to drilling optimization in order to lower drilling-related costs, reduce non-productive time (NPT) and reach deeper hydrocarbon reserves. Rate of penetration (ROP) is a measure of how fast the drilling process is; and therefore a key parameter to be optimized when drilling a well. Several ROP models have been developed in an attempt to investigate the interaction between the drill bit and formation rock, as well as the many other intricate factors that influence drilling. Knowledge of the different aspects that affect the drilling process is essential in achieving improved drilling performance.

In 1964, Bingham published the first rate of penetration model utilized industry-wide. This simplistic ROP correlation with weight-on-bit, rotary speed and bit diameter aimed to evaluate drilling performance in the field with respect to an idealized performance line. Bingham's model contains two coefficients ("a" and "b") to represent the rock properties of the formation being drilled (Bingham, 1964). Due to the great complexity of drilling interactions, the use of model coefficients to lump together drilling aspects that have no theoretical formulation is commonplace in literature. Such simplifications vary depending on each model's assumptions. They are necessary when approximating the effect of over twenty independent variables in drilling, many of which cannot be directly measured or are not completely understood (Winters *et al.*, 1987). By empirically calculating model coefficients that best fit field data from offset wells, ROP modeling provides a means to

select optimal drilling variables controlled at the rig, such as rotary speed and weight-on-bit, that will allow for faster drilling of a subsequent well in the same region.

The number and nomenclature of model coefficients vary from model to model, but all coefficients are contingent on the rock formation being drilled. Model coefficients calculated for a specific application are suitable when predicting ROP in future wells in the same field. However, no single set of coefficients can be used to apply a rate of penetration model accurately to multiple locations. The lithology dependence of ROP model coefficients, as well as model performance evaluated based on different types of rocks, is a topic explored during the course of this project.

Thanks to modern data acquisition technology, the oil and gas industry possesses an invaluable amount of high resolution drilling data, with up to the second information on the key drilling parameters included in ROP models published in literature: weight-on-bit (WOB), rotary speed (RPM) and flow rate. Large amounts of data are recorded while drilling. What data are relevant in ROP modeling? How reliable are the data? Can data outliers be detected and excluded?

Development of a system capable of data analytics, field data visualization, and straightforward calculation of ROP model coefficients is the main focus of this thesis. The software developed in this work, ROPPlotter, utilizes Excel VBA (Visual Basic for Applications) coding in data parsing, data filtering, and comparison of ROP model performance and coefficients by lithology. ROPPlotter is employed in drilling optimization case studies with field data from the Wider Windows Industrial Affiliate Program's sponsors. Each sponsor company has a different format of reporting data, and the program has the flexibility to work with any given data format. Plots are automatically formatted and coefficients for six ROP models previously published in literature can be calculated

with much ease. ROPPlotter is a valuable tool in analyzing the lithology dependence of ROP model coefficients and investigating model performance in different rock formations.

1.2 Evolution of ROP Modeling and Drilling Optimization in Literature

Rowley *et al.* (1961) empirically related penetration rate to weight-on-bit and rotary speed using a variation of linear and quadratic terms containing these two parameters. Acknowledging the deficiency in theoretical understanding of the drilling process, the investigators resorted to a quadratic surface and six model coefficients to incorporate flexibility in their model. Laboratory testing was conducted under controlled conditions, with Beekmanton dolomite rock samples and a field-sized roller-cone drill bit, to eliminate the effects of uncontrollable variables from the field. Then, the least-squares fit method was employed in obtaining the six model coefficients that best fit the quadratic surfaces to field data. The authors discuss selecting optimal WOBs and RPMs to reduce drilling cost as an innovative practice, freshly implemented in the industry. They concluded that ROP increases in concave upward fashion with increasing WOB, while increasing with a concave downward curvature with increasing RPM. Additionally, the negative effect of depth on ROP was demonstrated by simulating downhole pressure environments. Rowley *et al.* (1961) recommended high WOBs and low RPMs to improve drilling effectiveness.

Maurer (1962) applied a rock cratering theoretical approach to develop a rate of penetration formula for roller-cone bits operating under perfect cleaning conditions. In a perfect cleaning scenario, no rock fragments are left behind when the next bit tooth contacts the rock formation. Maurer's formulation relates ROP to WOB, RPM, bit diameter and rock strength with exact coefficients, as opposed to the empirical model coefficients in Rowley *et al.* (1961). Despite the theoretical foundation of the model, an empirical drillability constant is introduced to take into account downhole pressures and formation,

fluid and bit properties. In addition to the perfect cleaning equation, Maurer also adapted his model to reproduce imperfect cleaning conditions based on ROP-WOB and ROP-RPM charts from nine different authors. Maurer recognized that increasing weight-on-bit only improves ROP up to a point, where hole-cleaning issues become more influential and subsequent increases in WOB will have a negative impact on penetration rate. Additionally, it was shown that a higher-pressure differential across the bit leads to lower ROP. The author indicated that further work was needed to include depth, hydraulics and bit wear in the model.

Bingham published a weekly series of chapters in *The Oil and Gas Journal* between November 1964 and April 1965 (Bingham, 1964-1965). These publications served as a manual for drillers and drilling engineers, helping them understand the relative benefit of what could be done to improve drilling in different situations. By relating rate of penetration to weight-on-bit, rotary speed and bit diameter, Bingham evaluated drilling performance compared to the best possible drilling response in a rock formation with a given bit. Bingham emphasized the necessity of a scientific equation that defined the interaction between drill bit and formation rock, but accepted it was a hard endeavor to derivate such formulation due to complexity of drilling. Bingham also recognized that borehole cleaning is the main factor limiting drilling performance. Starting from Maurer's work on perfect cleaning (Maurer, 1962), Bingham derived a more generalized ROP relation, applicable to any drill bit type and formation being drilled. Straightforward application of this model deems it relevant in contemporary drilling optimization studies (Bataee *et al.*, 2010, Auwal *et al.*, 2012, and Barros, 2015).

Jorden and Shirley (1966) normalized rate of penetration by taking Bingham's equation (Bingham, 1964) and solving it for the "d exponent", well known to industry still today, to detect overpressured formations. Special attention was devoted to the bottom-

hole differential pressure, the difference between the drilling fluid hydrostatic pressure and rock formation pore pressure. The authors confirmed that a relation between the "d exponent" and differential pressure exists, although it cannot be described quantitatively. Jorden and Shirley (1966) concluded that overpressured formations are recognizable from a reverse in the trend of decreasing normalized ROP with depth. Hence, a formation fluid influx into the wellbore ("kick") can be prevented by increasing mud weight once an overpressured zone is encountered.

Eckel (1967) integrated the effect of drilling mud properties on ROP modeling. Using microbit tests, Eckel combined mud kinematic viscosity, flow rate, and bit nozzle diameter into a Reynolds number function. Strict bounds to this function define the model's limited range of application. The author envisioned application of this model to forecast ROP in future wells and to ensure proper treatment of drilling fluid on the field. Eckel (1967) recommended muds with low kinematic viscosity to produce maximum ROP.

As early as 1969, Young utilized a simplistic ROP model and computerized drilling control to evaluate rock formations and adjust WOB and RPM in order to minimize costs (Young, 1969). This ingenious concept of optimizing drilling parameters with drilling automation is still fought against and not widely applied in the oil and gas industry at the moment.

Bourgoyne and Young (1974) published the most comprehensive ROP model to date, taking into account eight different drilling parameters: formation strength, normal compaction trend, undercompaction, differential pressure, bit diameter and bit weight, rotary speed, tooth wear, and bit hydraulics. Eight model coefficients are computed to fit field data with a multiple regression approach. The investigators stated that if the WOB is too high, the disproportionate rate of bit wear might actually cause a negative effect on ROP. They emphasize that drilling optimization can achieved by selecting the appropriate

weight-on-bit, rotary speed, bit hydraulics, and mud types and properties. Such practice may reduce the cost of a well by 10% (Bourgoyne and Young, 1974). Bourgoyne and Young (1974) also employed ROP modeling to find an approximate value of formation pore pressure in wells drilled in the Gulf Coast Area.

Cunningham (1978) attempted an entirely empirical approach to ROP modeling, due to the great intricacy involved in drilling. Drilling strength, influenced by rock formation and type of roller-cone bit, is introduced as a property that greatly affects ROP. A relation between ROP and WOB, RPM, differential pressure and drilling strength was proposed. By determining rate of penetration for fixed values of WOB and RPM in a field test, drilling strength is measured and applied to forecast ROP.

Walker *et al.* (1986) tried to escape from the conventional technique of relating rate of penetration to WOB, RPM, flow rate and a rock formation parameter. Instead, the investigators resorted to relating ROP to weight-on-bit, physical rock properties and well depth. The experimenters derived an equation of general application for predicting ROP for roller cone bits, rather than utilizing offset well data to empirically calculate the rock formation constant. After conducting petrographic analyses and indentation tests on seven rock samples, the authors selected in-situ compressive strength and indentation peak force as the rock parameters with highest correlation to ROP. Walker *et al.* (1986) utilized triaxial rock strength tests and the Mohr-Coulomb failure criterion to develop a roller cone ROP equation dependent on WOB, borehole pressure, rock porosity, average grain size, and either in-situ formation compressive strength or indentation peak load.

In 1987, Warren published a famous three-term roller-cone bit ROP model that became the foundation for several future models (Winters *et al.*, 1987, and Hareland and Hoberock, 1993). Warren (1987) recognized that ROP is restricted by cuttings generation and cleaning, dividing drilling hampering effects into two groups: one for physical

mechanisms acting on the rock before it is broken, and one for processes that affect rock cuttings. New concepts of ratio of jet velocity to return velocity and modified jet impact force are introduced. While the model correctly predicts ROP in low differential pressure conditions, both cratering effects and cleaning problems hinder the accuracy of the model at high differential pressures. In those situations, model predictions can be used to identify which of these two phenomena is limiting ROP.

Winters *et al.* (1987) added a fourth term to the previous three-term ROP model for roller cone bits derived by Warren (Warren, 1987). Besides considering the rock's compressive strength as a drilling constraint, the investigators took into account another rock mechanical property: ductility. Rock ductility is the axial strain at failure, and the more ductile behavior a rock displays, the harder it is to drill through it. The model is formulated as the relative limiting contribution of indentation, offset, teeth, and hydraulics to ROP. Bit cone offset, a hard-to-measure geometrical property, is converted into a model coefficient to be determined empirically along three more coefficients. Winters *et al.* (1987) acknowledged that ROP models employ many simplifications, and therefore are not capable of general application. However, by repeated implementation, such models can be adjusted for valuable local interpretation.

Hareland and Hoberock (1993) modified the three-term Warren model (Warren, 1987) to produce a tricone bit ROP model that includes chip hold-down effects. The modified Warren model is employed in conjunction with Mohr circles to predict the maximum possible value of the minimum horizontal stress at any data point. This model capability can greatly benefit modern hydraulic fracturing design, which relies heavily on minimum horizontal stress values.

Focusing on cutter-rock interactions and applying the principle of conservation of mass, the drag bit model developed by Hareland and Rampersad (1994) includes the

number of cutters, cutter diameter, bit diameter, mechanical loading per cutter and formation rock compressive strength in its formulation. The authors indicated a tendency in the industry to opt for drag bits, which wear at a lower rate and are better suited for use with downhole motors than roller bits (Hareland and Rampersad, 1994). Three empirical coefficients account for lithology properties and hard-to-model factors. These coefficients can be calculated for a drag bit type in a specific field application and employed in the optimization of drilling parameters, drilling simulations and evaluation of bit performance. Rampersad *et al.* (1994) applied this drag bit model to generate Geological Drilling Logs (GDLs) for wells and minimize drilling costs.

Bratli *et al.* (1997), Gjelstad *et al.* (1998) and Nygaard *et al.* (2002) all reported successful implementation of GDLs and a drilling simulator equipped with three drilling rate models to optimize drilling parameters in the North Sea. An inverse formulation of the ROP models was utilized to obtain formation rock compressive strength. Consistent cost reduction of 10-25% was observed for future wells drilled in the North Sea employing optimization techniques.

Hareland *et al.* (2010) investigated how a roller cone insert fractures a rock crater in order to obtain a ROP formulation for roller cone bits as a function of several bit design parameters. Number of bit inserts in contact with rock, number of insert penetrations per revolution, chip formation angle and bit wear are embodied in this ROP model. The authors discussed the model's capability of real-time drilling simulation and optimization.

Motahhari *et al.* (2010) developed a drilling rate model designed specifically for PDC (polycrystalline diamond compact) bits and accounting for the influence of PDMs (positive displacement motors). Since PDC bits are the current industry standard, this model is appropriate for present-day optimization studies. Motahhari *et al.* (2010) stated that the torque at the drill bit is the key parameter in relating motor and bit performance, and that

the differential pressure across the motor is a function of the torque applied to it. The authors commented that if the optimization is performed at a single point instead of a section, the overall drilling performance for that entire interval might be impaired.

Bataee *et al.* (2010) obtained optimal WOB and RPM values for different bit sizes and at varied well depths in the Shadegan Field using ROP models introduced by Bingham (1964), Bourgoyne and Young (1974) and Warren model modified by Hareland and Hoberock (1993). Auwal *et al.* (2012) utilized the Bingham drilling rate model for optimization of drilling parameters in an unexplored area in the Gulf of Guinea.

Barros (2015) investigated the implementation of drag bit ROP models to field data from industry by using the software developed in this thesis: ROPPlotter. So far, in literature, there is no reference to a software that computes empirical model coefficients and evaluates the performance of ROP models in different applications.

1.3 ROPPlotter: Project Description and Capabilities

ROPPlotter is a data analysis and ROP modeling software developed in Microsoft Excel VBA (Visual Basic for Applications) that allows for ROP field data visualization and comparison of different ROP models. The program recognizes data headings from a field dataset spreadsheet and prompts the user to select the specific columns of data necessary for analysis (e.g. surface vs. downhole). Unrealistic data points can be flagged according to different criteria, creating data filters to remove unwanted data. After data have been imported selectively, an Excel Userform provides easy controls and great flexibility to determine the bounds displayed in the plot. Showing formation boundaries on the plot, color-coding field data inside/outside formations and zooming in on specific formation borders are some of the other functions available in this software.

Six ROP models from literature are included in ROPPlotter's library: Bingham (Bingham, 1964), Bourgoyne & Young (Bourgoyne and Young, 1974), Winters-Warren-Onyia Roller Bit (Winters *et al.*, 1987), Hareland Drag Bit (Hareland and Rampersad, 1994), Hareland Roller Cone Bit (Hareland *et al.*, 2010) and Motahhari PDC Bit (Motahhari *et al.*, 2010). The governing equations for these models are presented in Chapter 2. Each ROP model has its specific form that guides the user to input the necessary parameters for the selected model. Excel Solver is employed in determining the empirical coefficients of a specific model and the dataset utilized. User-specified coefficient bounds allow for a comprehensive analysis of parameter sensitivity and lithology influence on rate of penetration. Any combination of the six models can be displayed in the plot along with field data, and plots can be saved and exported as pictures for future reference and documentation.

Even though limited in computational power, Microsoft Excel VBA was chosen as the programming language for ROPPlotter since Excel is widely available. Excel's userforms ensure proper operation of the software, deeming the program error free. This software was created to facilitate data handling and visualization, and in an attempt to better understand how ROP model coefficients behave when fitting different models to field data. Summarizing ROPPlotter's general capabilities:

- Data format flexibility: ROPPlotter is designed to work with any data format provided by Wider Windows sponsor companies.
- Data parsing: Only data relevant to ROP model computations are imported into the spreadsheet, saving computational time.
- Data filtering: As previously stated, not all data can be trusted. This program allows for detection of data outliers based on absolute values or deviations from the mean

in specific sections of the well. The outliers can be removed and only filtered data is used for a more meaningful analysis.

- Evaluate different sections of the well: User-friendly control bars manage plot bounds. Zooming in on a rock formation section is as easy as the click of a button.
- Color-coding: For better visualization of field data, ROPPlotter is able to highlight a desired formation, split up the dataset according to lithology types (i.e. sandstone, limestone, shale), or detect data points according to a data filtering criterion.
- Overbalance analysis: Maurer (1962) verified that ROP is highly dependent on differential pressure. Visualization of overbalance data and ROP data side by side enhances comprehension of ROP trends in sections of the well.
- Neat plot formatting: Excel's default plot format is not visually appealing. By using Excel VBA coding, ROPPlotter applies a pre-defined plot scheme that is much clearer and well arranged.
- Save and export plots and useful data for future analysis: The ability to save plots and parsed data quickly is essential for continued work. This is another feature included in this program.
- Consistent way to compare ROP model coefficients and performance: Excel Solver adjusts ROP model coefficients to fit field data. ROPPlotter can execute Solver for a large set of data with a loop, without the need of human input every step of the way. Models are evaluated by average percent error in each lithology and overall for the entire well. Model coefficients are also displayed in similar fashion, offering a fast way to analyze how these coefficients vary from one formation to another.

1.4 Thesis Outline

There are six chapters in this thesis. Following the introductory chapter, Chapter 2 reviews the governing equations of the six ROP models from literature included in ROPPlotter's library. Chapter 3 discusses two different methods to calculate ROP model coefficients, and the factors affecting how well these coefficients fit field data. In Chapter 4, a detailed description of the ROPPlotter software is presented. Drilling optimization case studies using ROPPlotter results are reviewed in Chapter 5. Chapter 6 presents conclusions and future considerations resulting from this work.

Chapter 2: Review of ROP Models Included in ROPPlotter

In this chapter, the governing equations and basic principles of the six ROP models incorporated in ROPPlotter are presented in chronological order. These models encompass a wide range of applications. Bingham (Bingham, 1964) is a straightforward relation between ROP and WOB, RPM and bit diameter. Even though it was developed a long time ago, this ROP model is still relevant due to simple application encompassing all bit types. Contemporary optimization studies (Bataee *et al.*, 2010, Auwal *et al.*, 2012, and Barros, 2015) employ Bingham's model in finding the best drilling parameters for a region. Bourgoyne & Young (Bourgoyne and Young, 1974) is the most comprehensive ROP model to date, including correlations between eight parameters affecting drilling rate. Similar to Bingham's ROP model, B&Y can also be used with any bit type. Winters-Warren-Onyia (WWO) Roller Bit (Winters *et al.*, 1987) is a modification of the famous three-term roller cone bit ROP model developed by Warren (1987), adding a fourth term to account for the effect of rock ductility on ROP. Hareland Drag Bit (Hareland and Rampersad, 1994) provides a field-proven drag bit model emphasizing the influence of bit geometry. This ROP model has been applied in several optimization studies in the North Sea (Bratli *et al.*, 1997, Gjelstad *et al.*, 1998, and Nygaard *et al.*, 2002). The Hareland Roller Bit (Hareland *et al.*, 2010) model is founded on rock cratering with roller cone bits, also taking into account several bit geometry parameters. Motahhari PDC Bit (Motahhari *et al.*, 2010) is appropriate for modern drilling optimization applications, since PDC bits are the dominant bit type at the moment.

No model can perfectly predict ROP in every situation. They take into account different drilling parameters and have a varied number of model coefficients.

2.1 Bingham (Bingham, 1964)

Applicable to all bit types, Bingham's simplistic ROP relation is given by:

$$\frac{R}{N} = a\left(\frac{W}{D}\right)^{b} \tag{2.1}$$

where R is the penetration rate (ft/sec), N is the rotary speed (revolutions/sec), a and b are the dimensionless constants for each rock, D is the bit diameter (ft), and W is the bit load (lb). The model contains two coefficients (a and b), which account for the drillability of different rock formations (Bingham, 1964). It is important to note that the units in Bingham's work are slightly different from units commonly seen in the field today: ROP is usually reported in ft/hr, rotary speed in revolutions per minute, WOB in klb, and bit diameter in inches. Table 2.1 displays Bingham's suggested bounds for the a and b model coefficients:

Table 2.1: Model coefficients upper and lower bounds suggested by Bingham (1964).

ROP Model	**Bingham (1964)**	
Model Coefficients	a	b
Coeff. Lower Bound	2.60E-17	0.9
Coeff. Upper Bound	6.21E-08	3.0

In the table above, the bounds for the a coefficient are very small numbers and range over ten orders of magnitude. With Bingham's units, a slight variation in this coefficient might completely change model results. In Chapter 3 of this thesis, the importance of selecting appropriate upper and lower bounds for calculation of ROP model coefficients is discussed.

2.2 Bourgoyne & Young (Bourgoyne and Young, 1974)

Encompassing eight different factors influencing drilling rate, Bourgoyne & Young's exponential ROP relation is modeled as:

$$\frac{dD}{dt} = \text{Exp}\left(a_1 + \sum_{j=2}^{8} a_j x_j\right) \tag{2.2}$$

where D is the well depth (ft), t is the time (hr), a_1 is the formation strength parameter, a_2 is the normal compaction trend exponent, a_3 is the undercompaction exponent, a_4 is the pressure differential exponent, a_5 is the bit weight exponent, a_6 is the rotary speed exponent, a_7 is the tooth wear exponent, and a_8 is the hydraulic exponent. Coefficients a_1 through a_8 are determined with a multiple regression technique, using several data points to determine the eight unknowns that best fit a specific set of field data. The parameter x_2, representing the normal compaction drilling factor, can be calculated by:

$$x_2 = 10{,}000.0 - D \tag{2.3}$$

Next, the undercompaction drilling parameter is:

$$x_3 = D^{0.69}\left(g_p - 9.0\right) \tag{2.4}$$

where g_p is the pore pressure gradient of the rock formation (lb/gal). The pressure differential drilling parameter, x_4, is given by:

$$x_4 = D\left(g_p - \rho_c\right) \tag{2.5}$$

where ρ_c is the equivalent circulating mud density (ECD) at the bottom of the wellbore (lb/gal). As expected, Equation 2.5 illustrates an exponential decrease in ROP with increasing pressure overbalance at the bit. The fifth drilling parameter, accounting for the effect of bit weight, is:

$$x_5 = \ln\left(\frac{\frac{W}{d} - \left(\frac{W}{d}\right)_t}{4.0 - \left(\frac{W}{d}\right)_t}\right) \tag{2.6}$$

where W is the weight-on-bit (klb), d is the bit diameter (in), and the subscript t represents the threshold bit weight at which the bit begins to drill. The influence of rotary speed is included in the sixth drilling parameter:

$$x_6 = \ln\left(\frac{N}{100}\right) \tag{2.7}$$

where N is the rotary speed (RPM). It is interesting to note that both x_5 and x_6 are logarithmic terms in an exponential relation. In other publications that present Bourgoyne & Young's model as a multiplication between the eight drilling parameters, the fifth and sixth parameters are the only ones that do not appear in exponential form (Bataee *et al.*, 2010). The tooth wear drilling parameter is next:

$$x_7 = -h \tag{2.8}$$

where h is the fractional tooth height worn away. Lastly, the bit hydraulics drilling parameter is:

$$x_8 = \frac{\rho q}{350 \mu d_n} \tag{2.9}$$

where ρ is the mud density (lb/gal), q is the flow rate (gal/min), μ is the apparent viscosity at 10,000 sec^{-1} (cp), and d_n is the bit nozzle diameter (in).

Bourgoyne and Young (1974) discussed the implementation of their model in a drilling optimization study in the Gulf Coast Area. Bounds from model coefficient values obtained in this analysis are shown next:

Table 2.2: Model coefficient bounds obtained by Bourgoyne and Young (1974) in a Gulf Coast drilling optimization study.

ROP Model	**Bourgoyne & Young (1974)**							
Model Coefficients	a1	a2	a3	a4	a5	a6	a7	a8
Coeff. Lower Bound	2.71	1.00E-04	1.80E-04	4.30E-05	0.43	0.21	0.20	0.16
Coeff. Upper Bound	3.78	2.80E-04	9.00E-04	8.50E-05	1.2	0.72	0.41	0.61

Coefficient bounds from Table 2.2 are only applicable when predicting ROP in the Gulf Coast area with the same drill bit utilized by the authors. They are not global coefficient bounds, and may need to be expanded to suit other applications.

2.3 WWO Roller Bit (Winters *et al.*, 1987)

The Winters-Warren-Onyia Roller Bit ROP model is unique in that it equates the inverse of rate of penetration to four influencing factors (indentation, offset, teeth, hydraulics), representing their relative limiting contribution to ROP:

$$\frac{1}{R} = \frac{a\sigma^2 D^3 \varepsilon}{NW^2} + \frac{\varphi \sigma D^2}{NW\varepsilon} + \frac{b}{ND} + \frac{c\rho\mu D}{I_m} \tag{2.10}$$

where R is the penetration rate (ft/hr), a, b, and c are the dimensionless bit design constants, σ is the rock compressive strength (psi), D is the bit diameter (in), ε is the rock ductility (%), N is the rotary speed (rpm), W is the weight-on-bit (klb), φ is the cone offset coefficient (1/ft), ρ is the mud density (lb/gal), μ is the mud viscosity (cp), and I_m is the modified jet impact force (lbf). The modified jet impact force term in Eq. 2.10 (I_m) was presented by Warren (1987), in order to remove the influence of nozzle size on impact pressure:

$$F_{jm} = (1 - {A_v}^{-0.122})F_j \tag{2.11}$$

where A_v is the ratio of jet velocity to return velocity and F_j is the jet impact force (lbf). For a drill bit containing three jets, A_v is given by:

$$A_v = \frac{v_n}{v_f} = \frac{0.15{d_b}^2}{3{d_n}^2} \tag{2.12}$$

where v_n is the nozzle velocity (ft/sec), v_f is the return fluid velocity (ft/sec), d_b is the bit diameter (in) and d_n is the nozzle diameter (in). Furthermore, the jet impact force is:

$$F_j = 0.000516\rho q v_n \tag{2.13}$$

where ρ is the fluid density (lbm/gal) and q is the flow rate (gal/min). Once again, for a three jets bit, the nozzle velocity is:

$$v_n = \frac{418.3q}{{D_n}^2 + {D_n}^2 + {D_n}^2} \tag{2.14}$$

where D_n is the nozzle size number (1/32 in).

Indentation, offset, teeth, and hydraulics effects are represented by the first through fourth terms on the right hand side of Equation 2.10, respectively. By looking Eq. 2.10, it is clear that at low WOB, indentation is the limiting factor to ROP. The cone offset coefficient (φ), a hard-to-measure bit property, is empirically determined along with the three dimensionless bit design constants (a, b, and c) to match field data. Based on coefficient values for two bits from Winters *et al.* (1987), WWO Roller Bit model coefficient bounds are:

Table 2.3: Model coefficient bounds based on Winters *et al.* (1987).

ROP Model	**WWO Roller Bit (1987)**			
Model Coefficients	a	φ	b	c
Coeff. Lower Bound	0.0083	0.0123	1.303	0.0020
Coeff. Upper Bound	0.0101	0.0248	8.763	0.0023

Similar to the previous section, coefficient bounds in Table 2.3 are not universal to all applications.

2.4 Hareland Drag Bit (Hareland and Rampersad, 1994)

Hareland and Rampersad (1994) developed the first ROP model specific to drag bits presented in this work. Bit geometry is considered the primary factor affecting ROP:

$$ROP = \frac{14.14\, N_s\, RPM}{D_B}\left[\left(\frac{d_s}{2}\right)^2 cos^{-1}\left(1-\frac{4W_{mech}}{N_s {d_s}^2 \pi\sigma_c}\right) - \left(\frac{2W_{mech}}{N_s\pi\sigma_c}-\frac{4W_{mech}^2}{(N_s d_s \pi\sigma_c)^2}\right)^{0.5}\left(\frac{d_s}{2}-\frac{2W_{mech}}{N_s\pi\sigma_c d_s}\right)\right] \quad (2.15)$$

where N_s is the number of cutters, D_B is the bit diameter (in), d_s is the cutter diameter (in), W_{mech} is the mechanical loading (WOB) per cutter (lbs) and σ_c is the uniaxial compressive

rock strength (psi). Notice that Eq. 2.15 does not include any model coefficients in its formulation. They are introduced together in a single term:

$$COR = \frac{a}{(RPM^b \times WOB^c)} \tag{2.16}$$

where *a*, *b*, and *c* are cutter geometry correction factors. These three model coefficients are lumped into *COR* – a lithology coefficient that multiplies the right-hand side of Eq. 2.15. Both RPM and WOB are in the denominator of Eq. 2.16, suggesting that increasing these two parameters would have a negative influence on ROP. However, RPM and WOB are also found in the numerator of Eq. 2.15, and the combined effect depends on the values of the coefficients *b* and *c*. Coefficient bounds obtained with a diamond bit in a shale formation and in a limestone formation are provided in Table 2.4:

Table 2.4: Model coefficient bounds for a diamond bit in limestone/shale formations presented by Hareland and Rampersad (1994).

ROP Model	**Hareland Drag Bit (1994)**		
Model Coefficients	a	b	c
Coeff. Lower Bound	63.6	0.5397	0.585
Coeff. Upper Bound	185.4	0.8250	0.819

2.5 Hareland Roller Bit (Hareland *et al.*, 2010)

Analyzing how roller cone bit inserts induce rock cratering, the Hareland Roller Bit model equation is:

$$ROP = K\frac{80n_t\, m\, RPM^a}{{D_b}^2 tan^2\psi}\left(\frac{WOB}{100n_t\sigma_p}\right)^b W_f \tag{2.17}$$

where K is a comprehensive coefficient, n_t is the number of inserts in contact with the rock at the bottom, m is the number of insert penetrations per revolution, a and b are model coefficients, ψ is the chip formation angle, D_b is the bit diameter, σ_p is the ultimate strength of rock and W_f is the tooth wear function. The wear function is defined as:

$$W_f = 1 - \left(\frac{\Delta BG}{8}\right)^c \tag{2.18}$$

where ΔBG is the tooth dull grade, ranging from zero to eight, and c is a coefficient. Hareland *et al*. (2010) does not provide values or bounds for the c coefficient. The wear function in Eq. 2.18 is simplified as a constant in the model implementation on ROPPlotter.

Coefficient values presented for predicting rock strength with three bits in shale and limestone formations yield the coefficient bounds shown next:

Table 2.5: Hareland Roller Bit model coefficient bounds based on Hareland *et al*. (2010).

ROP Model	**Hareland Roller Bit (2010)**		
Model Coefficients	K	a	b
Coeff. Lower Bound	0.010	0.267	0.888
Coeff. Upper Bound	0.917	0.645	1.410

Depth, measured in meters, is the only mention to units in this publication. Therefore, coefficient values with field units will likely not fall within the bounds in Table 2.5.

2.6 Motahhari PDC Bit (Motahhari *et al.*, 2010)

Motahhari's PDC bit ROP model includes the effect of mud motors and assumes perfect bit cleaning. Its governing equation is:

$$ROP = W_f \left(\frac{G \times RPM_t^{\gamma} \times WOB^{\propto}}{D_B \times S}\right) \tag{2.19}$$

where W_f is the wear function, G is a model coefficient, RPM_t is the total bit rotary speed (RPM), WOB is the applied weight-on-bit (lbs), D_B is the bit diameter (in), S is the confined rock strength (psi), and α and γ are ROP model exponents. The wear function, W_f, is given by:

$$W_f = k_{wf}\left(\frac{WOB}{N_c}\right)^{\rho}\frac{1}{S^{\tau}{A_w}^{\rho+1}} \tag{2.20}$$

where k_{wf} is a wear function constant, ρ and τ are wear function exponents , N_c is the number of cutters on the bit face and A_w is the wear flat area underneath a cutter (in^2). Due to difficult implementation, the wear function in Eq. 2.20 is simplified as a constant when calculating the Motahhari PDC Bit model in ROPPlotter.

Influenced by bit geometry and interactions between drill bit and formation rock, the G coefficient in Eq. 2.19 is computed from offset well data along with the α and γ model exponents. Even though the authors discuss model application in producing formation strength logs, selecting PDMs and optimizing WOB and rotary speed for a well in Alberta, there is no information about model coefficient values or bounds.

Chapter 3: ROP Model Coefficients Calculations

Performance of ROP models is contingent on how model coefficients are computed. These coefficients are determined empirically to best fit field data in different applications. This chapter discusses methods to calculate ROP model coefficients using Excel Solver and factors affecting these calculations. Marathon (Marathon Oil Corporation) field data for the vertical section of a horizontal well is analyzed with the ROPPlotter software (described in detail in Chapter 4) for illustration purposes.

3.1 ROP Model Coefficients Summary

The following table summarizes the model coefficients of the ROP models presented in Sections 2.1 through 2.6:

Table 3.1: Coefficients of ROP models included in ROPPlotter.

Model	Coefficients	Description
Bingham (1964)	a, b	Dimensionless constants for each rock
Bourgoyne & Young (1974)	a_1-a_8	Various drilling parameters
Winters-Warren-Onyia Roller Bit (1987)	a, b, c φ	Dimensionless bit design constants Cone offset coefficient
Hareland Drag Bit (1994)	a, b, c COR	Cutter geometry correction factors Lithology correction factor (lumps a, b, c)
Hareland Roller Bit (2010)	K a, b	Comprehensive coefficient Coefficients
Motahhari PDC Bit (2010)	G γ, α	Bit geometry, cutter-rock coefficient of friction ROP model exponents

Table 3.1 shows that ROP models in literature have a varying number of model coefficients. Arranging the models in increasing order of model coefficients: Bingham (2), Hareland Drag Bit (3), Hareland Roller Bit (3), Motahhari PDC Bit (3), WWO Roller Bit (4) and Bourgoyne & Young (8).

3.2 Excel Solver Methods to Calculate Model Coefficients

In the early stages of this project, all model coefficients calculations were performed by exactly matching model ROP to field ROP at certain intervals with the Single Point ROP Matching method. Further investigation determined that if model coefficients are computed by minimizing the error between model ROP and field ROP for an entire rock formation, the accuracy of the models increases and the computational time is greatly reduced. ROPPlotter offers both methods of calculating coefficients, Single Point ROP Matching and Minimum Formation Error.

3.2.1 Single Point ROP Matching

In this method, Excel Solver iterates through model coefficients within defined bounds to exactly match model ROP to field ROP for a single data point. Running Excel Solver is a time-consuming task when applied to thousands of rows of data. This procedure can be sped up by matching ROP at intervals of 10ft, 25ft, or 50ft of well depth instead of at all data points. Then, a set of model coefficients for a rock formation is obtained from the average value of coefficients computed for data points within that lithology.

Applications of this method with a resolution of 50ft are demonstrated with Bingham's model and Marathon field data. Greenhorn Limestone, presented in Figure 3.1, is the shallowest formation in the dataset:

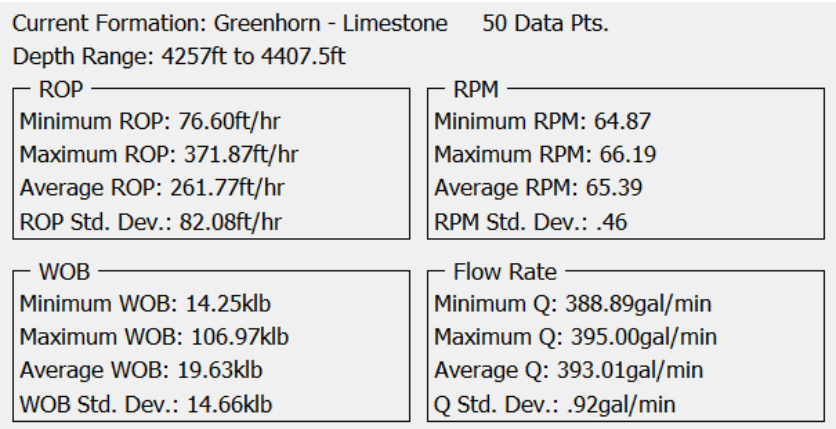

Figure 3.1: Data statistics for Greenhorn Limestone formation.

Within this lithology, there is high variation in ROP (295ft/hr difference between minimum and maximum values) and WOB (92klbs difference between minimum and maximum values). Standard deviations for these parameters are correspondingly high. Meanwhile, RPM stays fairly constant throughout the formation, resulting in a low RPM standard deviation value. Bingham's formulation does not include flow rate, which can be disregarded in this example. Three data points are selected for model coefficient calculations when employing the Single Point ROP Matching method at data points every 50ft to this 150.5ft long rock formation:

Table 3.2: Greenhorn Limestone data points for Single Point ROP Matching (50ft) method.

1	Depth (ft)	ROP (ft/hr)	WOB (klbs)	RPM	a	b	Matched ROP (ft/hr)
2	4257	261.2	16.5670969	66	1.591777199	1.42674	261.1999992
23	4308.25	87.83044729	15.2972428	65.7364	0.786577534	0.948446	87.83044749
38	4364.5	320.2252223	17.2135926	64.9933	1.739644651	1.538559	320.2252218

Averaging out the three values for Bingham's model coefficients a and b in Table 3.2, a set of coefficients to fit the Greenhorn Limestone formation is obtained: a = 1.3727, b = 1.3046. Utilizing these coefficient values, the average percent error for the Bingham model

in the whole formation is 74.88%. This high error value illustrates a shortcoming of the Single Point ROP Matching method at intervals: the set of coefficients computed for a formation relies only on data points selected by a depth criterion (three out of fifty data points for the Greenhorn Limestone formation in the example above). In formations with big variations in surface parameters, the values of model coefficients will also encompass a wide range and may yield formation coefficients that do not fit field data accurately.

On the other end of the spectrum, the Lodgepole Limestone is deepest formation in dataset:

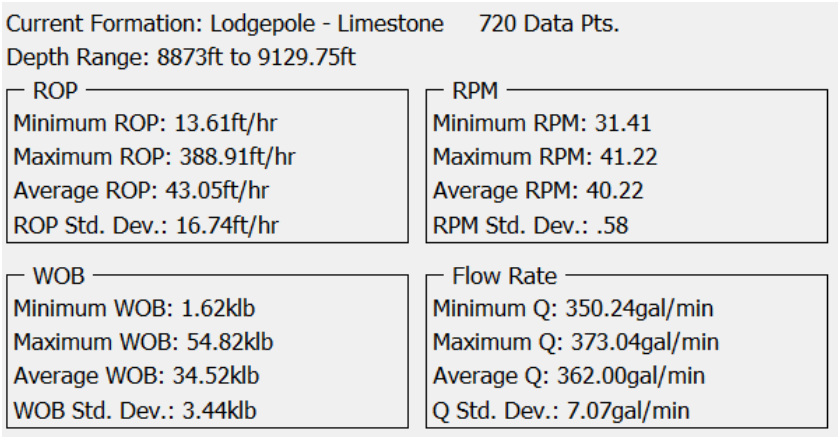

Figure 3.2: Lodgepole Limestone formation data statistics.

Even though there is still high variation in ROP (375ft/hr difference between minimum and maximum values) and WOB (53klbs difference between minimum and maximum values) in the Lodgepole Limestone formation, the standard deviation values for these two parameters in this lithology are much lower than in the previously analyzed Greenhorn Limestone formation. Five data points are selected throughout 256.75ft of rock formation for computation of Bingham's model coefficients:

Table 3.3: Data points for Single ROP Matching (50ft) method in Lodgepole Limestone formation.

1	Depth (ft)	ROP (ft/hr)	WOB (klbs)	RPM	a	b	Matched ROP (ft/hr)
6798	8909	38.86	35.1464143	40	0.9713649	0.0001	38.859999
6934	8959.25	46.18087609	33.5226105	39.8699	1.035327934	0.083553	46.18087511
7071	9009.75	38.51774959	34.0262831	39.8875	0.965527329	0.0001	38.51774859
7215	9060.25	39.07571287	35.1757486	39.8089	0.971162881	0.00767	39.07571294
7362	9110.75	35.17727112	35.8179225	40	0.879307707	0.0001	35.17727012

Taking the mean of the coefficient values from Table 3.3 yields Bingham's model coefficients $a = 0.9645$, $b = 0.0183$ for the Lodgepole Limestone formation. The average percent error in the formation is 8.17%, compared to 74.88% for the Greenhorn Limestone formation. Therefore, at least for this dataset, Bingham's model is able to predict ROP at depth much better than at surface, due to slower average ROP and less variation in drilling parameters.

Applying the Single Point ROP Matching method at all data points requires as many Excel Solver iterations as the number of data points. In order to save computational time in long datasets, calculating coefficients at every 50ft relies only on select data points in that formation, as shown above. The Minimum Formation Error method, presented in the next section, overcomes some of the limitations of the Single Point ROP Matching method by reducing the number of Excel Solver iterations required, while also equally weighing all data points in each formation.

3.2.2 Minimum Formation Error

The Minimum Formation Error method employs the minimization function of Excel Solver, instead of the matching function used with Single Point ROP Matching. Solver finds a set of model coefficients that minimize the average percent error between model ROP and field ROP for all data points in a rock formation:

$$Avg.\%\ Error = \frac{\sum_1^N \frac{|Model\ ROP - Field\ ROP|}{Field\ ROP}}{N} \times 100\% \quad (3.1)$$

where N is the number of data points in a formation. It is essential to take the absolute value of the difference between model and field ROP, or model overestimating and underestimating effects might cancel out and yield an unrealistically low error. The average percent error concept is also later employed to evaluate the performance of ROP models systematically.

Referring back to the Greenhorn Limestone lithology presented in Fig. 3.1, the Minimum Formation Error method minimizes error between model ROP and field ROP for all 50 data points in the formation. The resulting Bingham model coefficients a = 3.7080 and b = 0.0010 yield an average percent error of 37.63% in the Greenhorn Limestone formation, a much lower error value compared to 74.88% obtained with the Single Point ROP Matching method. Furthermore, the Minimum Formation Error method requires only one iteration of Excel Solver while Single Point ROP Matching with 50ft resolution required three iterations, one for each of the selected data points in Table 3.2.

In the Lodgepole Limestone (Fig 3.3) example, one Solver iteration is needed to minimize error in all 720 formation data points with the Minimum Formation Error method, yielding Bingham model coefficients a = 1.0321 and b = 0.0010 and average percent error in the formation of 7.40%. If the Single Point ROP Matching was applied at all data points in the Lodgepole Limestone formation, 720 Excel Solver iterations would have been required.

Table 3.4 summarizes the average percent error and Bingham model coefficients for the Greenhorn Limestone and Lodgepole Limestone formations with the two methods to calculate model coefficients:

Table 3.4: Comparison between Single Point ROP Matching (50ft) and Minimum Formation Error methods with Bingham model for two different formations in Marathon dataset.

Solver Method	**Single Point ROP Matching (50ft)**	**Minimum Formation Error**	**Single Point ROP Matching (50ft)**	**Minimum Formation Error**
Limestone Formation	**Greenhorn**	**Greenhorn**	**Lodgepole**	**Lodgepole**
Average Percent Error	74.88%	37.63%	8.17%	7.40%
***a* Coefficient**	1.3727	3.7080	0.9645	1.0321
***b* Coefficient**	1.3046	0.0010	0.0183	0.0010

It is important to note that both Bingham model coefficients had a defined lower bound (0.001) and upper bound (10) in the calculations above. Coefficient *b* is at the lowest allowed value in both limestone formations when using the Minimum Formation Error method. The importance of model coefficient bounds will be discussed in Section 3.3.1.

The following table explores how the two methods to calculate model coefficients, including all different resolutions of Single Point ROP Matching, fare with the Bingham model for all twenty rock formations in the Marathon dataset:

Table 3.5: Single Point ROP Matching and Minimum Formation Error results with Bingham model for all twenty formations in Marathon dataset.

Solver Method (Resolution)	**Single Point ROP Matching (all data pts.)**	**Single Point ROP Matching (10ft)**	**Single Point ROP Matching (25ft)**	**Single Point ROP Matching (50ft)**	**Minimum Formation Error**
Run Time	> 1 hour	4 minutes	100 seconds	35 seconds	15 seconds
Solver Iterations	7,414	488	195	98	20
Bingham Error - By Formation					
Greenhorn - Limestone	96.71%	45.75%	40.80%	74.88%	37.63%
Newcastle - Sandstone	63.50%	21.67%	21.99%	43.27%	17.96%
Dakota - Sandstone	309.62%	20.56%	22.34%	96.01%	20.52%
Swift - Shale	42.13%	38.38%	37.17%	48.08%	35.81%
Rierdon - Limestone	62.96%	29.11%	25.78%	38.43%	24.51%
Piper - Limestone	35.05%	34.57%	42.48%	34.84%	24.71%
Spearfish - Sandstone	28.70%	18.92%	19.58%	26.77%	18.34%
Pine Salt - Sandstone	81.65%	115.16%	111.70%	126.89%	49.70%
Broom Creek - Sandstone	47.85%	45.05%	54.87%	39.15%	38.54%
Tyler - Sandstone	52.20%	54.39%	49.96%	46.42%	32.58%
Kibbey Lime - Limestone	23.90%	22.17%	22.31%	27.51%	21.61%
Kibbey Lime - Shale	14.09%	14.96%	15.70%	14.12%	13.96%
Charles - Sandstone	40.92%	64.10%	68.20%	42.75%	31.25%
Charles - Limestone	40.83%	39.88%	45.20%	79.32%	25.83%
Ratcliffe - Sandstone	28.87%	21.70%	30.84%	28.38%	21.47%
Base Last Salt - Limestone	9.74%	19.88%	14.20%	100.00%	9.29%
Base Last Salt - Sandstone	13.21%	12.28%	24.56%	13.36%	12.10%
Base Last Salt - Limestone	18.63%	15.91%	16.73%	100.00%	15.88%
Mission Canyon - Limestone	16.11%	19.58%	13.04%	14.05%	12.10%
Lodgepole - Limestone	8.02%	7.53%	7.69%	8.17%	7.40%
Bingham Error - Entire Dataset	**41.80%**	**38.34%**	**38.00%**	**43.17%**	**23.67%**

Table 3.5 shows that the number of iterations and computational time are significantly reduced with the Minimum Formation Error method. In every one of the twenty lithologies, the average percent error is lowest with the Minimum Formation error method. Remarkably, error results for different resolutions of the Single Point ROP Matching method do not follow a pattern. Computing model coefficients for all data points does not always result in an averaged set of coefficients that better fits a formation than when model coefficients are only calculated for a few points in the formation. With a resolution of 50ft, the Single Point ROP Matching method skips some formations entirely, since they are not

longer than 50ft. Thus, the average percent error in those formations (Base Last Salt Limestones in Table 3.5) is 100%.

The comparison between Minimum Formation Error and Single Point ROP Matching (50ft resolution) is extended to all six ROP models included in ROPPlotter:

Table 3.6: Overall average percent error for six ROP models with Marathon dataset.

ROP Model	Bingham (1964)	Bourgoyne & Young (1974)	Hareland Drag Bit (1994)	Hareland Roller Bit (2010)	Motahhari PDC Bit (2010)	WWO Roller Bit (1987)
50ft Match ROP Overall Error	43.17%	48.34%	80.20%	705.78%	59.52%	36.60%
Min. Form. Err. Overall Error	23.67%	26.65%	46.96%	22.52%	28.14%	24.30%

Unrealistic large errors for some models in Table 3.6 indicates that the selected model coefficient bounds did not allow the model to fit field data properly (more in Section 3.3.1). Consistent with previous results, the Minimum Formation Error method performs better with all six ROP models. Therefore, Minimum Formation Error is the preferred method to calculate model coefficients and will be employed for the remainder of this work.

3.2.3 Minimum Formation Error (RMSE)

Root-mean-squared error, or RMSE, is a concept widely applied in mathematics and statistics. Instead of minimizing the average percent error, the Minimum Formation Error method can be modified to reduce RMSE for a rock formation:

$$RMSE = \sqrt{\frac{\sum_1^N (Model\ ROP - Field\ ROP)^2}{N}} \tag{3.2}$$

Marathon field data and the Bingham ROP model are again utilized for comparison between minimizing average percent error or RMSE for each formation:

Table 3.7: Bingham error comparison between RMSE and average percent error minimization with Marathon dataset.

Solver Method (Resolution)	**Minimum Formation Error (RMSE)**	**Minimum Formation Error (% Error)**
Bingham Error - By Formation		
Greenhorn - Limestone	44.82%	44.64%
Newcastle - Sandstone	20.11%	20.11%
Dakota - Sandstone	29.28%	29.05%
Swift - Shale	46.26%	44.88%
Rierdon - Limestone	30.67%	29.44%
Piper - Limestone	29.49%	28.42%
Spearfish - Sandstone	28.64%	27.00%
Pine Salt - Sandstone	75.44%	51.10%
Broom Creek - Sandstone	53.00%	43.97%
Tyler - Sandstone	43.33%	37.30%
Kibbey Lime - Limestone	28.15%	27.96%
Kibbey Lime - Shale	16.68%	16.68%
Charles - Sandstone	46.47%	37.22%
Charles - Limestone	35.72%	28.64%
Ratcliffe - Sandstone	36.90%	33.84%
Base Last Salt - Limestone	11.88%	11.83%
Base Last Salt - Sandstone	16.17%	16.03%
Base Last Salt - Limestone	28.66%	28.66%
Mission Canyon - Limestone	16.27%	14.39%
Lodgepole - Limestone	8.57%	8.15%
Bingham Error - Entire Dataset	**32.78%**	**27.42%**

For all formations in Table 3.7, a lower Bingham error is obtained when minimizing average percent error. Therefore, the Minimum Formation Error (RMSE) method is discarded moving forward. Error values for Minimum Formation Error (average percent

error) are slightly higher than in Table 3.5 because the lower bound of Bingham's *b* coefficient was increased from 0.001 to 0.5 (discussed in Section 3.3.1).

3.2.4 Minimum Formation Error and Bourgoyne & Young Model

When varying all eight B&Y model coefficients in a single iteration of the Minimum Formation Error method, Excel Solver was not able to obtain satisfying results. The other five ROP models in ROPPlotter had no similar issues. A possible explanation is that Solver does not know how to proceed when there are too many coefficients to fit a wide range of data. Tests varying eight, four, two and finally only one model coefficient in each Solver iteration were performed:

Table 3.8: Error comparison when varying different number of B&Y model per Solver iteration.

Coefficients Varied Per Iteration	a1-a8	a1-a4 a5-a8	a1-a2 a3-a4 a5-a6 a7-a8	a1, a2, a3, a4, a5, a6, a7, a8
Run Time	**20 seconds**	**38 seconds**	**70 seconds**	**123 seconds**
Solver Iterations	**20**	**40**	**80**	**160**
B&Y Error - By Formation				
Greenhorn - Limestone	86.39%	74.89%	60.79%	45.68%
Newcastle - Sandstone	92.05%	85.61%	76.28%	19.80%
Dakota - Sandstone	92.76%	86.95%	78.85%	26.98%
Swift - Shale	94.61%	91.12%	86.18%	44.40%
Rierdon - Limestone	99.13%	99.13%	98.91%	27.77%
Piper - Limestone	88.22%	79.04%	67.23%	27.59%
Spearfish - Sandstone	91.75%	85.19%	75.74%	25.54%
Pine Salt - Sandstone	81.72%	69.56%	54.65%	49.75%
Broom Creek - Sandstone	85.12%	74.51%	59.33%	43.00%
Tyler - Sandstone	87.80%	79.45%	66.25%	35.20%
Kibbey Lime - Limestone	82.46%	70.92%	55.09%	25.93%
Kibbey Lime - Shale	86.28%	76.92%	62.03%	15.87%
Charles - Sandstone	87.20%	77.54%	63.76%	37.79%
Charles - Limestone	88.53%	79.67%	66.80%	28.04%
Ratcliffe - Sandstone	92.49%	86.59%	77.89%	32.04%
Base Last Salt - Limestone	88.26%	79.04%	65.44%	11.43%
Base Last Salt - Sandstone	87.44%	77.30%	63.50%	15.23%
Base Last Salt - Limestone	95.49%	92.06%	86.91%	25.27%
Mission Canyon - Limestone	96.06%	96.06%	94.37%	15.00%
Lodgepole - Limestone	92.65%	87.07%	47.72%	7.34%
B&Y - Entire Dataset	**90.07%**	**83.54%**	**70.91%**	**26.65%**

As seen in Table 3.8 above, the Bourgoyne & Young model has a much lower average percent error when varying only one coefficient per Solver iteration. Even though the number of iterations and computational time both increase, the drastic reduction in error merits variation of each coefficient separately for the B&Y model.

3.3 Factors Affecting Model Coefficients Calculations with Excel Solver

There are three main factors that affect Excel Solver's ability to accurately fit model coefficients to ROP field data: coefficient value bounds, coefficient initial guess and coefficient resolution.

3.3.1 Coefficients Value Bounds

By restricting the model coefficients to minimum and maximum bounds, no single parameter affecting ROP dominates the behavior of the model or has its effect neglected. In determining Bingham model coefficients with the Minimum Formation Error method for two lithologies in Section 3.2.2, a value of $b = 0.001$ is obtained. Table 3.4 shows low model average percent error using this coefficient value. Looking back at Bingham's formulation (Eq. 2.1), model coefficient b is the WOB term exponent. By selecting values of $b = 0.001$ for the two limestone formations, Excel Solver effectively eliminates the influence of WOB on ROP. Figures 3.1 and 3.2 display high variation in WOB within the formations, so neglecting the effect of WOB on ROP produces lower average percent errors between model ROP and field ROP.

Figure 3.3 displays the Bingham model, with lower coefficient bounds of 0.001 and upper coefficient bounds of 10, and ROP field data for the entire Marathon dataset:

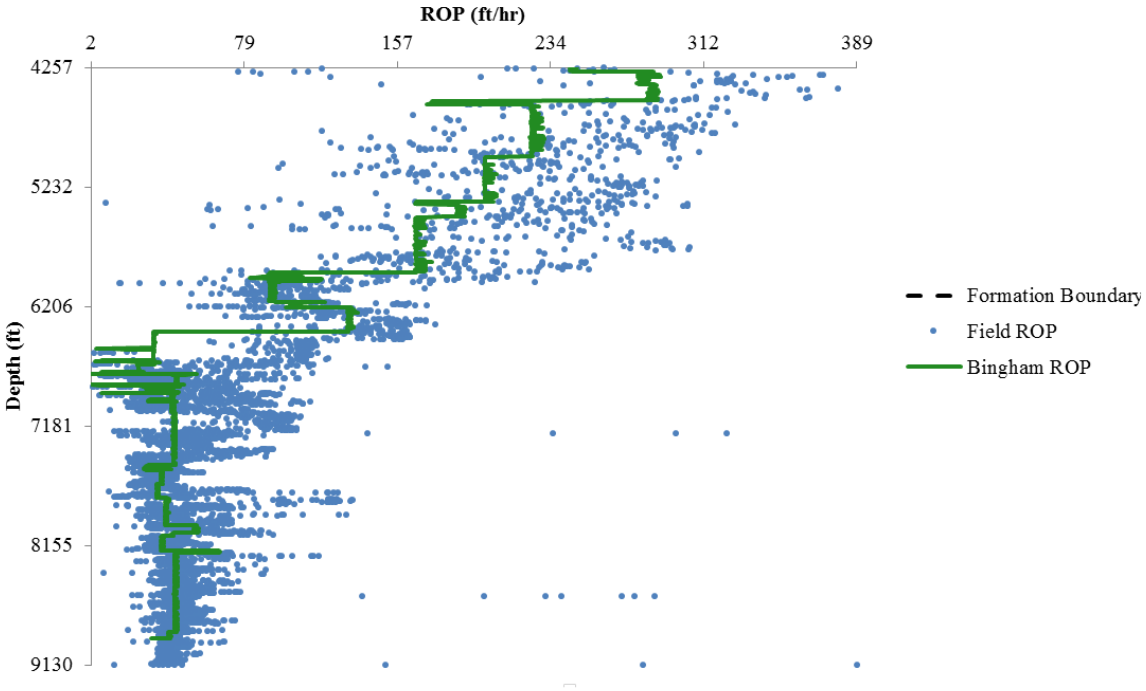

Figure 3.3: Bingham model fit to Marathon data with coefficient lower bounds = 0.001 and upper bounds = 10.

Bingham's ROP model does not show much scatter in the figure above. In fact, the lower bound value of the *b* coefficient (*b* = 0.001) is utilized in all formations, resulting in the unrealistically constant model fit in Figure 3.3. Raising the lower bound of the *b* coefficient to 0.5, the fit becomes a little more erratic:

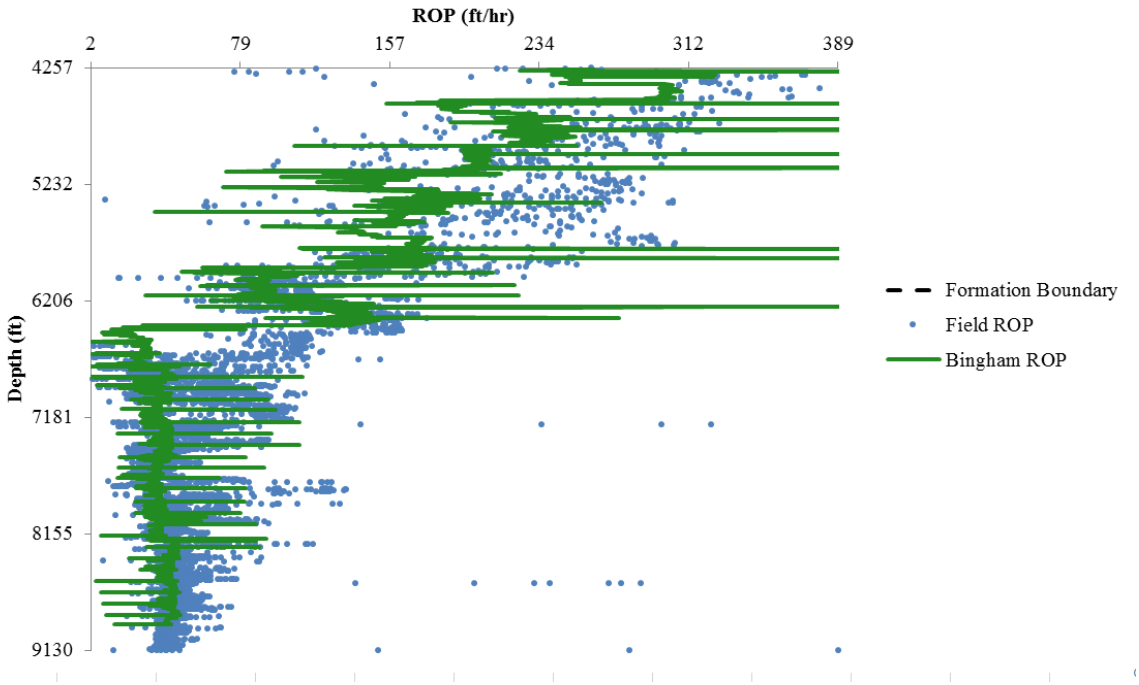

Figure 3.4: Bingham model fit increasing the lower bound of coefficient *b* to 0.5.

A *b* coefficient lower bound of 0.5 ensures WOB variations are not completely ignored by the model. Even though model accuracy might be reduced, the model becomes more representative. Actually, the average percent error with these coefficient bounds does not change by much in a number of lithologies:

Table 3.9: Bingham error comparison for different *b* coefficient lower bounds.

"b" Coefficient Lower Bound	**L.B. = 0.001**	**L.B. = 0.5**
Bingham Error - By Formation		
Greenhorn - Limestone	37.63%	44.64%
Newcastle - Sandstone	17.96%	20.11%
Dakota - Sandstone	20.52%	29.05%
Swift - Shale	35.81%	44.88%
Rierdon - Limestone	24.51%	29.44%
Piper - Limestone	24.71%	28.42%
Spearfish - Sandstone	18.34%	27.00%
Pine Salt - Sandstone	49.70%	51.10%
Broom Creek - Sandstone	38.54%	43.97%
Tyler - Sandstone	32.58%	37.30%
Kibbey Lime - Limestone	21.61%	27.96%
Kibbey Lime - Shale	13.96%	16.68%
Charles - Sandstone	31.25%	37.22%
Charles - Limestone	25.83%	28.64%
Ratcliffe - Sandstone	21.47%	33.84%
Base Last Salt - Limestone	9.29%	11.83%
Base Last Salt - Sandstone	12.10%	16.03%
Base Last Salt - Limestone	15.88%	28.66%
Mission Canyon - Limestone	12.10%	14.39%
Lodgepole - Limestone	7.40%	8.15%
Bingham Error - Entire Dataset	**23.67%**	**27.42%**

Table 3.9 exhibits an increase of less than 4% in the Bingham model average percent error for the entire dataset when the lower bound of the *b* coefficient is raised from 0.001 to 0.5.

In Chapter 2, Tables 2.1 through 2.5 display model coefficient bounds determined according to model applications provided by each ROP model author. Those coefficients were obtained for a specific field and, in some cases, with outdated drill bits. Therefore, they should not be taken as global coefficient bounds. Coefficient bound values (Tables 2.1-2.5) can be used as a guide and adapted to fit each model implementation. New studies require a throughout analysis in determining realistic bounds for model coefficients.

ROPPlotter allows for user-defined minimum and maximum bounds for each ROP model coefficient to be computed by the program.

3.3.2 Coefficients Initial Guess

An initial guess for each model coefficient is provided to Excel Solver in each iteration. Starting from the initial guesses, Solver varies the coefficients in increments, seeking to minimize the average percent error between model ROP and field ROP. If the error does not differ by a considerable amount after a number of increments, the result converged and the iteration is over. Hence, if coefficient initial guesses yield a model ROP value too many orders of magnitude off from field ROP, Excel Solver might converge to an unreasonable solution.

3.3.3 Coefficients Resolution

Model coefficients resolution refers to the interval of data points that utilizes the same set of coefficients for model ROP calculations. It is not to be confused with Excel Solver resolution used with the Single Point ROP Matching method. In this method, even though ROP model coefficients are calculated at certain intervals (e.g. every 50ft), those values are averaged out to produce a set of coefficients for each rock formation. Therefore, the model coefficients resolution for all examples in this chapter is defined by lithology.

There are two extremes concerning model coefficient resolution. With the highest resolution, where coefficients may change for every single data point, the model will perfectly match field data with zero error. On the other hand, if one set of model coefficients is used to fit an entire dataset containing many different rock formations, model performance will likely be lousy. Both extremes will result in modeling problems, either underfitting or overfitting data. Throughout this thesis, ROP model coefficients resolution is always determined by rock formations.

Chapter 4: ROPPlotter

This chapter illustrates the capabilities of the ROPPlotter software. Step-by-step explanation of commands (with pictures) is included. Program implementation examples are demonstrated with Marathon (Marathon Oil Corporation) field data, since it is a complete dataset that spans twenty different lithologies in a 4,873ft vertical section of a horizontal well. The main Excel userform that controls most ROPPlotter functions is the "Plotter" form:

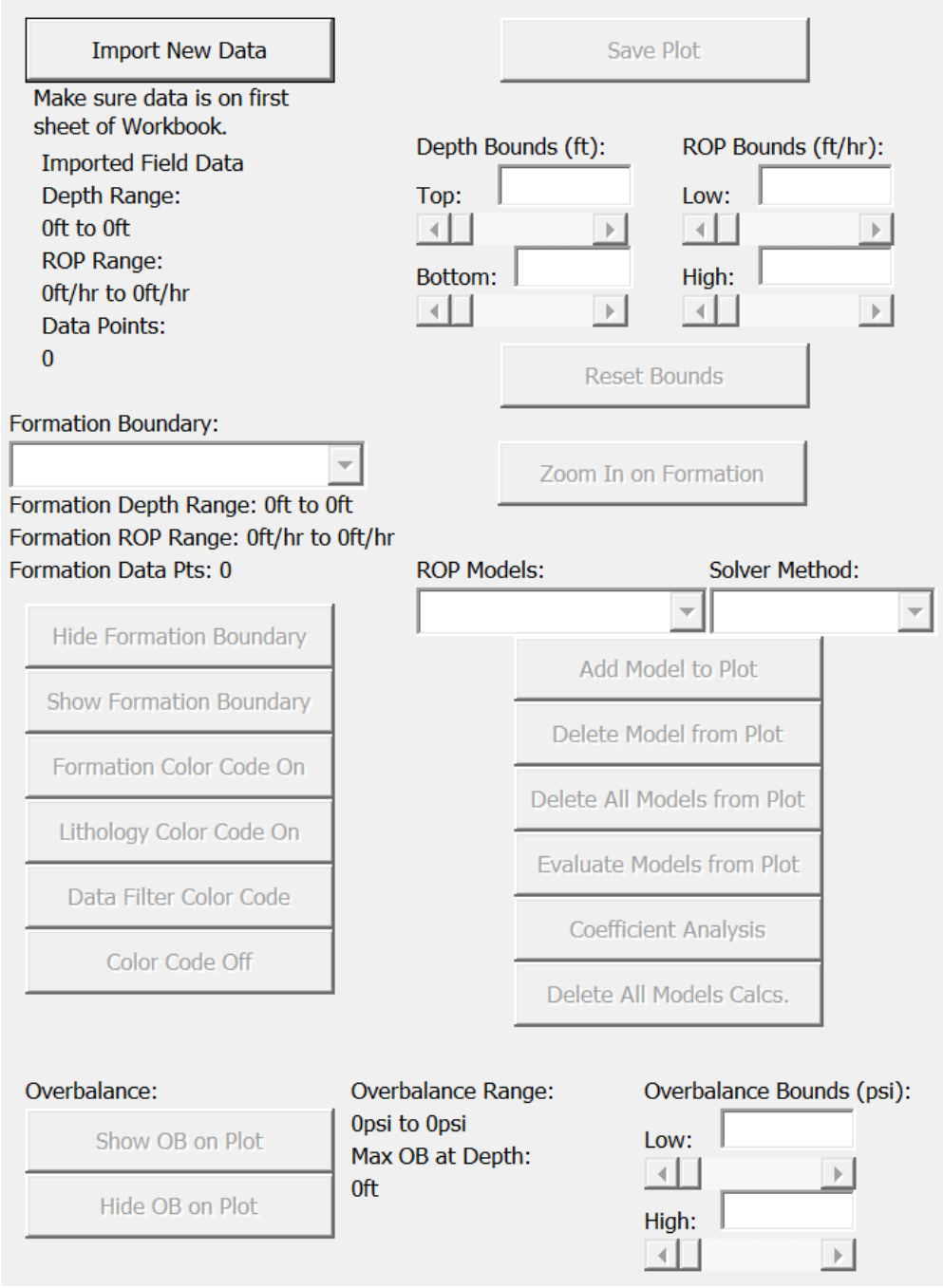

Figure 4.1: Plotter form with main program commands.

As seen in Figure 4.1, most command buttons are deactivated because no field data has been imported. Functionalities of each command button will be presented later. The first step is to import data from another Excel spreadsheet.

4.1 Importing Data

4.1.1 Selecting Appropriate Data Headings

By clicking on the "Import New Data" button (Fig. 4.1), the user can select the desired dataset for analysis. Once a file is selected, VBA code automatically detects the data headings in the chosen sheet and the following form is displayed:

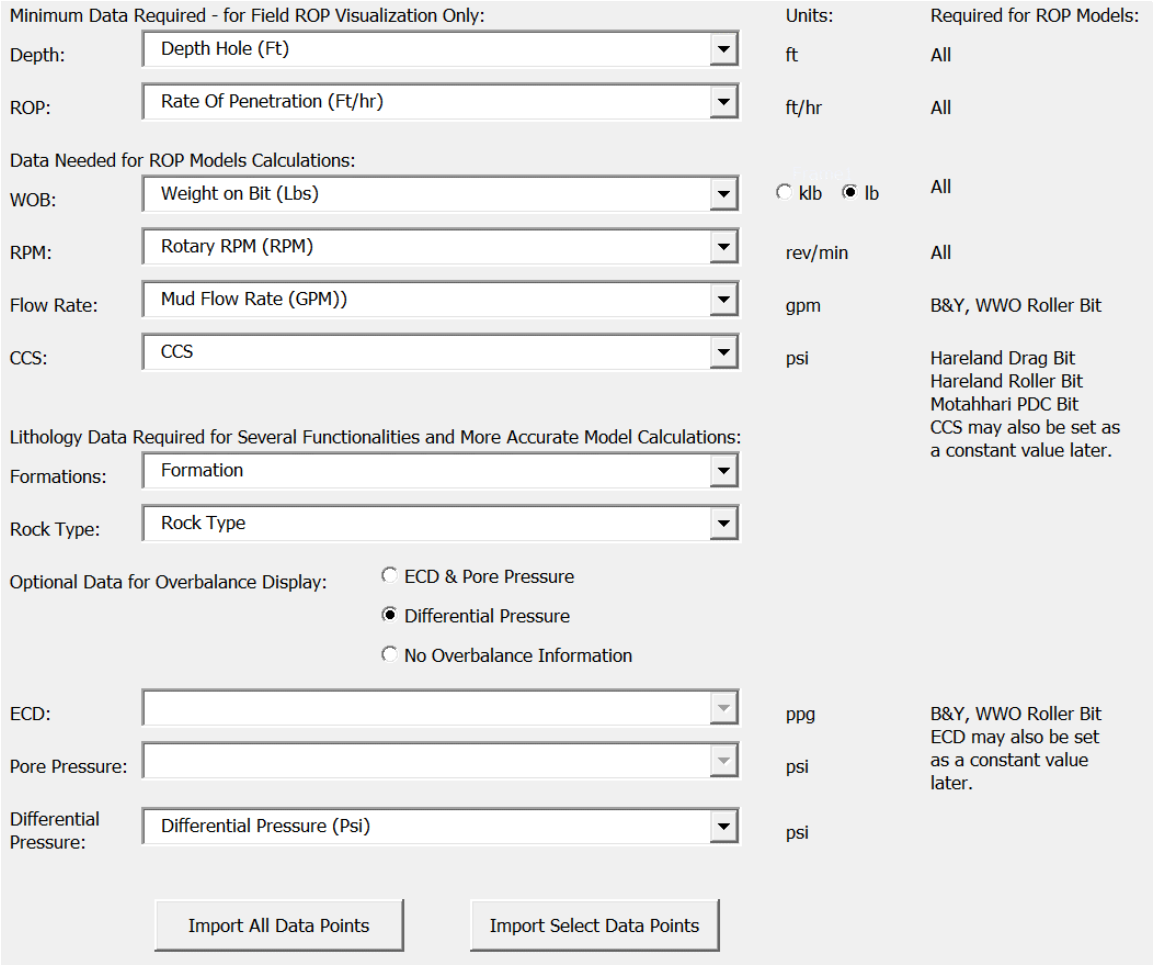

Figure 4.2: Headings form with Marathon field data.

Data headings in Figure 4.2 represent parameters variable at every data point recorded while drilling the well. They are divided into four categories: data for field ROP visualization, data for ROP model calculations, lithology data, and overbalance data. Units for each drilling parameter are indicated on the headings userform in Fig 4.2, and weight-on-bit can be reported in either pounds or kilopounds. With only depth and ROP data, no model calculations can be performed. WOB and RPM information is required for all six ROP models in ROPPlotter. The data headings form also indicates which models need additional data: flow rate and ECD for the B&Y and WWO Roller Bit models and rock

confined compressive strength (CCS) for the Hareland Drag Bit, Hareland Roller Bit and Motahhari PDC Bit models. Since CCS and ECD are parameters not always reported by industry standard, the program allows for their input as constant values later when calculating coefficients for ROP models. Constants needed to compute ROP models, such as bit diameter and number of bit nozzles, are defined when implementing each model. Lithology data is essential in defining model coefficients resolution, as discussed in Section 3.3.3. A single set of coefficients will fit the entire dataset if no information about rock formations is available. Optional overbalance data can be visualized by subtracting pore pressure from ECD, or with differential pressure information.

Most datasets include various measurements for each of the parameters necessary for ROP model analysis. ROPPlotter looks for key terms in the selected spreadsheet and populates the lists of headings for each parameter. Some companies record both surface and downhole data and the form in Figure 4.2 allows the user to choose the type of data to be studied. For the dataset in this example, five different values of RPM may be selected:

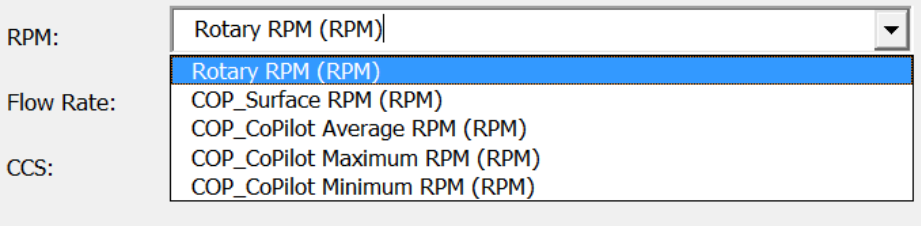

Figure 4.3: Different choices for RPM data headings in the given dataset.

After selecting the appropriate data headings, the user has the choice of importing all data points in the selected file or going through a data filtering process. The "Import All Data" button (see Fig. 4.2) is useful when performing a quick analysis, but data outliers will most likely be present. For a more meaningful application of ROP models, it is necessary to remove data points that deviate greatly from their neighboring points.

4.1.2 Data Filtering

Data outliers can be detected and removed by clicking on the "Import Select Data" button (Fig. 4.2), launching the data filtering form:

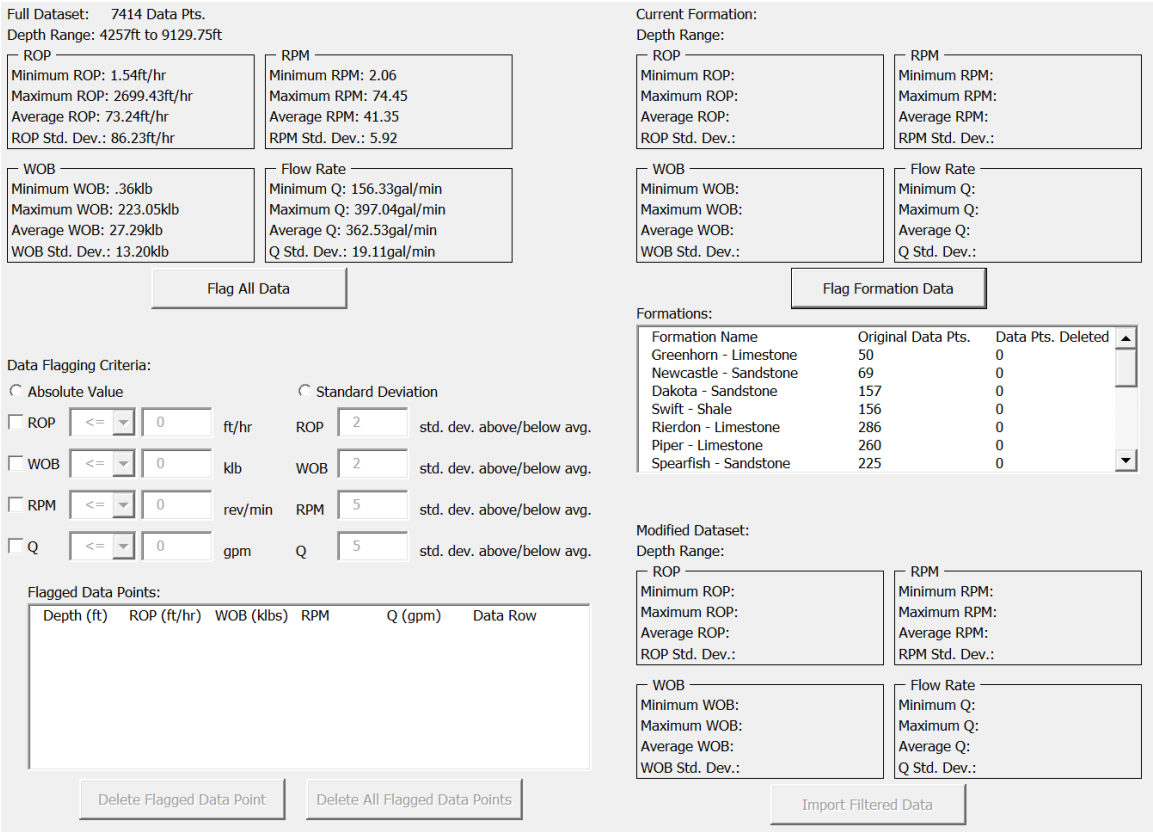

Figure 4.4: Data filtering userform.

The data filtering form has many different capabilities, explained separately in the next sections.

4.1.2.1 ROP, RPM, WOB, and Flow Rate Statistics

The top left-hand corner of the form in Fig. 4.4 summarizes important information about the key parameters for all data points in the dataset (no outliers excluded yet).

Minimum, maximum, average, and standard deviation values for ROP, RPM, WOB and flow rate (Q) are given for the full dataset:

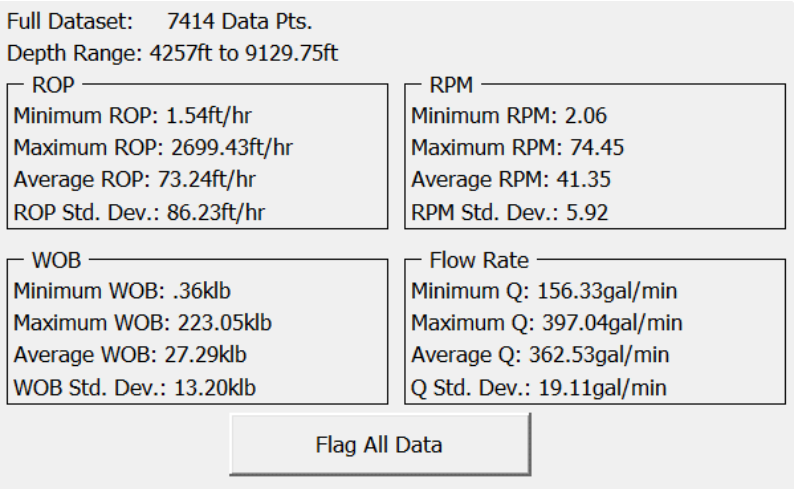

Figure 4.5: Zoom-in visualization of the full dataset statistical parameters.

Figure 4.5 shows that some of the data gathered in the given spreadsheet is almost certainly inaccurate. While the average ROP is 73.24ft/hr, the maximum is 2,699.43ft/hr, which is an unrealistic rate of penetration value. Weight-on-bit values display similar behavior. Flagging (detection) of such data outliers is accomplished with two distinct techniques.

4.1.2.2 Data Flagging Methods

The first and quickest data flagging method is to examine the entire dataset at once, by clicking on the "Flag All Data" button shown in Figure 4.5. A more in-depth evaluation of data outliers may be done formation-by-formation, with the formation list and "Flag Formation Data" button in Fig. 4.6 below:

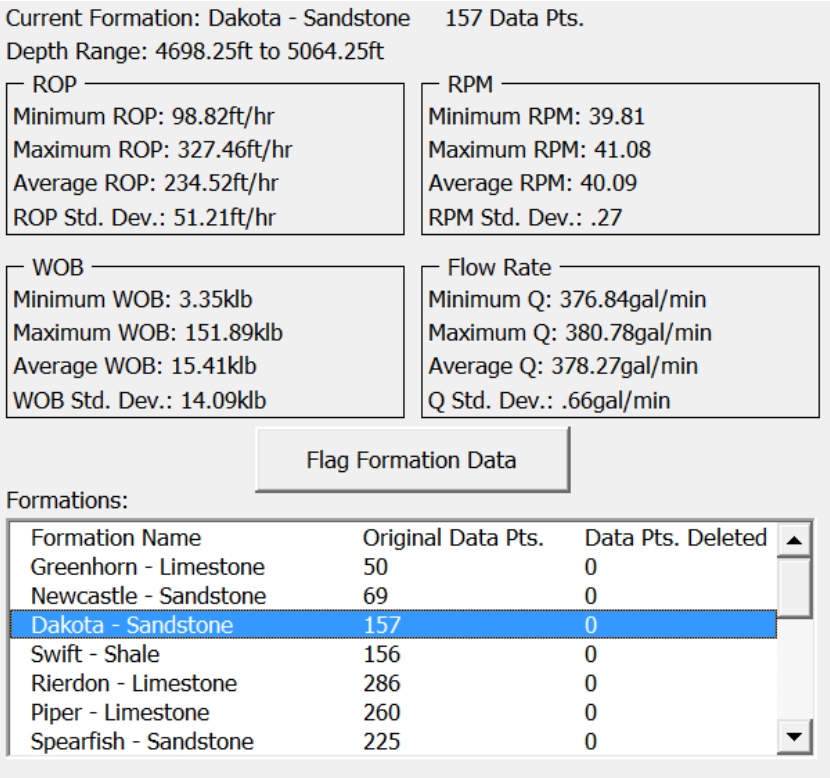

Figure 4.6: List of formations and parameter statistics for the Dakota Sandstone lithology.

The formation flagging method is only available if lithology data was previously selected in the headings form in Fig. 4.2. In this case, a list of all the rock formations is automatically populated (see Fig. 4.6 above). By selecting a formation, parameter statistics for that specific lithology (e.g. Dakota Sandstone) can be analyzed. Once a formation has been investigated using one of the two data flagging criteria (described next), data points can be deleted. The rightmost column of the formations list is updated constantly, displaying how many data outliers have been deleted in each formation in comparison with the original number of data points.

4.1.2.3 Data Flagging Criteria

ROPPlotter accomplishes data flagging, or detection of outlier data points, with two distinct criteria: absolute value or standard deviation. Just below the statistical information for the whole dataset, presented in Fig. 4.5, the flagging criteria can be selected:

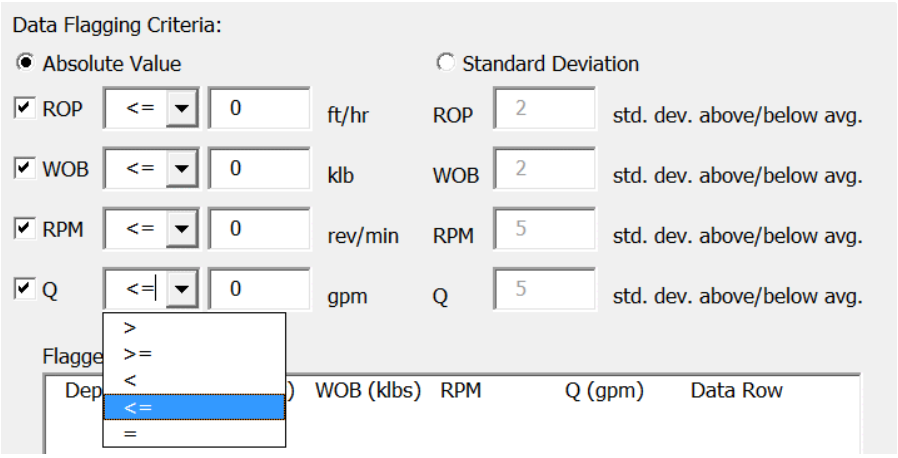

Figure 4.7: Two distinct data flagging criteria (absolute value selected).

Looking at the figure above, the absolute value criterion can be set to flag points greater than, greater than or equal to, less than, less than or equal to, or equal to a defined value. The user can flag points based on absolute value for any or all of the four key parameters (ROP, WOB, RPM and flow rate). The default absolute value flagging setting, shown in Fig. 4.7, is recommended for every single dataset. Eliminating data points with parameter values less than or equal to zero is essential, since negative parameter values might cause problems in model calculations. The standard deviation criterion detects data points with values above or below a defined number of standard deviations from the parameter average.

Either data flagging criteria (absolute value or standard deviation) can be utilized in conjunction with either data flagging method (all data or formation-by-formation).

Depending on which data flagging method is chosen, one of the two criteria choices in Figure 4.7 might be more appropriate. If a quick analysis is desired, the "Flag All Data" button can be used together with the absolute value criterion to detect data points in the entire dataset above or below a chosen threshold value. On the other hand, a more elaborate study may be performed by selecting the standard deviation criterion and working with the "Flag Formation Data" button for each lithology.

4.1.2.4 Excluding Data Outliers

Once the "Flag All Data" button (Fig. 4.5) or the "Flag Formation Data" button (Fig. 4.6) is clicked, with a data flagging criterion selected, the flagged data points box in the bottom left-hand corner of the data filtering form is populated:

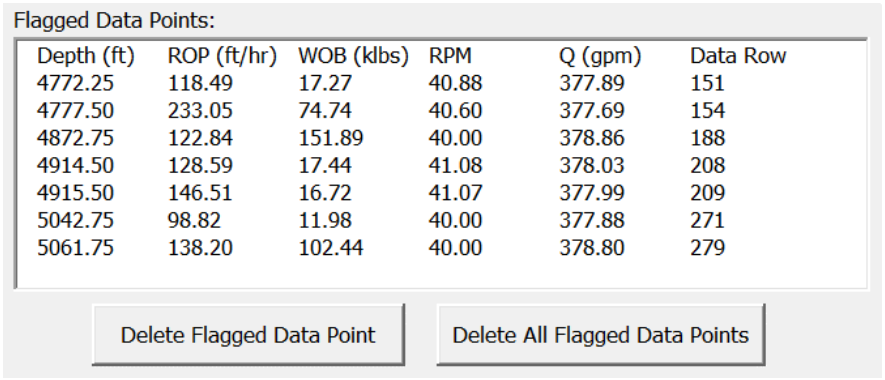

Figure 4.8: Flagged data points for Dakota Sandstone formation with standard deviation criterion. Points were flagged for ROP and WOB two standard deviations above/below average and RPM and flow rate five standard deviations above/below average.

The data outliers might be excluded all at once ("Delete All Flagged Data Points" button) or one at a time ("Delete Flagged Data Point" button). In this example, the flexibility in choosing which points to delete is essential. By looking at Figures 4.6 and 4.8, it is clear that the third and the last flagged data points should be removed, as their WOB values are

much higher than the average for the Dakota Sandstone formation. However, the five remaining data points in Fig. 4.8 were flagged due to a very low standard deviation in flow rate. They are accurate data points that should be included in the analysis.

4.1.2.5 Modified Dataset Statistics

As one or more flagged data points are deleted, the statistical information for the modified dataset (full dataset without the excluded outliers) on the bottom right-hand corner of the data filtering form (Fig. 4.4) is updated:

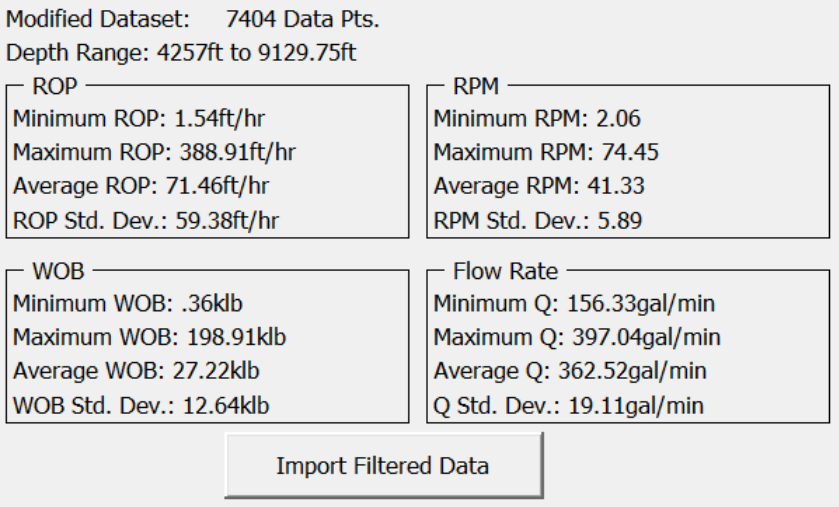

Figure 4.9: Modified dataset statistics achieved by deleting all data points with ROP absolute value greater than or equal to 400ft/hr and WOB absolute value greater than or equal to 200klb.

By performing a simple data flagging study (entire dataset with absolute value criterion) and removing 10 out of 7414 total data points, it is possible to see major improvement in the modified dataset in relation to the original full dataset (Fig. 4.5). Maximum ROP originally was 2,699.43ft/hr, with a standard deviation of 86.32ft/hr. Maximum ROP in the modified dataset is capped at 388.91ft/hr (a more realistic value) with standard deviation

of 59.38ft/hr. Similar improvement can be seen for WOB values. The illustrations that follow in this chapter are obtained with the modified dataset represented in Figure 4.9. By performing a formation-by-formation analysis, even better and more consistent results can be obtained. After the user is satisfied with the modified dataset statistics, the "Import Filtered Data" button stores such data in ROPPlotter for further investigation.

4.2 Plotter Form Commands

Data has now been imported into ROPPlotter, either by using the "Import All Data" button (see Fig. 4.2) or the "Import Filtered Data" button (Fig 4.9). The Plotter form is again displayed, but now with a plot next to it containing ROP field data:

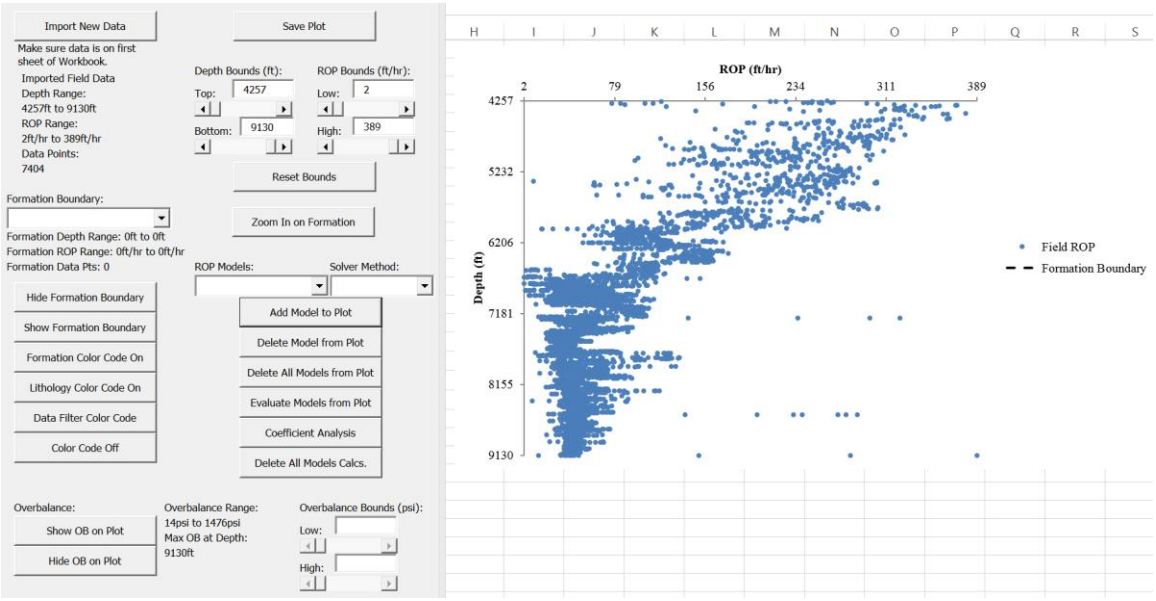

Figure 4.10: Plotter form and plot displaying ROP field data.

The Plotter form and the plot besides it work together, and any commands executed in the form are reflected on the plot. The command buttons are now activated and specific information about the dataset is displayed.

4.2.1 Changing Plot Bounds

On the right side of the Plotter form, bound boxes and bars offer a straightforward manner to edit the plot's depth and ROP bounds:

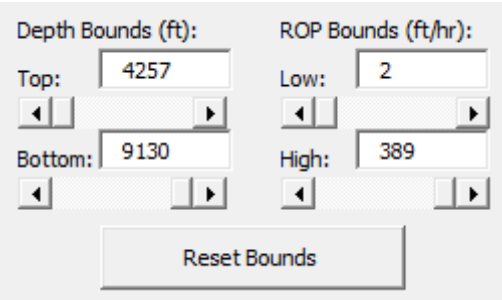

Figure 4.11: Depth and ROP bounds boxes and bars.

Clicking on or dragging the bound bars, or typing in a number into the bound boxes, automatically updates the axes bounds on the visualized plot. The "Reset Bounds" button changes the depth and ROP bounds to the minimum and maximum values from field data.

4.2.2 Zoom-in on Formation

Similar to the formation list in the data filtering form (Fig 4.6), the formation boundary box on the left side of the Plotter form contains a list of all the formations in the given dataset:

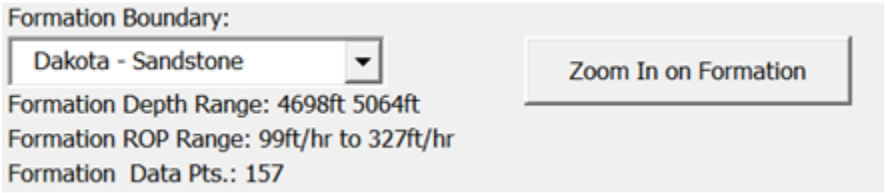

Figure 4.12: Formation boundary list box and zooming-in button.

By choosing a formation from this drop-down list, formation boundary lines are displayed in the plot to indicate where the formation starts and ends. The plot depth bounds will be

adjusted to include the entire formation and an extra fifty feet above and below it, while the ROP bounds will range from the minimum to the maximum ROP values encountered in that lithology:

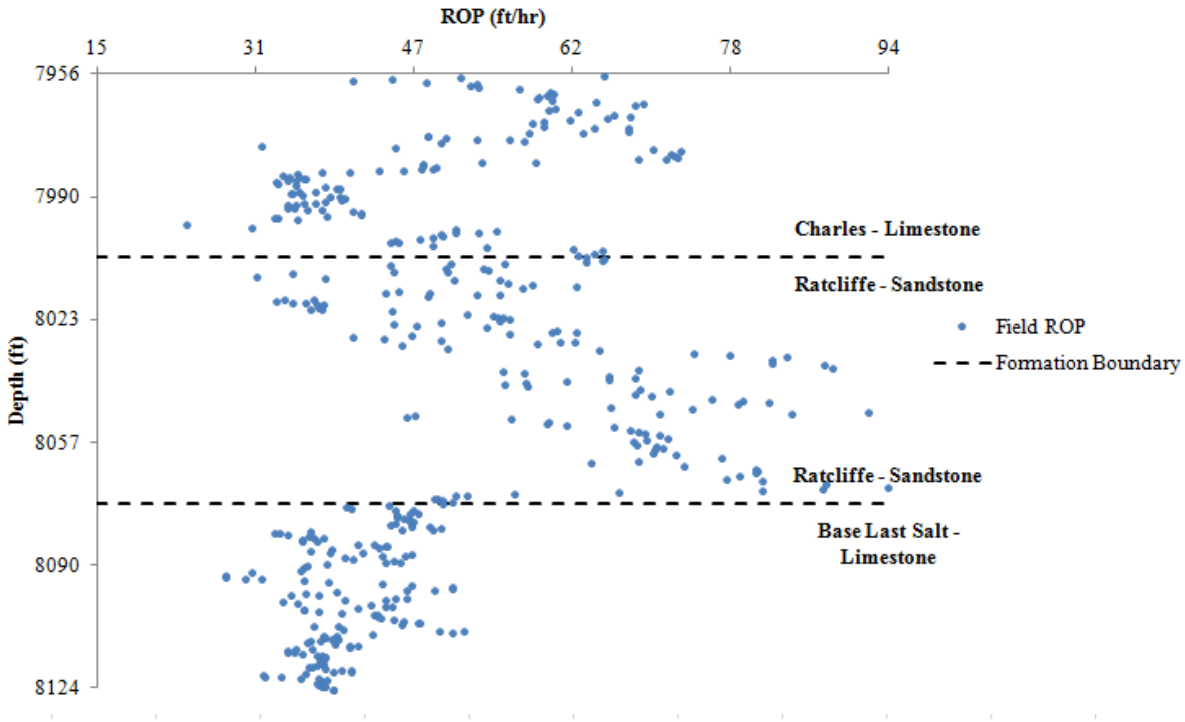

Figure 4.13: Ratcliffe Sandstone ROP field data with formation boundaries.

If the plot bounds are changed, it is possible to return to this default configuration shown above by simply clicking on the "Zoom-in on Formation" button (Fig. 4.12). It is worthwhile to investigate how field ROP varies across formation boundaries. As the lithology shifts from the Charles Limestone to the Ratcliffe Sandstone, a gradual increase in rate of penetration is observed. On the other hand, the well experiences a sharp decrease in ROP when transitioning between Ratcliffe Sandstone and Base Last Salt Limestone. The

two buttons underneath the formation boundary list box control whether or not the formation boundary lines shown in Figure 4.13 are visible or hidden:

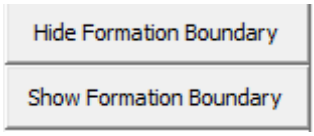

Figure 4.14: Hide and show formation boundary buttons.

4.2.3 Color-coding

Below the two buttons in Figure 4.14, four other command buttons govern color-coding for a specific formation, by lithology, or with a data filtering criterion:

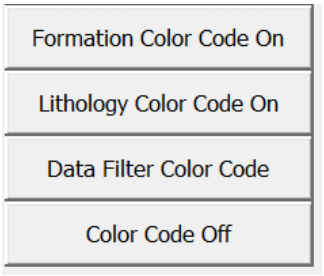

Figure 4.15: Formation, lithology, data filter and no color-coding buttons.

4.2.3.1 Formation Color Coding

When the "Formation Color Code On" option is chosen, the field ROP inside the selected formation (Fig 4.12) is displayed in a different color:

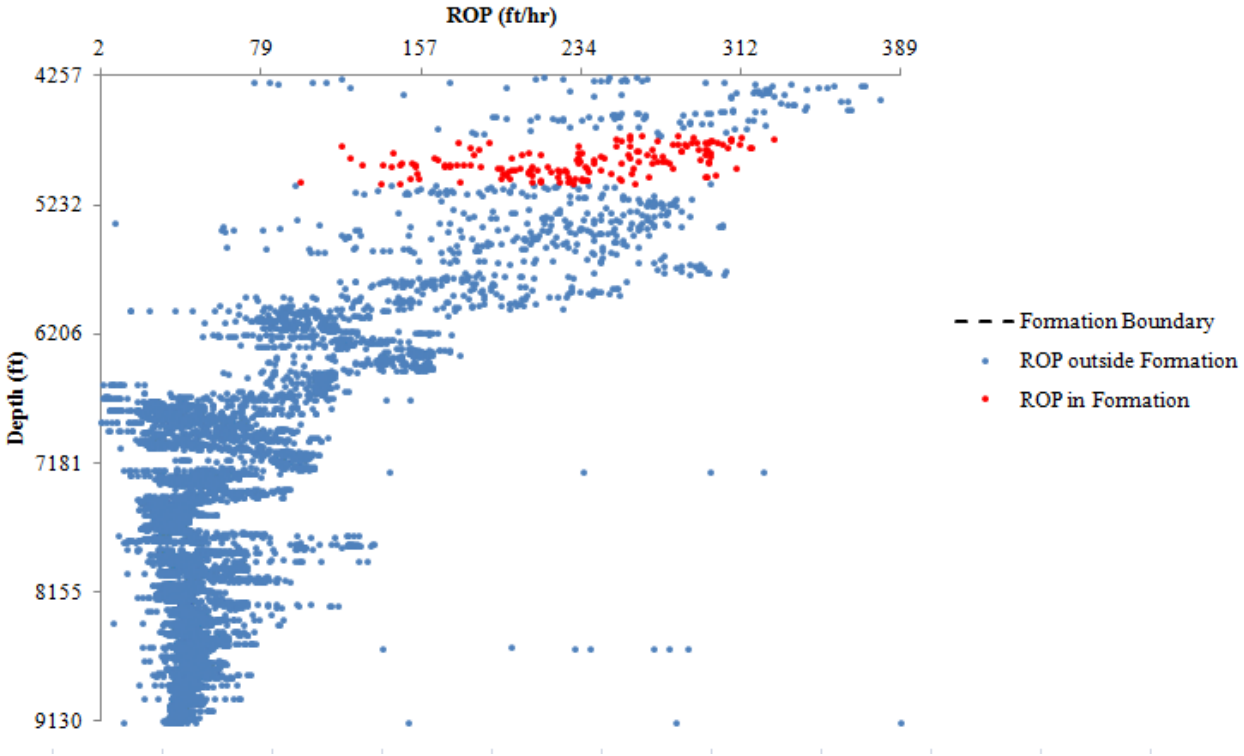

Figure 4.16: Formation color-coding for Dakota Sandstone formation (boundary lines hidden).

Color-coding can also be used in conjunction with formation boundary lines (hidden above).

4.2.3.2 Lithology Color Coding

The "Lithology Color Code On" button (Fig 4.15) color-codes the entire well based on rock type, yielding a fine representation of how field ROP changes for different types of rock:

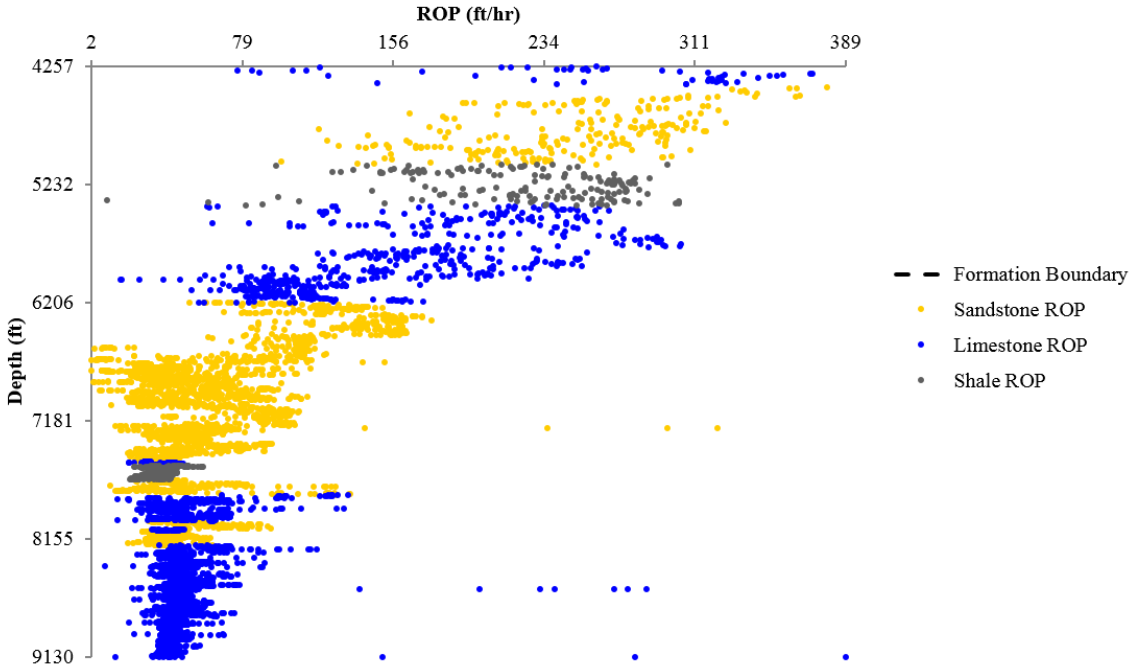

Figure 4.17: Lithology color-coding for the entire well.

Default colors from standard geologic representations identify sandstones (yellow), limestones (blue) and shales (gray).

4.2.3.3 Data Filter Color Coding

The third and final color-coding option highlights data points according to a data flagging criterion for the whole dataset. Clicking "Data Filter Color Code" button (Fig 4.15) launches the following form:

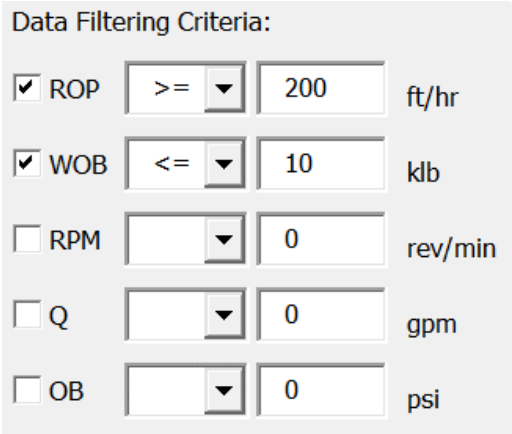

Figure 4.18: Data filter color-coding userform.

Notice that the form in the figure above is similar to data flagging by absolute value criterion presented when removing data outliers in Figure 4.7, but it additionally offers data flagging according to overbalance (OB). One, or all five drilling parameters in Fig 4.18, may be selected for color-coding using the checkboxes next to each parameter.

Color-coding points with ROP greater than or equal to 200ft/hr in the Marathon dataset:

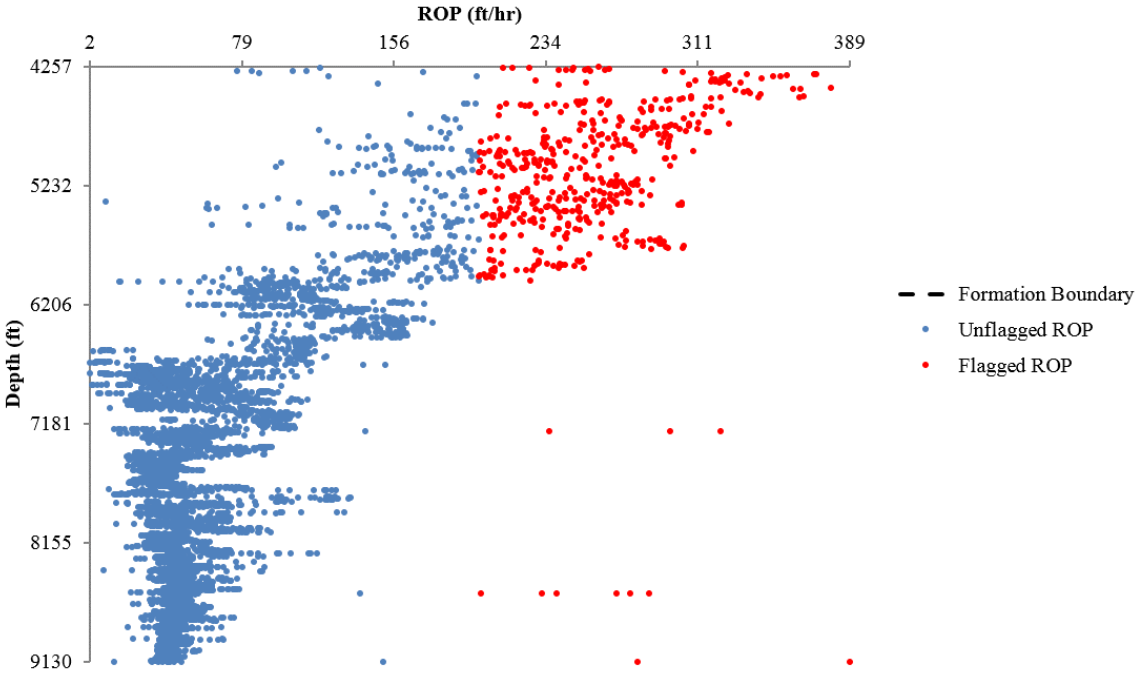

Figure 4.19: Data filtering color-coding for points with ROP greater than or equal to 200ft/hr.

As expected, filtering points according to ROP creates a vertical line at the ROP value selected. Data filter color-coding becomes more valuable when detecting points based on other drilling parameters. Points with WOB lower than or equal to 10klb are highlighted next:

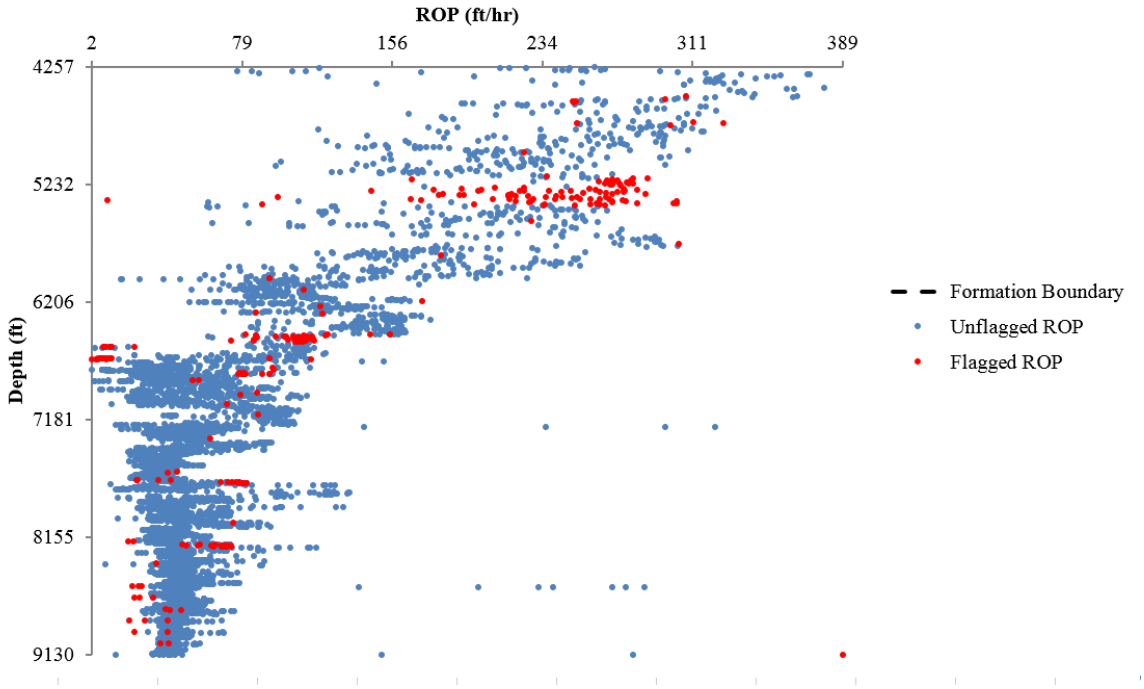

Figure 4.20: Data filtering color-coding for points with WOB lower than or equal to 10klb.

Figure 4.20 shows that low WOB data points are scattered throughout the dataset. However, there is a concentration of flagged points (red) around 5250ft. It is possible that this section of the well could have been drilled faster if higher WOB values were applied.

One of the current industry areas of interest is sliding drilling, when the top drive is not spinning and RPM approaches or is equal to zero. Filtering points with RPM less than or equal to 5rev/min in the Marathon dataset:

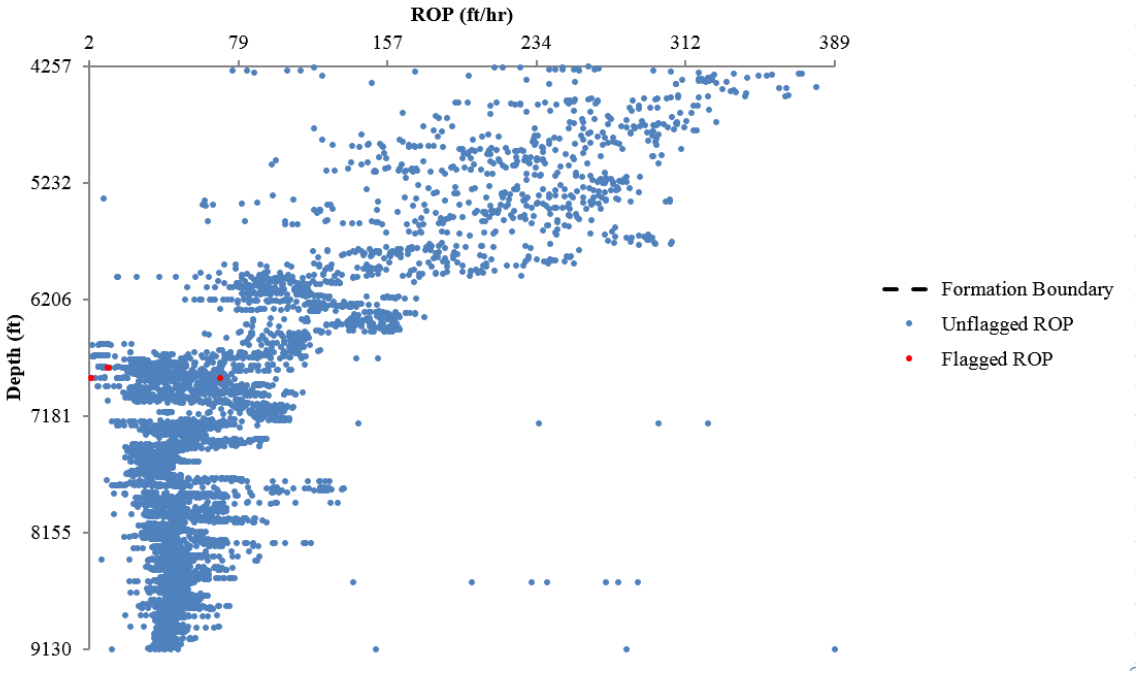

Figure 4.21: Data filtering color-coding for points with RPM lower than or equal to 5rev/min.

Only three data points were detected according to this criterion, meaning that sliding drilling was not performed in this well.

4.2.4 Overbalance Analysis

As previously discussed in Chapter 1, increasing differential pressure at the drill bit has been shown to have a negative impact on ROP due to the chip hold-down effect. Consequently, overbalance display capabilities are included in ROPPlotter at the bottom of the Plotter form:

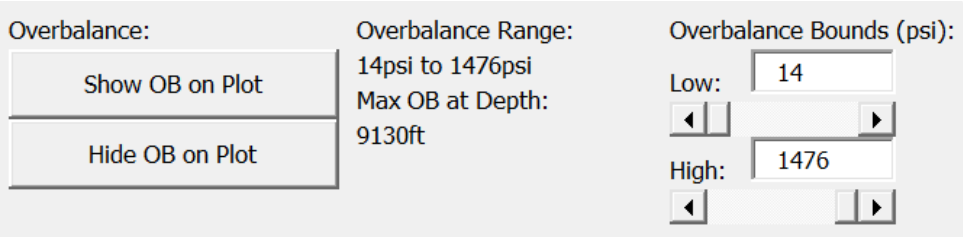

Figure 4.22: Overbalance information, controls and axis bound boxes.

The two command buttons on the left side of Fig. 4.22 control whether or not overbalance is displayed on the plot. If so, differential pressure is plotted on a secondary axis and the bound boxes above control the axis bounds.

Figure 4.23 illustrates overbalance and field ROP for the Marathon dataset:

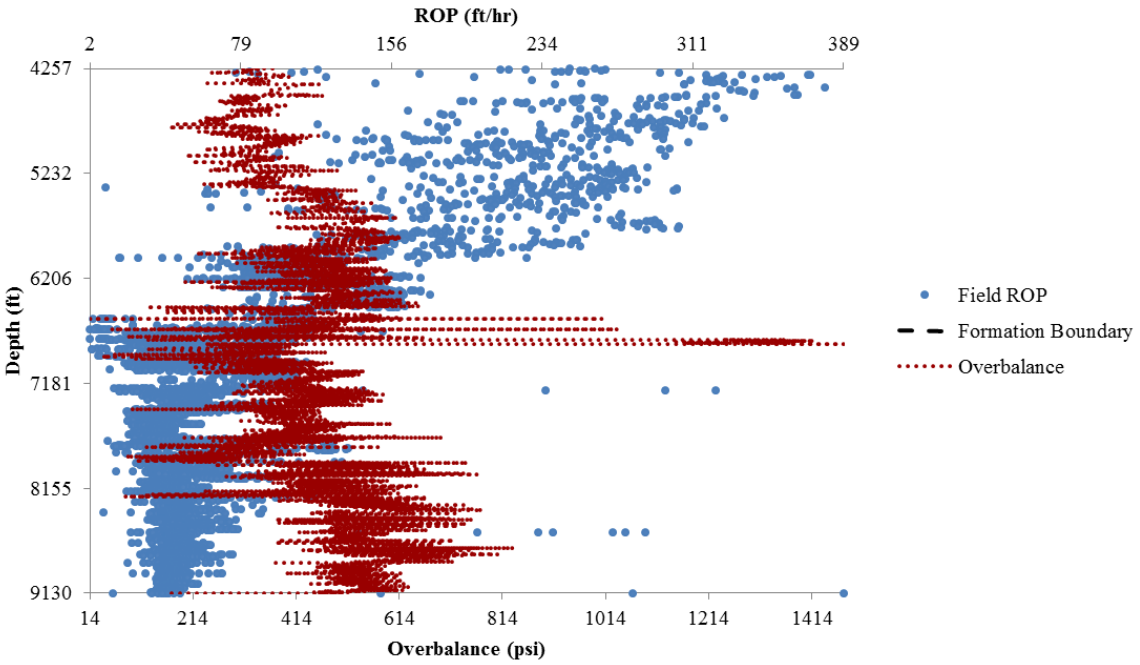

Figure 4.23: Differential pressure and field ROP for Marathon dataset.

It is hard to make observations regarding overbalance when the whole well is being shown. Zooming-in on a specific rock formation:

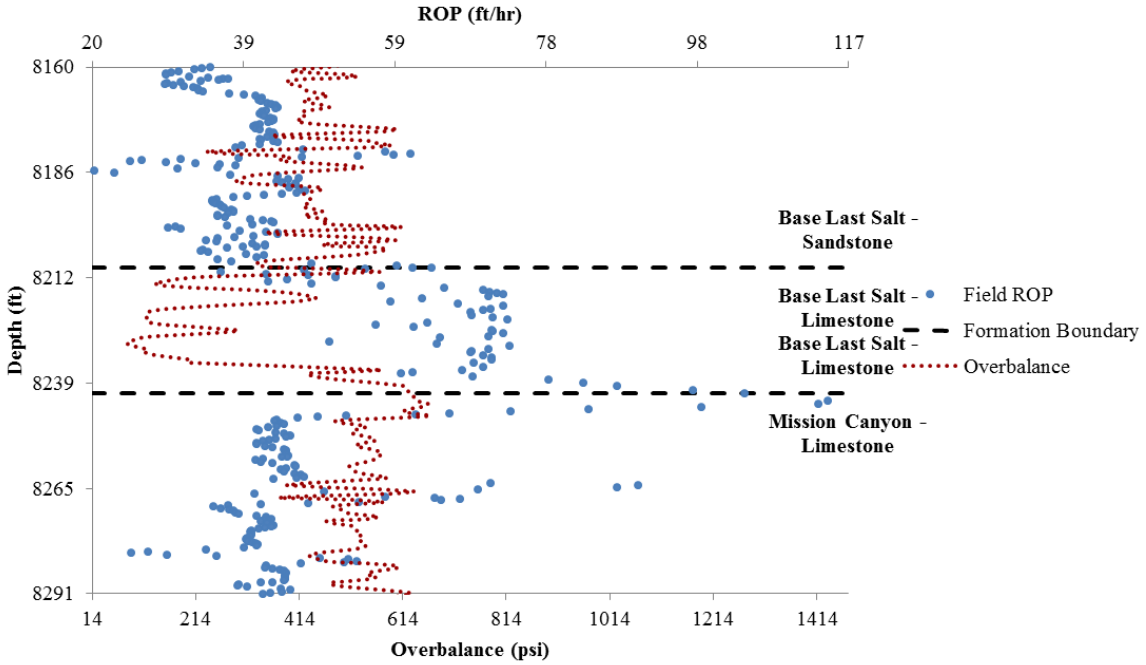

Figure 4.24: Overbalance analysis on Base Last Salt Limestone formation.

In the figure above, there is a significant increase in ROP when transitioning from the Base Last Salt Sandstone formation to the Base Last Salt Limestone formation. A corresponding decrease in differential pressure at the bit happens at the same lithology boundary, implying that Base Last Salt Limestone formation is likely overpressured. Figure 4.24 represents a drilling break when the drill bit penetrates an overpressured formation, a phenomenon commonly experienced in the field.

4.2.5 Saving Plots

Any of the plots worked in association with the Plotter form can be stored in the spreadsheet by clicking on the "Save Plot" button on the top right-hand corner of the Plotter form:

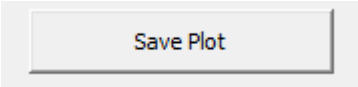

Figure 4.25: Save plot command button.

The plots saved with the "Save Plot" button above can be exported to picture files for future analysis (described in Section 4.3).

4.2.6 Applying ROP Models

The bottom right-hand part of the Plotter form is dedicated to the application and comparison of ROP models:

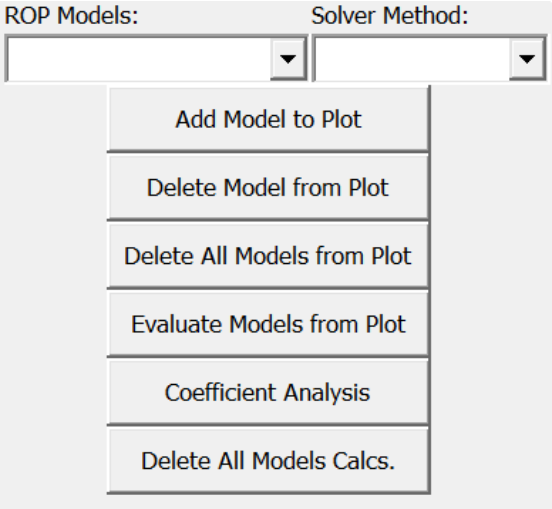

Figure 4.26: Command buttons for application and comparison of ROP models.

The ROP models box provides a list of the six ROP models in ROPPlotter: Bingham, Bourgoyne & Young, Hareland Drag Bit, Hareland Roller Bit, Motahhari PDC Bit, and Winters-Warren-Onyia Roller Bit. One of the biggest benefits of utilizing Excel VBA coding in this software is being able to execute Solver in loop to evaluate model coefficients. Since Solver can only be used for one cell at a time, automation of this process

saves a considerable amount of human time and effort. The method by which model coefficients are calculated is selected from the Solver method box.

4.2.6.1 Solver Method

The Solver method box offers the choice between Minimum Formation Error and Single Point ROP Matching with different resolutions:

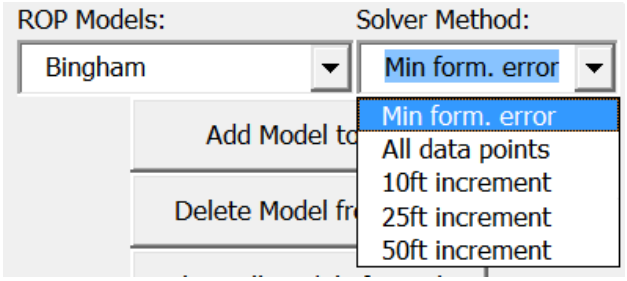

Figure 4.27: List of Solver methods to calculate ROP model coefficients.

Once computations start, ROPPlotter allows the option to cancel model calculations if the estimated time left is excessive:

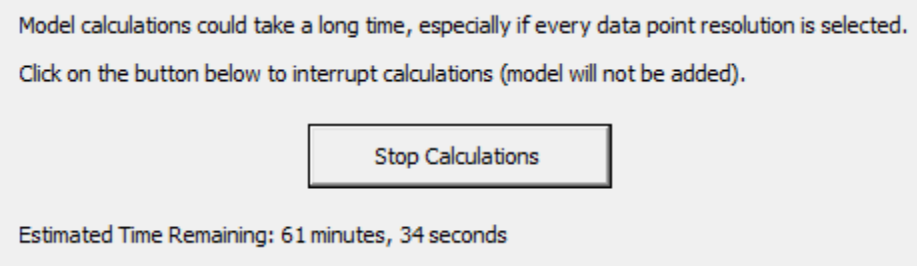

Figure 4.28: Bingham model coefficient calculations performed with the Single Point ROP Matching method at every data point.

As seen in Figure 4.28, it would take over an hour to compute model coefficients for the Bingham model in every single data point in this dataset (7,404 rows of data). With the Minimum Formation Error method, the estimated calculation time is reduced to less than

thirty seconds. The "Stop Calculations" button interrupts model calculations in case the user decides the computational expense is too much.

4.2.6.2 Bingham (Bingham, 1964)

After selecting the Bingham model in the ROP models list box and the Minimum Formation Error Solver method, a click of the "Add Model to Plot" button (Fig. 4.26) will launch a model-specific userform inquiring for additional information to compute Bingham model coefficients:

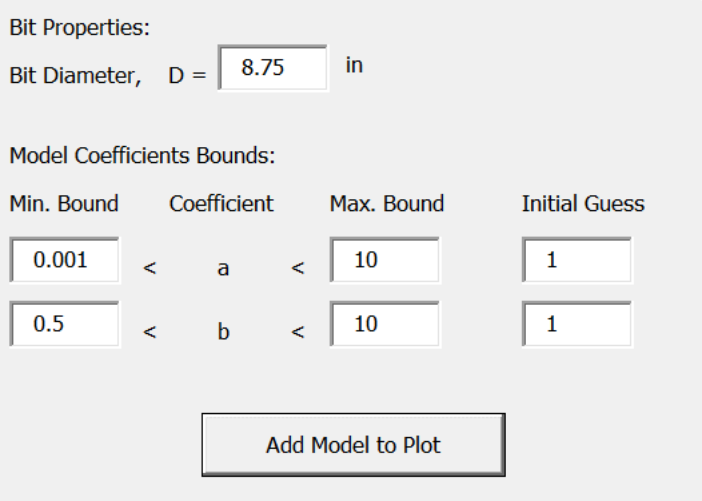

Figure 4.29: Bingham model form.

Simplest of all ROP models, Bingham only requires the bit diameter to complete its application. This value is stored and shared between forms for easier implementation of subsequent models. The form in Figure 4.29 allows for user-specified model coefficient bounds and coefficient initial guess. By selecting "Add Model to Plot" in the above picture, the Bingham model is displayed on the plot once model coefficients are calculated:

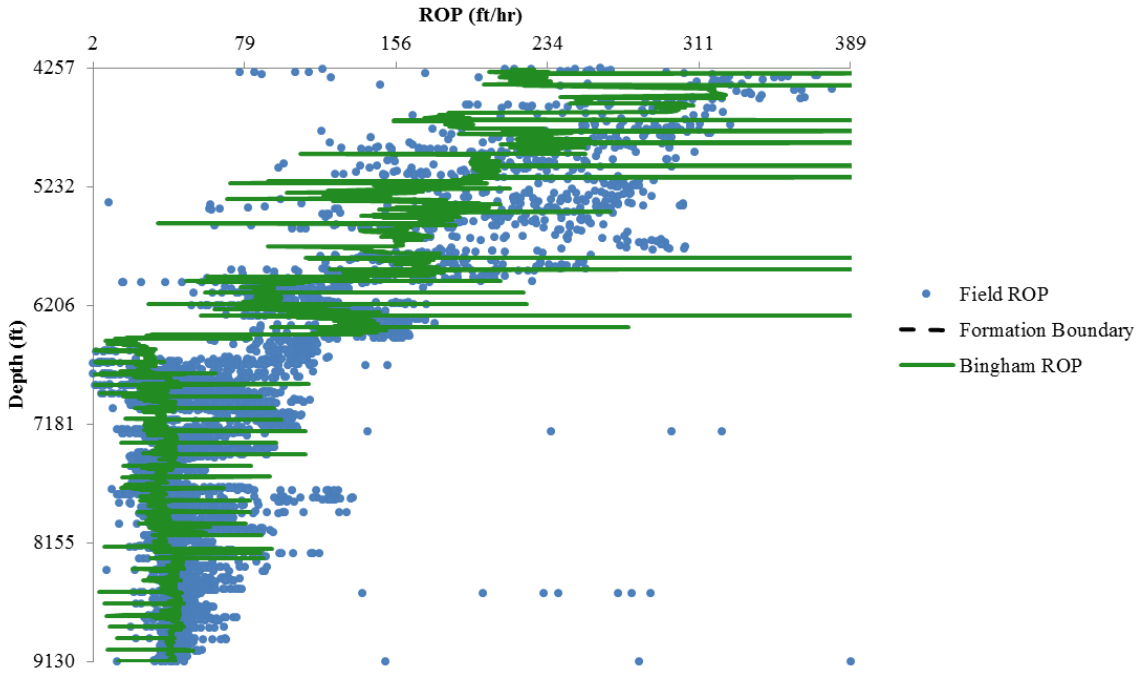

Figure 4.30: Bingham ROP and field ROP for the entire well. Model coefficient bounds and initial guess values from Figure 4.29.

Model calculations are stored in the program, so that if the "Delete Model from Plot" or the "Delete All Models from Plot" buttons (Fig. 4.26) are used to remove a model from the plot, it can be quickly re-added without the need to perform Solver calculations again. The “Delete All Models Calculations” button (Fig 4.26) deletes the saved model computations, a necessity when utilizing different parameters or model coefficient bounds values. By zooming in on formation boundaries, discontinuities are observed for the ROP predicted by the Bingham model:

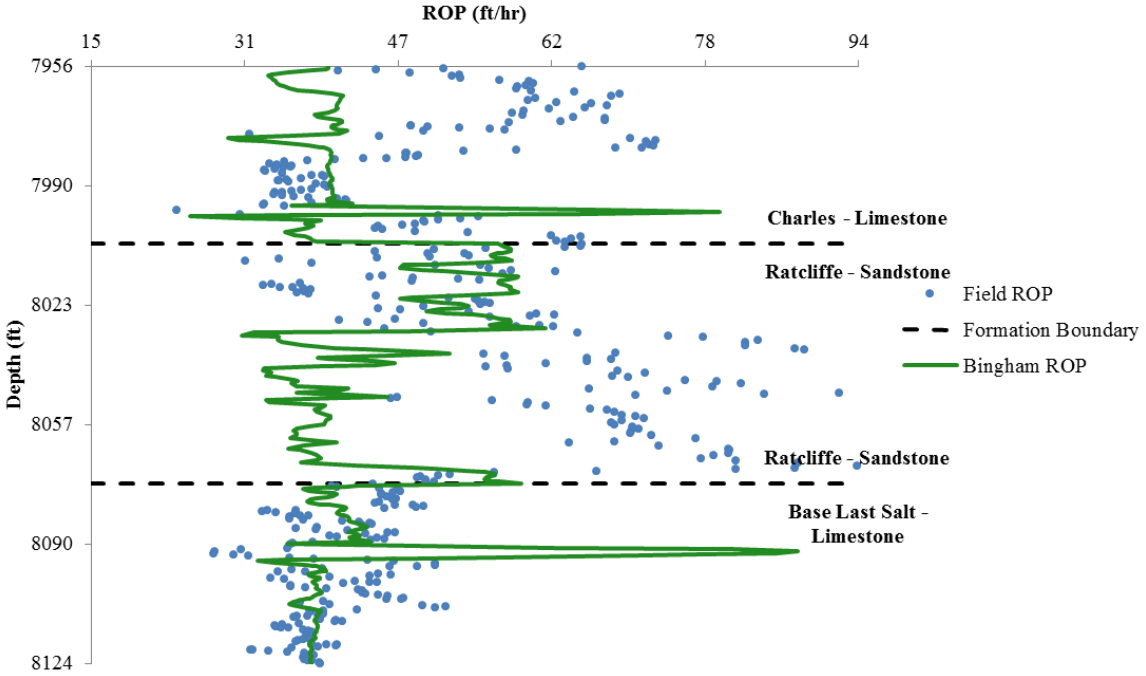

Figure 4.31: Bingham ROP and field ROP for the Ratcliffe Sandstone formation.

Discontinuities in model ROP across formation boundaries are expected, since a new set of model coefficients is calculated for each formation. Figure 4.31 shows that Bingham's model correctly adjusts to a higher ROP at the top of the Ratcliffe Sandstone formation. However, it stays fairly constant throughout most of that section, while the field ROP steadily increases. Bingham ROP matches up pretty well when transitioning from Ratcliffe Sandstone to Base Last Salt Limestone, as the field ROP decreases.

4.2.6.3 Bourgoyne & Young (Bourgoyne and Young, 1974)

Similar to the procedure to compute Bingham's ROP, Bourgoyne & Young's model is selected in the ROP models list box and a click of the "Add Model to Plot" button (Fig. 4.26) shows the following form:

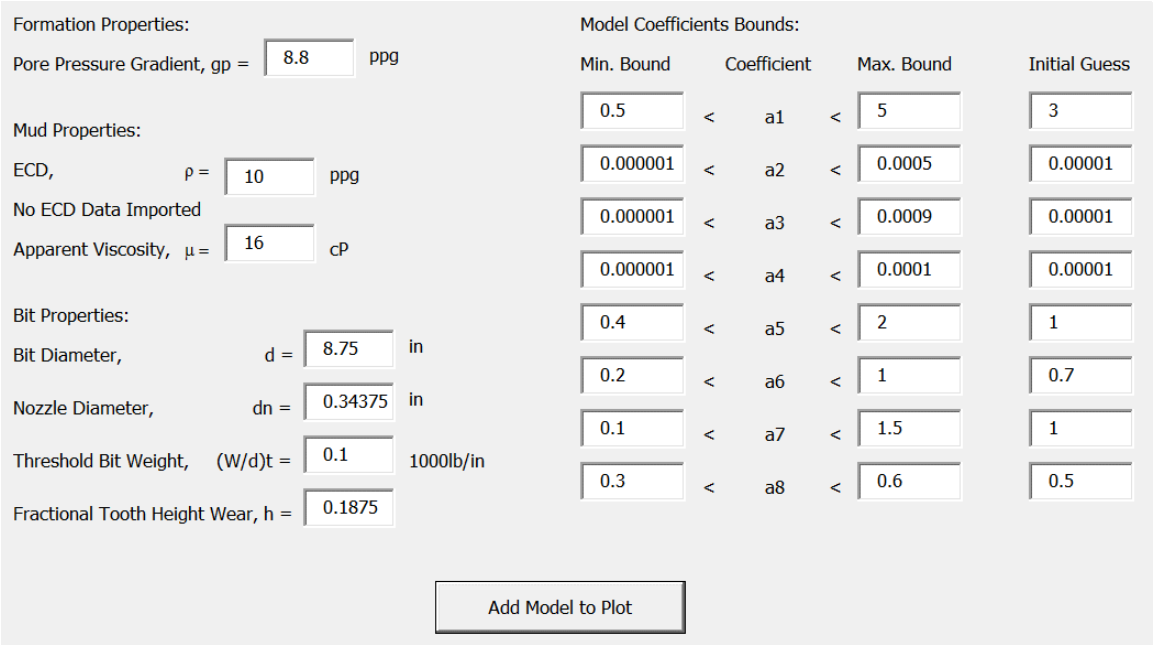

Figure 4.32: Formation, mud, and bit properties needed for application of the Bourgoyne & Young model.

Since Bourgoyne & Young's model is much more extensive than Bingham's, more information is needed in order to compute model coefficients. Note that a label under ECD announces “No ECD Data Imported”, indicating that no point-by-point ECD data heading was designated when importing data with the data headings form (Fig. 4.2). Minimum bound, maximum bound, and initial guess for each of the eight model coefficients are inputs in Fig. 4.32. With the above form filled out, the "Add Model to Plot" button will start coefficient calculations and include this model in the plot:

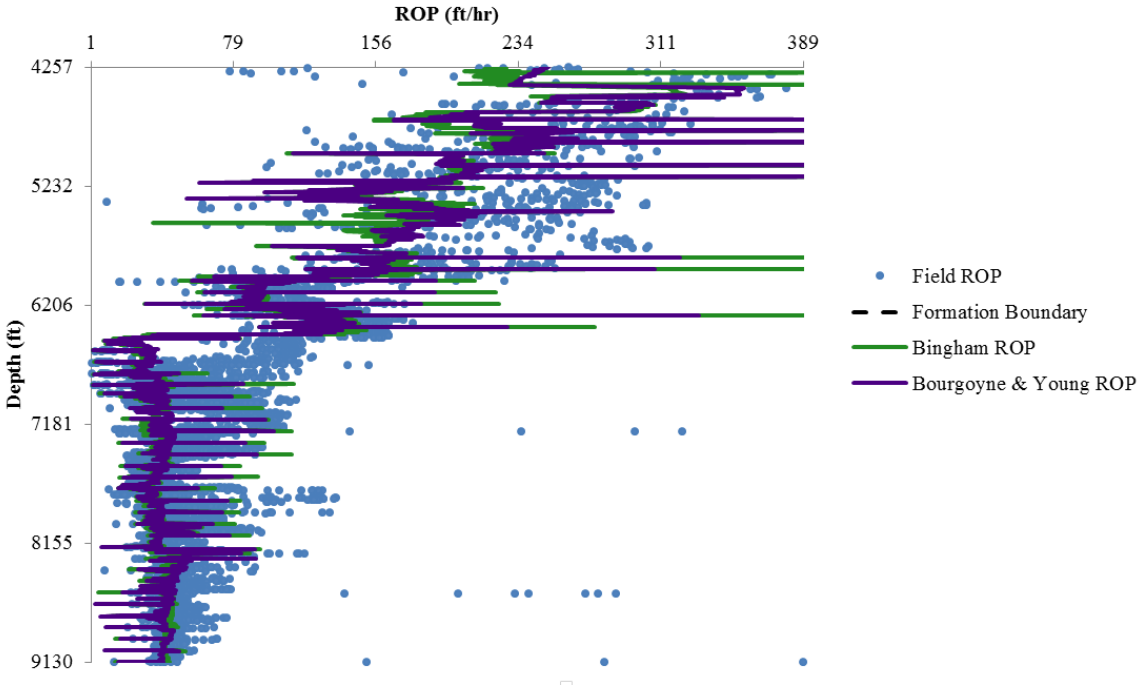

Figure 4.33: Bingham ROP, Bourgoyne & Young ROP and field ROP for Marathon dataset. Model coefficient bounds and initial guess values for B&Y model from Figure 4.32.

When two or more models are displayed on the plot, a view of the entire well becomes cluttered. Meaningful results are obtained when zooming-in on formation boundaries:

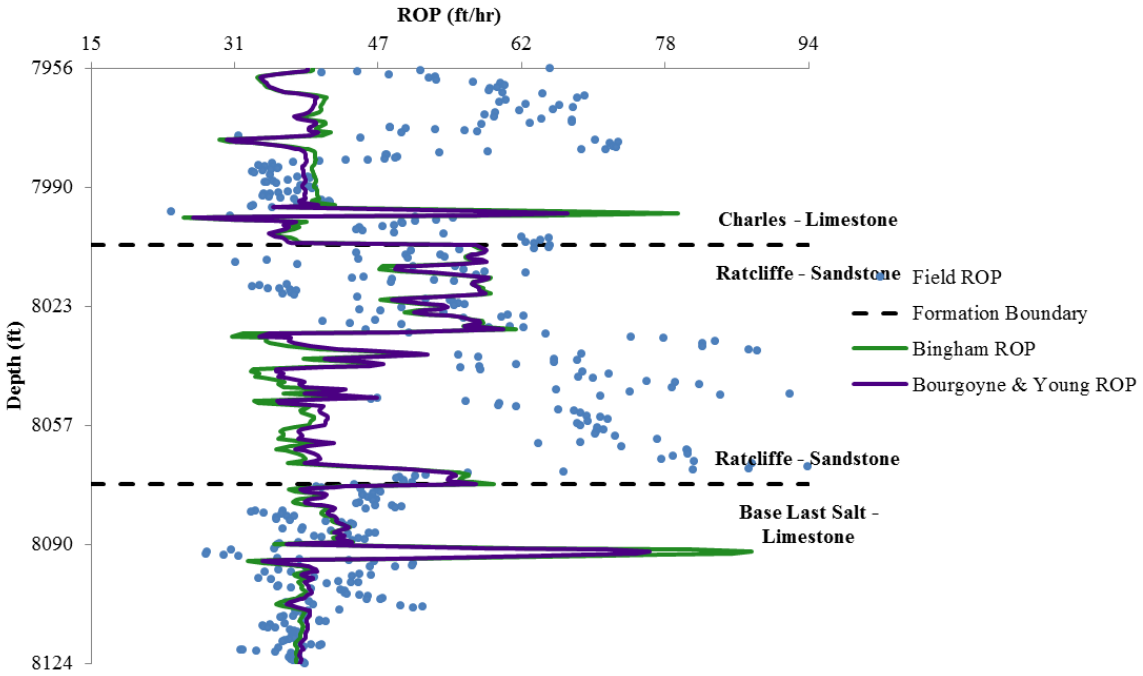

Figure 4.34: Bingham ROP, Bourgoyne & Young ROP and field ROP for the Ratcliffe Sandstone formation.

Figure 4.34 displays a lot of overlap between the two ROP models, even overshooting at the same data points. At the top of the Base Last Salt Limestone formation, in a well depth of around 8,090ft, both models highly deviate from their behavior for a small data interval while field ROP remains contained. This suggests that the Bingham and B&Y models are highly sensitive to the same drilling parameter, either WOB or RPM since those are the only two varying parameters considered in Bingham's formulation. Analyzing parsed data for the interval in question:

Table 4.1: Field data between 8089.75ft to 8095.25ft in the Marathon dataset.

Depth (ft)	ROP (ft/hr)	WOB (klbs)	RPM
8089.75	37.8442051	39.25952386	39.8308
8090	35.78	36.5193228	40
8090.25	35.5174525	30.54729322	40.2514
8091.5	35.1679052	93.23310968	41.0837
8092	30.39	156.7874168	41
8092.5	27.7353195	183.0196252	41.0192
8093	27.6259857	173.3168607	41.1335
8093.5	29.5998929	140.3830952	41.2658
8093.75	31.2236537	119.1745782	41.3147
8094.25	35.4559735	75.2142584	41.3295
8094.5	37.949006	55.63844851	41.2762
8095	43.4	29.2355112	41
8095.25	46.1881486	24.96645105	40.7656

Table 4.1 shows a substantial rise in WOB values from 8091.5ft to 8094.5ft. Meanwhile, field ROP and RPM do not deviate much from their mean values in the same interval, confirming that the behavior of both Bingham and B&Y models is mainly governed by WOB values in this example. The rapid increase in WOB from 8091.5ft to 8094.5ft might have been caused by sensor malfunction. When importing data, such points could have been removed by employing data flagging with the standard deviation criterion for that formation. Without those data points, both model fits would likely improve.

4.2.6.4 WWO Roller Bit (Winters *et al.*, 1987)

Implementation of the Winters-Warren-Onyia Roller Bit model requires the input of rock compressive strength and ductility for each formation. The model userform addresses this necessity:

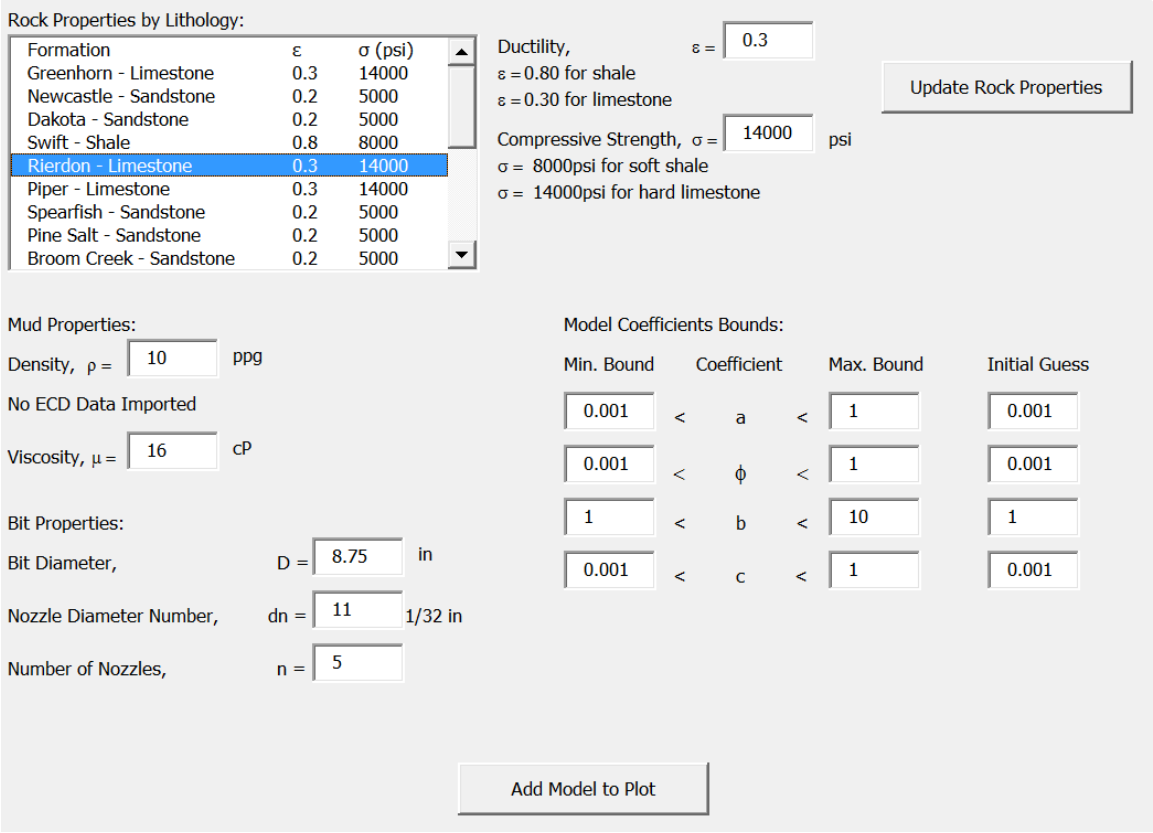

Figure 4.35: Required parameters in WWO Roller Bit form.

The list box displayed on the top left-hand corner of Figure 4.35 is automatically populated with all lithologies in the dataset and pre-determined ductility and compressive strength values for each formation, based on the rock type (shale, sandstone, or limestone). Those values can be easily changed for any formation by selecting it in the formations box, entering new values on the ductility and compressive strength boxes, and clicking on the "Update Rock Properties" button:

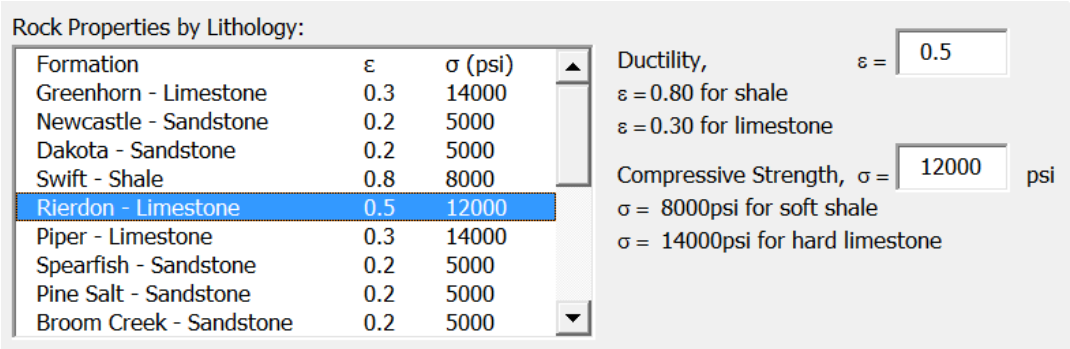

Figure 4.36: Rierdon Limestone rock properties updated to a ductility of 0.5 (previously 0.3) and compressive strength of 12,000psi (previously 14,000psi).

After entering the appropriate ductility and compressive strength for each formation (or leaving them as the default values) and the other required properties in Fig. 4.35, clicking on the "Add Model to Plot" button will display the WWO Roller Bit model on the plot:

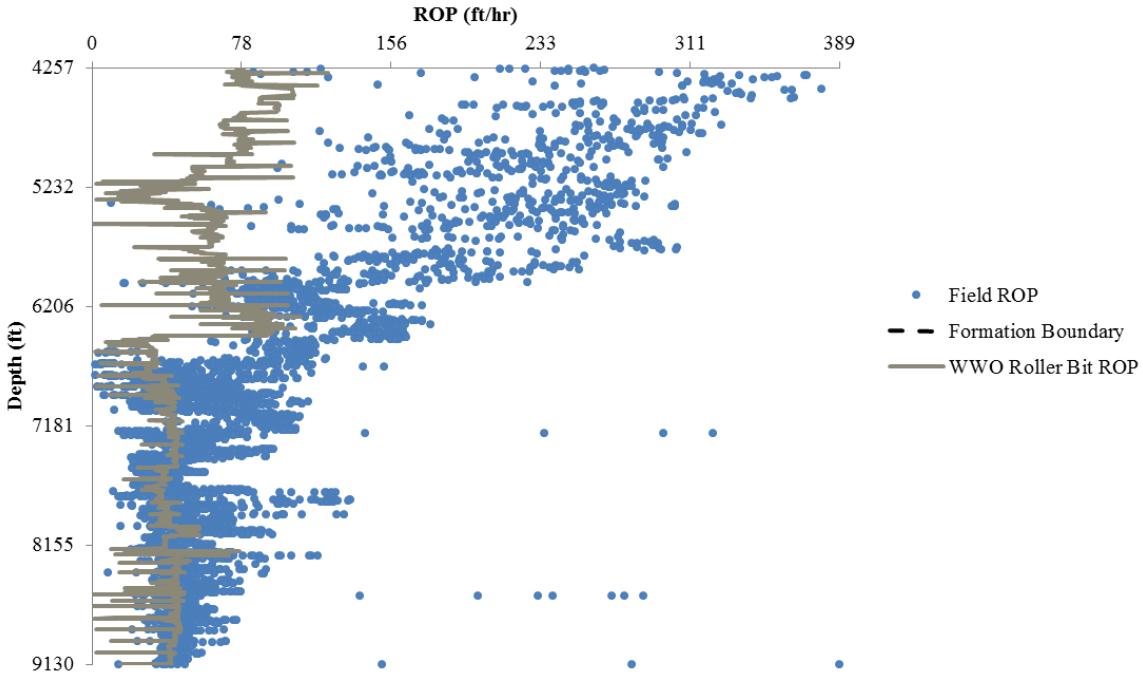

Figure 4.37: WWO Roller Bit ROP and field ROP for Marathon dataset. Model coefficient bounds and initial guess values from Figure 4.35.

ROP is grossly underestimated by the model in the shallower sections of the well with the selected coefficient bounds (Fig 4.35). The WWO Roller Bit model is more accurate at depth. The model's overall average percent error is only 29.48%, as more data points were recorded with the slower ROP experienced in the deeper segments of the well. However, application of this roller bit model to a well drilled with a drag bit is not appropriate.

4.2.6.5 Hareland Drag Bit (Hareland and Rampersad, 1994)

Multiple bit geometry parameters and model coefficient bounds required for calculation of coefficients for the Hareland Drag Bit model are presented below:

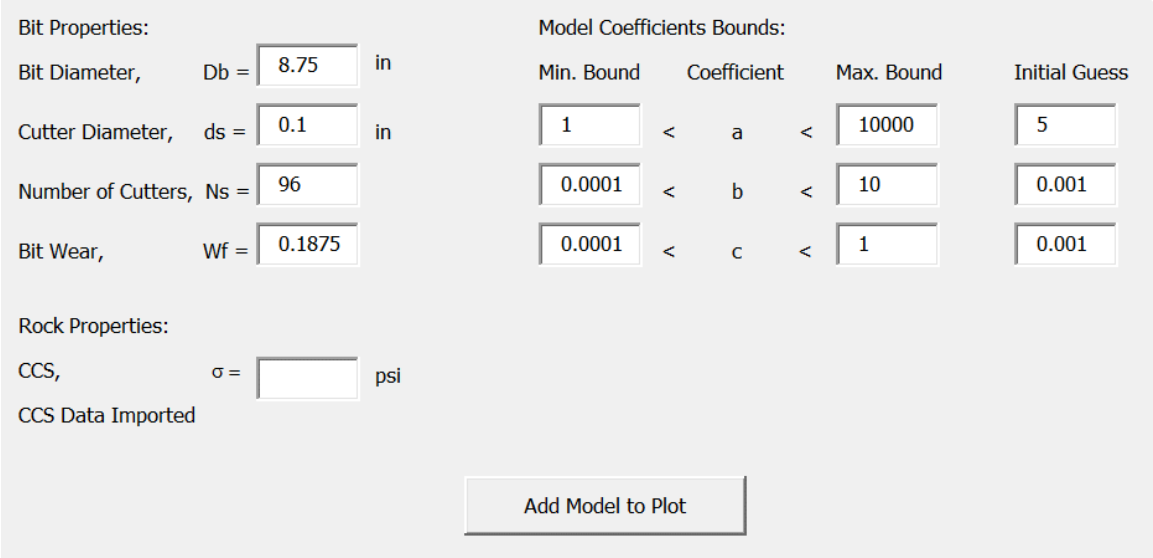

Figure 4.38: Hareland Drag Bit model userform.

Contrary to ECD, a CCS data heading was selected when importing data earlier in this chapter. The "CCS Data Imported" label under the CCS parameter in Fig. 4.38 reflects that selection, and point-by-point data is utilized in model calculations instead of a constant value. After Solver calculations of model coefficients, Hareland Drag Bit ROP is added to the plot:

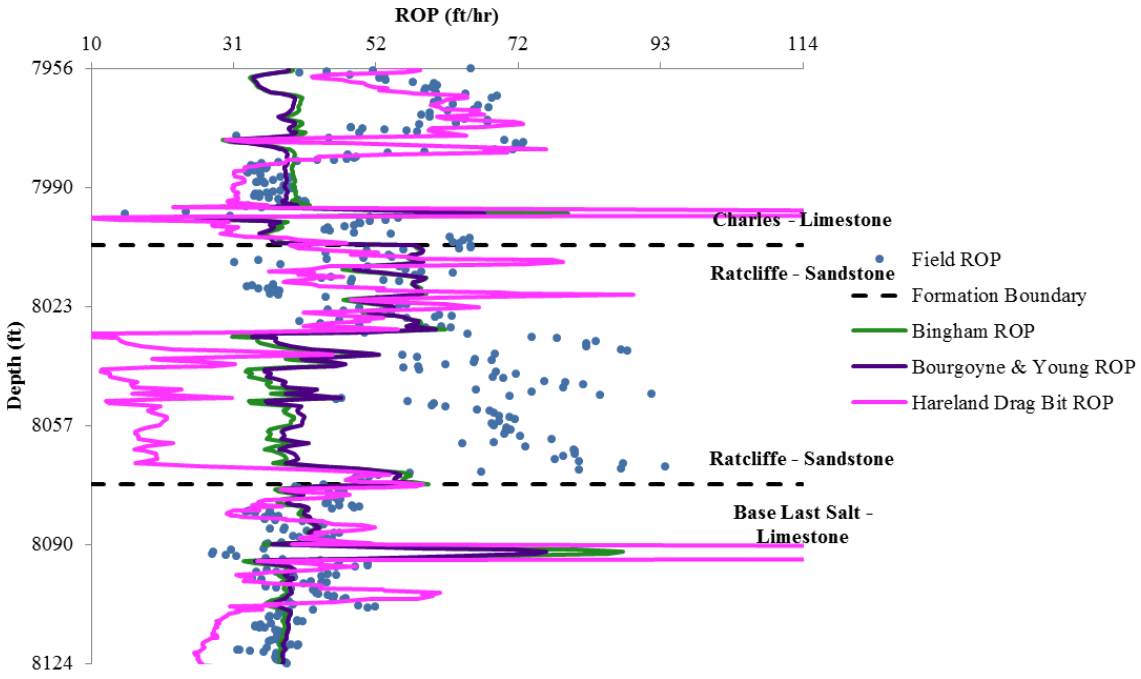

Figure 4.39: Bingham ROP, Bourgoyne & Young ROP, Hareland Drag Bit ROP and field ROP for the Ratcliffe Sandstone formation. Model coefficient bounds and initial guess values for Hareland Drag Bit model from Figure 4.38.

Hareland Drag Bit ROP varies more than both Bingham ROP and B&Y ROP in Fig. 4.39. The Hareland Drag bit model produces a much better fit to field data at the bottom of the Charles Limestone formation, but overly underestimates ROP for the second half of the Ratcliff Sandstone formation. Similar to Bingham and B&Y, Hareland Drag Bit ROP overshoots around 8,090ft well depth.

With three ROP models displayed on the plot, even a zoomed-in formation view becomes congested. Since the model calculations are stored in ROPPlotter, the command buttons in Fig. 4.26 ("Add Model to Plot", "Delete Model from Plot", and "Delete All Models from Plot") can be used to alternate between the models being compared.

4.2.6.6 Hareland Roller Bit (Hareland *et al.*, 2010)

The Hareland Roller Bit model form contains many bit properties, and bounds for the three model coefficients:

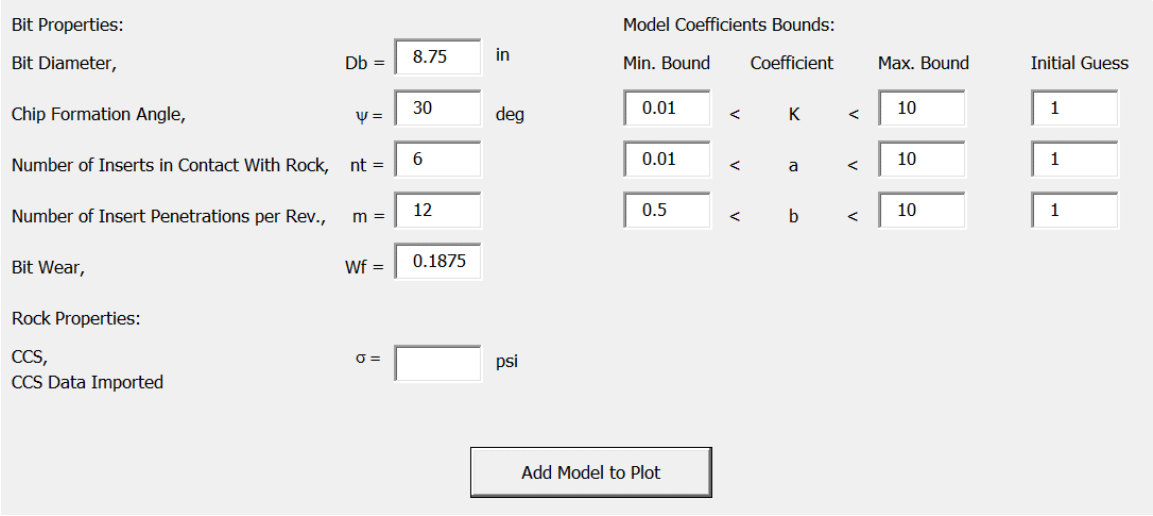

Figure 4.40: Parameters for the Hareland Roller Bit model.

Some of the parameters in Fig 4.40 are specific to roller cone bits. Since the example well was drilled with a drag bit, values for these parameters were selected based on an average roller bit. A minimum bound of 0.5 is imposed on the *b* coefficient, the exponent of the WOB term just as in Bingham's model. Zooming-in on the Pine Salt Sandstone formation following model coefficient calculations:

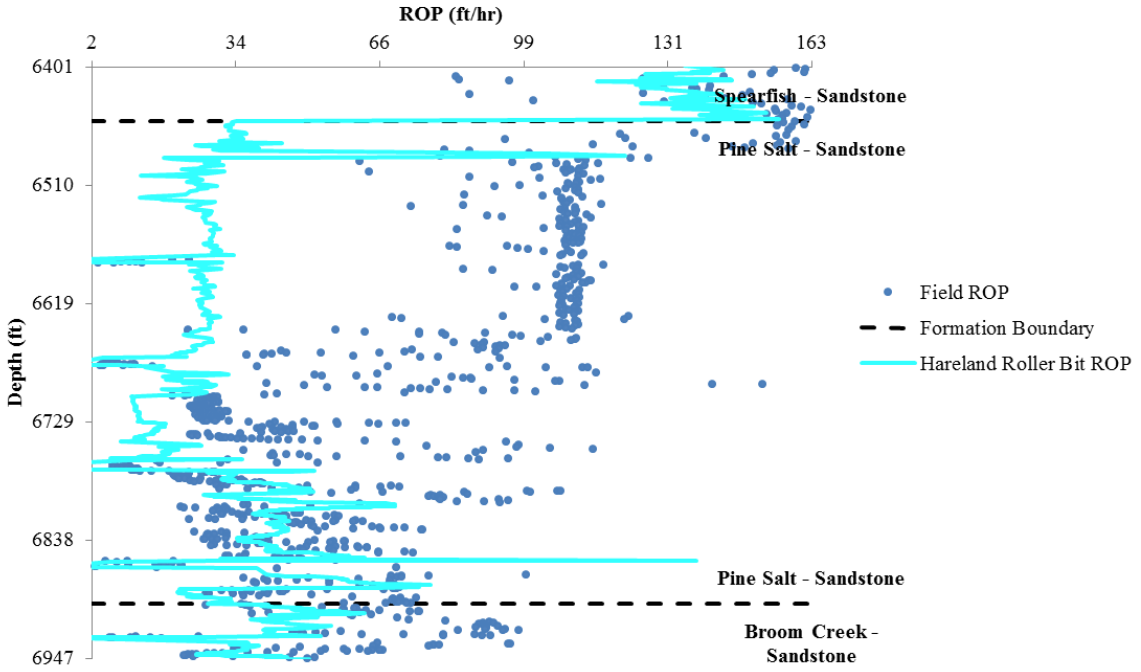

Figure 4.41: Hareland Roller Bit ROP and field ROP in the Pine Salt Sandstone formation. Model coefficient bounds and initial guess values from Figure 4.40.

At the top of the Pine Salt Sandstone, field ROP is much higher than predicted by the Hareland Roller Bit model. Otherwise, the model fits field data accurately. The model ROP decreases drastically across the Spearfish/Pine Salt formations boundary due to a new set of model coefficients.

4.2.6.7 Motahhari PDC Bit (Motahhari *et al.*, 2010)

Lastly, the Motahhari PDC Bit model is added to the plot by following the same procedure used for other models:

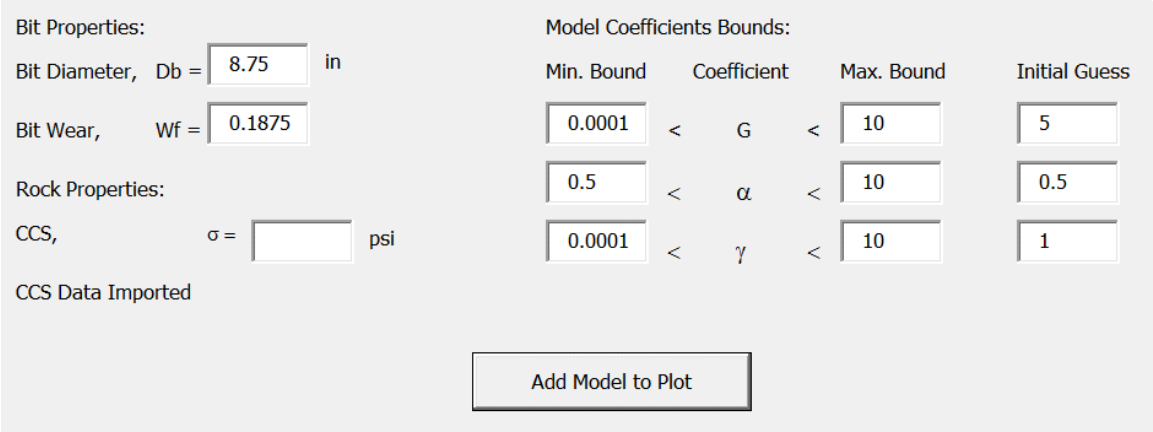

Figure 4.42: Input properties for the Motahhari PDC Bit model.

Comparing Motahhari PDC Bit and three other ROP models on the Charles Sandstone formation:

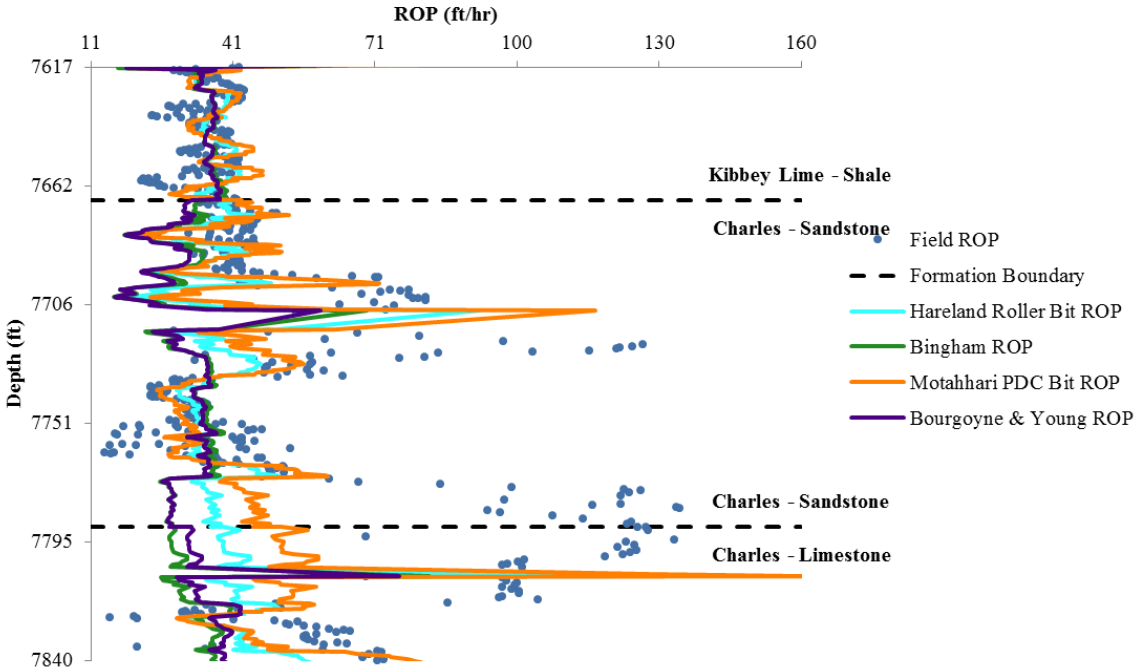

Figure 4.43: Hareland Roller Bit ROP, Bingham ROP, Motahhari PDC Bit ROP, Bourgoyne & Young ROP and field ROP for the Charles Sandstone formation. Model coefficient bounds and initial guess values for Motahhari's model from Figure 4.42.

In Figure 4.43, all four ROP models predict an increase in ROP around 7706ft, which actually happens a few feet later. A plausible explanation is that a change in WOB at the surface is instantaneously sensed by the ROP models, and only experienced downhole after a lag time. As previously discussed, having four models on the plot makes it hard to comprehend the models' behavior fully. Comparing two models at a time is more appropriate:

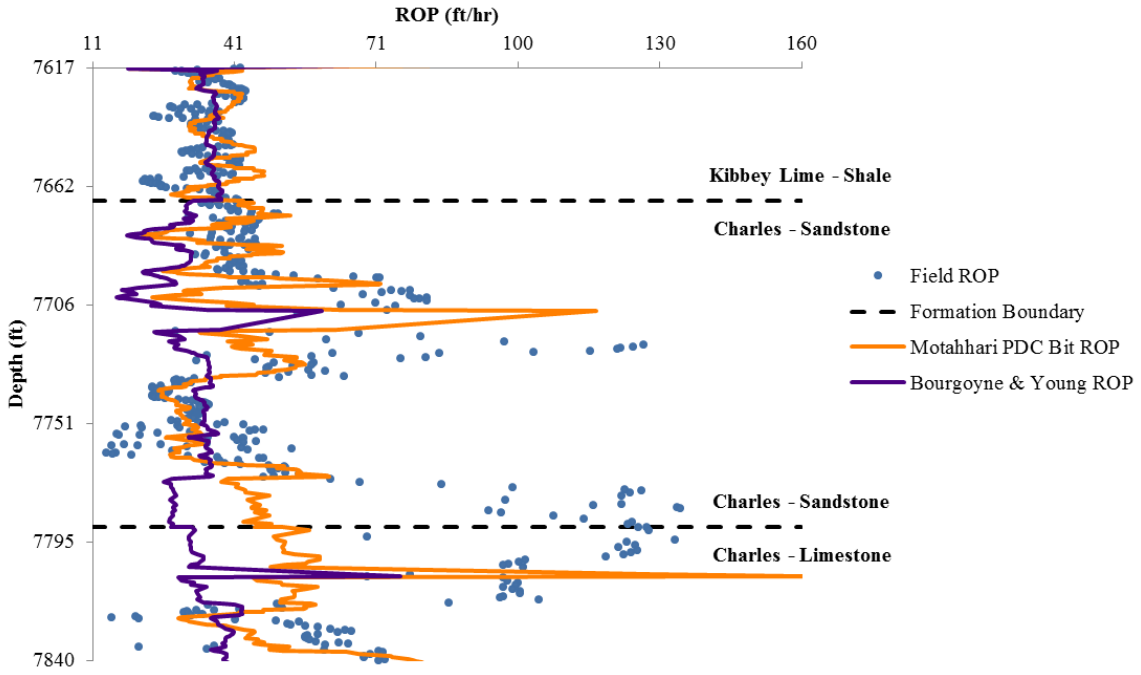

Figure 4.44: Bourgoyne & Young ROP, Motahhari PDC Bit ROP and field ROP for the Charles Sandstone formation.

The Motahhari PDC Bit model matches field data well throughout Charles Sandstone formation. Conversely, Bourgoyne & Young ROP underestimates field ROP in much of this section, staying more or less constant in the whole formation.

4.2.7 Comparing ROP Models and Coefficients by Lithology

While visual representation and comparison of ROP models is of great value, numerically quantifying model performance and analyzing model coefficients enhances understanding of each model. The last two command buttons in Figure 4.26 offer those capabilities:

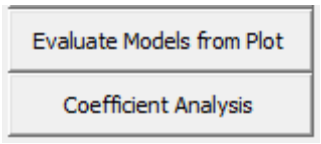

Figure 4.45: Evaluate models and coefficient analysis buttons in the Plotter form.

4.2.7.1 Model Performance

Using the concept of average percent error, presented in Equation 3.1, the "Evaluate Models from Plot" button launches a table indicating the best ROP model for each formation and the best overall model for the dataset:

Formation Name	Bingham	Bourgoyne & Young	Hareland Drag Bit	Hareland Roller Bit	Motahhari PDC Bit	WWO Roller Bit	Best Model in Formation
Greenhorn - Limestone	44.64%	38.31%	96.33%	43.90%	44.81%	64.29%	Bourgoyne & Young
Newcastle - Sandstone	20.11%	18.65%	66.94%	24.92%	37.01%	65.82%	Bourgoyne & Young
Dakota - Sandstone	29.05%	26.44%	68.04%	31.60%	48.16%	65.47%	Bourgoyne & Young
Swift - Shale	44.88%	44.78%	60.08%	37.64%	45.54%	80.83%	Hareland Roller Bit
Rierdon - Limestone	29.44%	27.75%	54.03%	24.94%	31.60%	63.58%	Hareland Roller Bit
Piper - Limestone	28.42%	27.43%	96.81%	33.92%	55.17%	39.09%	Bourgoyne & Young
Spearfish - Sandstone	27.00%	26.60%	81.62%	25.59%	28.03%	33.04%	Hareland Roller Bit
Pine Salt - Sandstone	51.10%	48.74%	78.59%	60.29%	67.18%	48.44%	WWO Roller Bit
Broom Creek - Sandstone	43.97%	43.06%	61.36%	36.64%	35.95%	39.96%	Motahhari PDC Bit
Tyler - Sandstone	37.30%	34.26%	76.16%	29.74%	44.56%	33.29%	Hareland Roller Bit
Kibbey Lime - Limestone	27.96%	25.37%	55.08%	38.66%	51.55%	18.31%	WWO Roller Bit
Kibbey Lime - Shale	16.68%	15.68%	33.20%	17.59%	20.19%	14.46%	WWO Roller Bit
Charles - Sandstone	37.22%	37.85%	41.80%	30.45%	28.86%	33.64%	Motahhari PDC Bit
Charles - Limestone	28.64%	28.14%	35.31%	23.70%	23.02%	26.93%	Motahhari PDC Bit
Ratcliffe - Sandstone	33.84%	32.16%	48.86%	33.01%	33.95%	24.90%	WWO Roller Bit
Base Last Salt - Limestone	11.83%	11.45%	14.43%	8.83%	9.70%	10.46%	Hareland Roller Bit
Base Last Salt - Sandstone	16.03%	15.37%	58.23%	16.94%	23.15%	12.22%	WWO Roller Bit
Base Last Salt - Limestone	28.66%	25.51%	48.39%	25.27%	22.69%	40.55%	Motahhari PDC Bit
Mission Canyon - Limestone	14.39%	16.80%	16.80%	12.03%	11.54%	13.92%	Motahhari PDC Bit
Lodgepole - Limestone	8.15%	7.60%	11.36%	8.30%	8.99%	7.20%	WWO Roller Bit
Entire Dataset	27.42%	26.80%	48.02%	26.19%	30.85%	29.48%	Hareland Roller Bit

Figure 4.46: Comparison of model performance formation-by-formation in the Marathon dataset.

The average percent error is measured in each formation and overall for each ROP model. Formation-by-formation error analysis is useful to distinguish which model works best for a certain type of rock. It is important to note that, in this dataset, the overall error is biased towards error in the deeper formations, since the ROP is slower and more data points are taken at depth. In Chapter 3, the shallowest formation, Greenhorn Limestone, contained 50 data points while the deepest formation, Lodgepole Limestone, contained 720 data points.

From Figure 4.46, Bingham's model correlates fairly well with ROP field data (27.42% overall error), even though it is not the best model for any one formation. Bourgoyne & Young, the most complete of all models, has the second best performance overall (26.80% error). Hareland Roller Bit has the best overall model performance for this dataset (26.19% error), but should be regarded for illustration purposes only, as this well was drilled with a PDC bit. While no deterministic conclusions can be made from a single well dataset, analyzing ROP models with data from several wells in the same field makes it possible to elect which model works best for a specific application.

4.2.7.2 Coefficient Analysis

In order to easily compare model coefficients and see how they change by lithology, clicking the "Coefficient Analysis" button (Fig. 4.45) unveils a dynamic model coefficients table:

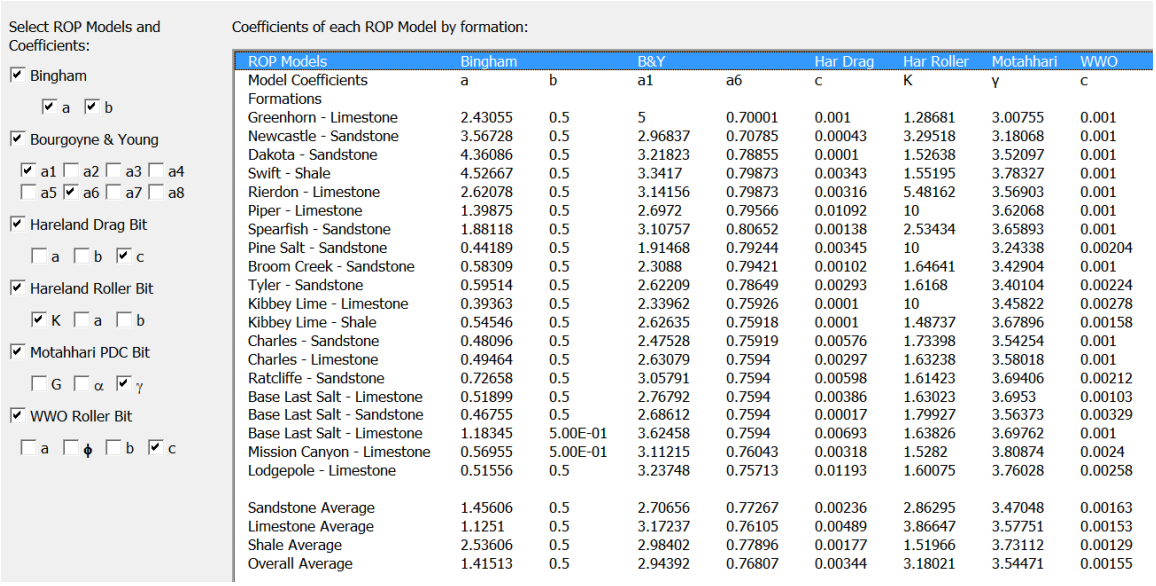

ROP Models	Bingham		B&Y		Har Drag	Har Roller	Motahhari	WWO
Model Coefficients	a	b	a1	a6	c	K	γ	c
Formations								
Greenhorn - Limestone	2.43055	0.5	5	0.70001	0.001	1.28681	3.00755	0.001
Newcastle - Sandstone	3.56728	0.5	2.96837	0.70785	0.00043	3.29518	3.18068	0.001
Dakota - Sandstone	4.36086	0.5	3.21823	0.78855	0.0001	1.52638	3.52097	0.001
Swift - Shale	4.52667	0.5	3.3417	0.79873	0.00343	1.55195	3.78327	0.001
Rierdon - Limestone	2.62078	0.5	3.14156	0.79873	0.00316	5.48162	3.56903	0.001
Piper - Limestone	1.39875	0.5	2.6972	0.79566	0.01092	10	3.62068	0.001
Spearfish - Sandstone	1.88118	0.5	3.10757	0.80652	0.00138	2.53434	3.65893	0.001
Pine Salt - Sandstone	0.44189	0.5	1.91468	0.79244	0.00345	10	3.24338	0.00204
Broom Creek - Sandstone	0.58309	0.5	2.3088	0.79421	0.00102	1.64641	3.42904	0.001
Tyler - Sandstone	0.59514	0.5	2.62209	0.78649	0.00293	1.6168	3.40104	0.00224
Kibbey Lime - Limestone	0.39363	0.5	2.33962	0.75926	0.0001	10	3.45822	0.00278
Kibbey Lime - Shale	0.54546	0.5	2.62635	0.75918	0.0001	1.48737	3.67896	0.00158
Charles - Sandstone	0.48096	0.5	2.47528	0.75919	0.00576	1.73398	3.54254	0.001
Charles - Limestone	0.49464	0.5	2.63079	0.7594	0.00297	1.63238	3.58018	0.001
Ratcliffe - Sandstone	0.72658	0.5	3.05791	0.7594	0.00598	1.61423	3.69406	0.00212
Base Last Salt - Limestone	0.51899	0.5	2.76792	0.7594	0.00386	1.63023	3.6953	0.00103
Base Last Salt - Sandstone	0.46755	0.5	2.68612	0.7594	0.00017	1.79927	3.56373	0.00329
Base Last Salt - Limestone	1.18345	5.00E-01	3.62458	0.7594	0.00693	1.63826	3.69762	0.001
Mission Canyon - Limestone	0.56955	5.00E-01	3.11215	0.76043	0.00318	1.5282	3.80874	0.0024
Lodgepole - Limestone	0.51556	0.5	3.23748	0.75713	0.01193	1.60075	3.76028	0.00258
Sandstone Average	1.45606	0.5	2.70656	0.77267	0.00236	2.86295	3.47048	0.00163
Limestone Average	1.1251	0.5	3.17237	0.76105	0.00489	3.86647	3.57751	0.00153
Shale Average	2.53606	0.5	2.98402	0.77896	0.00177	1.51966	3.73112	0.00129
Overall Average	1.41513	0.5	2.94392	0.76807	0.00344	3.18021	3.54471	0.00155

Figure 4.47: Coefficients table with select model coefficients from all six ROP models.

Checkboxes on the left side of the table in Fig. 4.47 permit selection of the model coefficients to be displayed. Due to space constraints, this flexibility is essential. The average value of model coefficients for each rock type is shown at the bottom of table, offering valuable information to determine model behavior in different lithologies.

4.3 Exporting Plots

By clicking on the "Save Plot" button, presented in Section 4.2.5, the desired plot is stored in the “Plots” worksheet of ROPPlotter. This worksheet contains three command buttons:

Figure 4.48: Command buttons in Plots worksheet.

The "Launch Plotter" button is used to launch the Plotter form, the main frame of work discussed earlier. Selecting the "Delete All Plots" option will discard the stored plots, while the "Export All Plots" option will launch a new form:

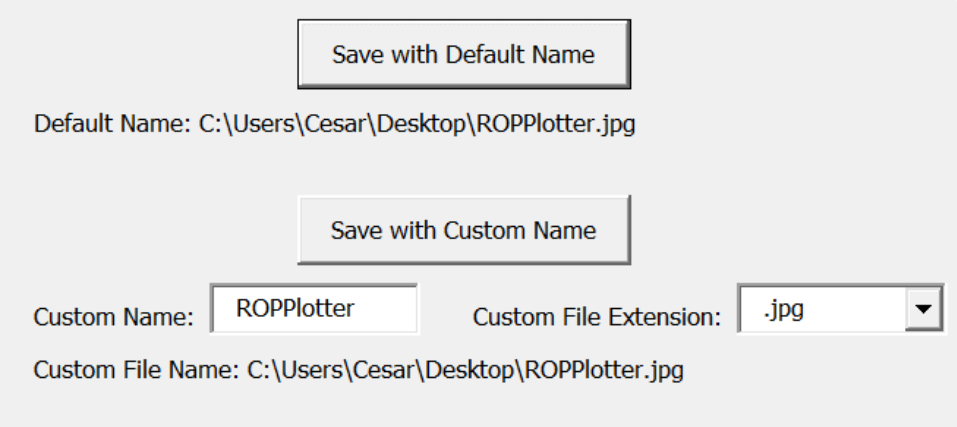

Figure 4.49: Export plots form.

Names and different extensions for the picture files can be chosen in the form in Fig 4.49. By clicking on either "Save with Default Name" or "Save with Custom Name" buttons, all the plots in the Plots worksheet are saved in the same folder as ROPPlotter. Picture files are extremely helpful for including these plots in reports and for future analysis.

4.4 Exporting Parsed Data

Data imported and employed in ROP model coefficients calculations (Section 4.1) is saved in the “Data” worksheet of ROPPlotter. This worksheet contains two command buttons that work similarly to the buttons in the Plots worksheet:

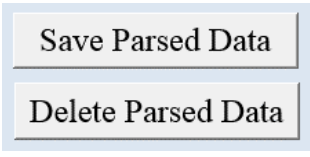

Figure 4.50: Command buttons in Data worksheet.

Parsed data refers to the data obtained from the original dataset that is actually useful for the applications of ROP models (data headings selected in Section 4.1.1). The "Delete Parsed Data" button erases all the data imported, whereas the "Save Parsed Data" button allows the user to export this valuable data to a new spreadsheet:

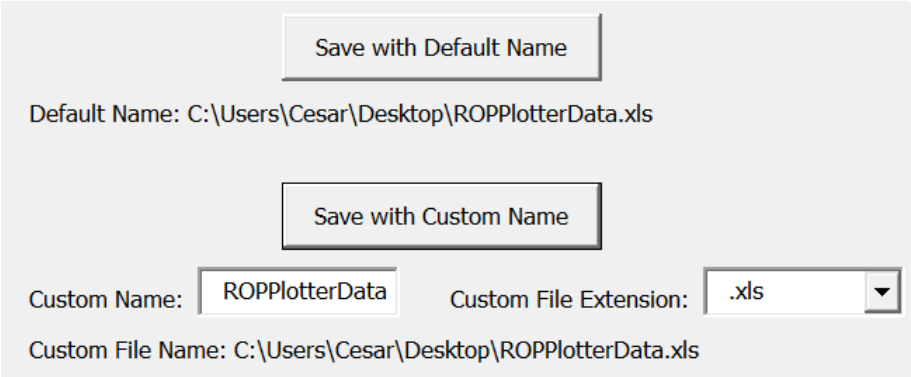

Figure 4.51: Save parsed data form.

Having the same features as the export plots form (Figure 4.49), the save parsed data form provides an easy method to store dissected data for subsequent investigation.

Chapter 5: ROPPlotter Case Studies

Chapter 5 illustrates two sample applications of the ROPPlotter software to drilling optimization. ROPPlotter is employed in testing which ROP model is appropriate for each example, calculating a set of model coefficients that are later used to produce ROP prediction tables. Marathon (Marathon Oil Corporation) and NOV (National Oilwell Varco) datasets are analyzed in two separate optimization studies.

5.1 Surface vs. Downhole Measurements with Marathon Dataset

Marathon's 4,873ft vertical section of a horizontal well dataset, previously utilized in Chapter 3 and Chapter 4, contains information about both surface and downhole drilling parameters. This study compares ROP model performance with these two collections of parameters, providing optimization tables computed with model coefficients that result in the best model fit to field ROP data.

5.1.1 Surface Measurements

For convenience, surface data headings selected in Figure 4.2 are shown again:

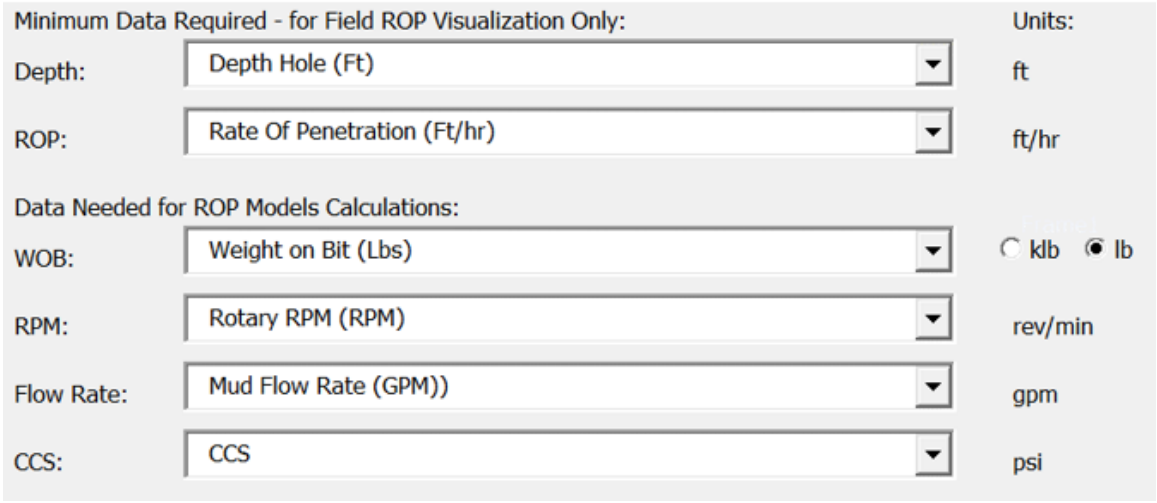

Figure 5.1: Surface data headings for Marathon dataset.

5.1.1.1 Data Statistics

Figure 5.2 displays ROP, WOB, RPM and flow rate statistics for the data headings in Fig 5.1, encompassing all data points of the Marathon dataset:

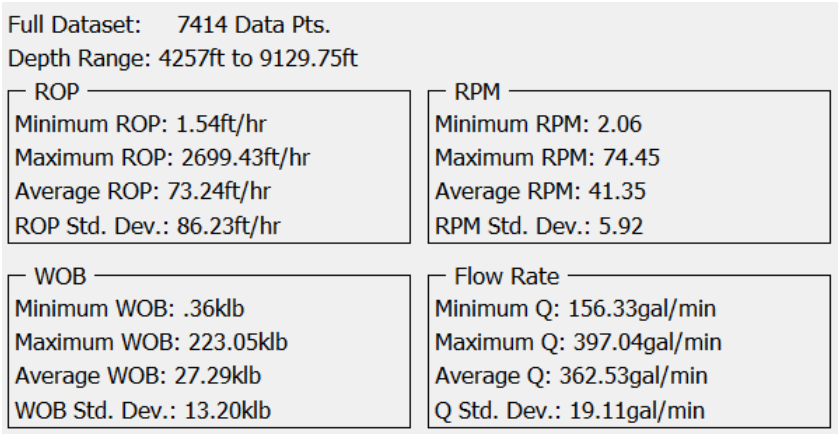

Figure 5.2: Statistics for surface parameters with the Marathon dataset.

In order to eliminate some of the erratic data behavior of this dataset, an in-depth formation-by-formation data flagging analysis with standard deviation criterion is performed.

5.1.1.2 Modified Data Statistics

The data filtering form presented in Chapter 4 facilitates detection and removal of data outliers. Points with ROP or WOB two standard deviations away from the mean or with RPM or flow rate five standard deviations above/below average were excluded. Data statistics for the modified dataset are displayed below:

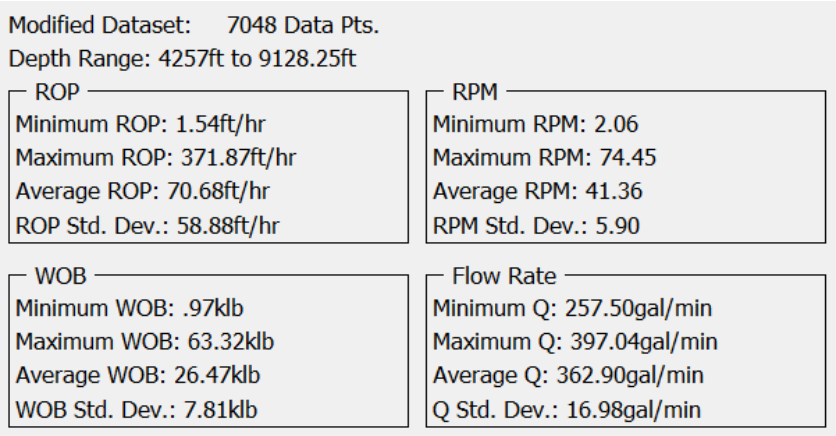

Figure 5.3: Modified data statistics for surface parameters with the Marathon dataset.

Comparing Figures 5.2 and 5.3, there is a noteworthy decrease in standard deviation for ROP and WOB parameters. The maximum ROP value is 371.87ft/hr (2,699.43ft/hr previously) and the maximum WOB is 63.32klb (223.05klb previously). Although 366 data points were removed from the original 7,414-point dataset, representation of the different segments of the well is not compromised, as 7,048 data points remain.

5.1.1.3 ROP Models Average Percent Error

Out of the six ROP models in ROPPlotter, two are roller cone bit models (WWO Roller Bit and Hareland Drag Bit) and will be left out of this analysis since the well was drilled with a drag bit. Model coefficient bounds are the same as in Chapter 4. Table 5.1 presents the average percent error for the remaining four models in each lithology and overall:

Table 5.1: Average percent error for Bingham, B&Y, Hareland Drag Bit, and Motahhari PDC Bit models with filtered Marathon surface data.

Rock Formation	Bingham Error	Bourgoyne & Young Error	Hareland Drag Error	Motahhari PDC Error
Greenhorn - Limestone	28.17%	28.06%	43.00%	34.00%
Newcastle - Sandstone	18.83%	16.71%	53.98%	36.09%
Dakota - Sandstone	21.34%	20.41%	58.41%	47.19%
Swift - Shale	27.63%	30.00%	45.55%	32.66%
Rierdon - Limestone	23.37%	21.99%	44.53%	29.16%
Piper - Limestone	18.20%	17.83%	45.59%	29.19%
Spearfish - Sandstone	16.55%	17.47%	27.58%	18.85%
Pine Salt - Sandstone	48.19%	46.58%	53.56%	56.27%
Broom Creek - Sandstone	40.10%	39.56%	39.22%	30.51%
Tyler - Sandstone	36.17%	33.42%	57.73%	40.81%
Kibbey Lime - Limestone	21.54%	19.74%	19.84%	34.42%
Kibbey Lime - Shale	13.05%	12.40%	23.13%	16.84%
Charles - Sandstone	34.19%	34.96%	36.39%	25.87%
Charles - Limestone	23.88%	23.93%	22.49%	19.28%
Ratcliffe - Sandstone	33.05%	31.35%	47.58%	32.89%
Base Last Salt - Limestone	11.39%	11.00%	14.32%	9.97%
Base Last Salt - Sandstone	11.70%	11.60%	20.10%	15.45%
Base Last Salt - Limestone	25.18%	22.47%	43.44%	18.80%
Mission Canyon - Limestone	12.39%	14.76%	13.11%	10.05%
Lodgepole - Limestone	7.33%	6.86%	9.87%	8.14%
Entire Dataset	**23.88%**	**23.68%**	**32.37%**	**25.85%**

Bourgoyne & Young's model has the best fit for surface parameters in this Marathon data example. There is major enhancement in the performance of all four ROP models when compared to results obtained with the Marathon dataset in Chapter 4 (Figure 4.46), filtered only for data points with ROP values greater than or equal to 400ft/hr and WOB greater than or equal to 200klb. Hareland Drag Bit is the most improved model, reducing its average overall error from 48.02% to 32.37%. If a single model is applied for optimization of the entire dataset, Bourgoyne & Young is the appropriate choice. In a formation-by-

formation optimization exercise, the table above can be consulted to determine which model works best for the formation being drilled. As an example, the Motahhari PDC Bit model should be implemented for optimization of drilling parameters in the Base Last Salt Limestone formation.

5.1.2 Downhole Measurements

Depth, ROP, WOB, RPM, and flow rate are also reported with a downhole measurement tool in the Marathon dataset:

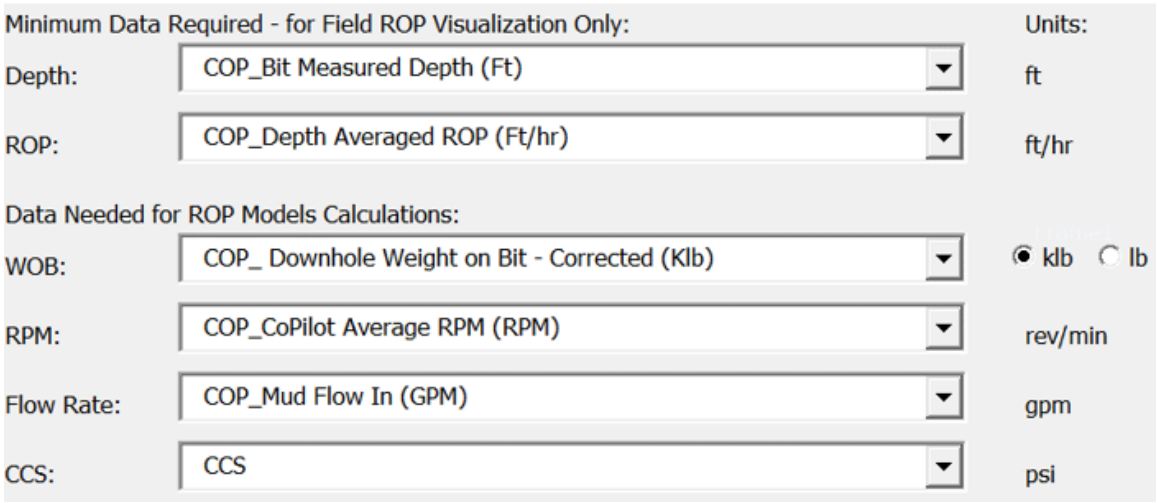

Figure 5.4: Data headings for downhole parameters with Marathon data.

CCS is the only data heading common to Figure 5.1 and Figure 5.4 above.

5.1.2.1 Data Statistics

Statistics for downhole measurements differ considerably from surface parameters statistics:

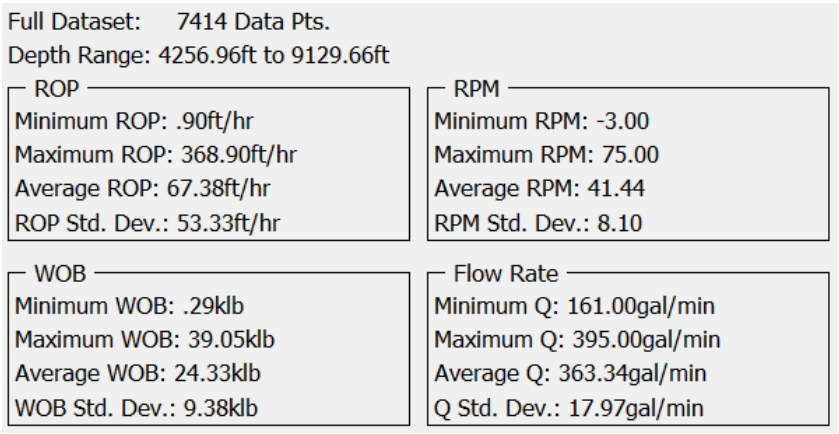

Figure 5.5: Statistics for downhole parameters with the Marathon dataset.

Maximum values of ROP (368.90ft/hr) and WOB (39.05klb) are much lower compared to surface parameter statistics in Fig. 5.2, indicating the odd nature of high values of maximum ROP (2,699.43ft/hr) and maximum WOB (223.05klb) with surface measurements. Averages for all four parameters do not deviate by much.

5.1.2.2 Modified Data Statistics

Besides applying the same data filtering criteria as with surface data, all negative RPM values (Fig 5.5) were removed for downhole parameter analysis:

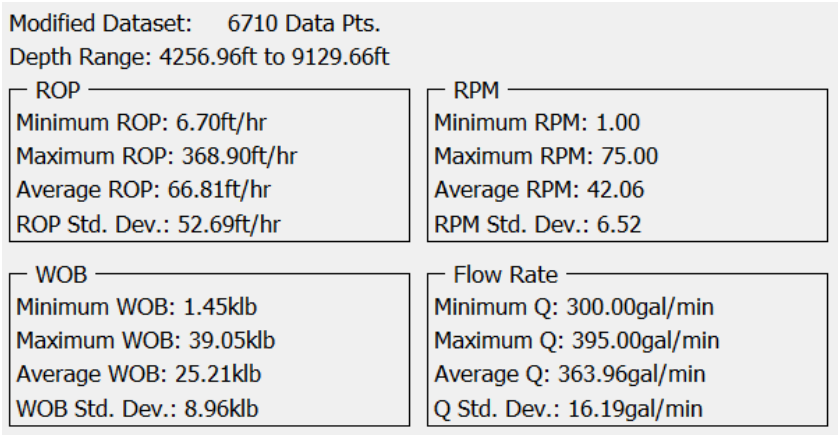

Figure 5.6: Modified data statistics for downhole parameters with the Marathon dataset.

Standard deviations for all four parameters decreased in relation to Figure 5.5. The data filtering process removed 704 points, almost twice as much as with surface measurements (366 points). When compared to the modified Marathon dataset for surface data (Fig. 5.3), the data in Fig. 5.6 has a lower ROP standard deviation but slightly higher WOB standard deviation.

5.1.2.3 ROP Models Average Percent Error

The following table summarizes average percent error for the four ROP models with the modified downhole data statistics:

Table 5.2: Average percent error for Bingham, B&Y, Hareland Drag Bit, and Motahhari PDC Bit models with filtered Marathon downhole data.

Rock Formation	Bingham Error	Bourgoyne & Young Error	Hareland Drag Error	Motahhari PDC Error
Greenhorn - Limestone	19.35%	21.71%	59.05%	41.06%
Newcastle - Sandstone	13.62%	11.46%	51.89%	38.88%
Dakota - Sandstone	17.61%	15.03%	61.26%	49.67%
Swift - Shale	25.31%	25.04%	61.63%	47.63%
Rierdon - Limestone	23.64%	22.89%	45.93%	42.01%
Piper - Limestone	20.45%	19.45%	41.64%	31.38%
Spearfish - Sandstone	22.13%	22.39%	24.78%	29.05%
Pine Salt - Sandstone	45.08%	43.11%	45.53%	50.88%
Broom Creek - Sandstone	44.45%	43.99%	52.27%	41.41%
Tyler - Sandstone	38.43%	35.52%	50.13%	36.90%
Kibbey Lime - Limestone	13.43%	13.62%	12.06%	13.65%
Kibbey Lime - Shale	15.06%	16.11%	20.55%	20.51%
Charles - Sandstone	31.69%	32.21%	32.73%	35.44%
Charles - Limestone	27.08%	26.57%	28.82%	33.35%
Ratcliffe - Sandstone	38.68%	36.06%	51.01%	48.80%
Base Last Salt - Limestone	14.90%	13.27%	12.55%	20.18%
Base Last Salt - Sandstone	14.50%	14.12%	16.04%	17.98%
Base Last Salt - Limestone	27.71%	25.51%	56.67%	31.91%
Mission Canyon - Limestone	13.60%	14.85%	13.68%	19.29%
Lodgepole - Limestone	9.11%	8.39%	10.37%	11.74%
Entire Dataset	**24.57%**	**24.01%**	**31.51%**	**30.34%**

Once again, the Bourgoyne & Young model has the lowest error average for the entire dataset. Table 5.3 summarizes model performance results for surface and downhole data:

Table 5.3: Model ROP error comparison for surface vs. downhole data.

Data Analyzed	Bingham Error	Bourgoyne & Young Error	Hareland Drag Error	Motahhari PDC Error
Marathon Surface Data	23.88%	23.68%	32.37%	25.85%
Marathon Downhole Data	24.57%	24.01%	31.51%	30.34%

Overall, the Hareland Drag Bit model is the only model with lower average percent error using downhole data. However, the Bingham model performs better with downhole measurements in the first eight rock formations (see Tables 5.1 and 5.2), up to the Pine Salt Sandstone lithology. Bourgoyne & Young's model also fits most of that segment better with downhole data. The Motahhari PDC Bit model has higher error with downhole measurements in most formations. As previously discussed when analyzing model performance in Chapter 4, the overall dataset error relies heavily on the deeper formations in this Marathon example, since more data points are recorded in a slower ROP setting. Hence, downhole measurements deserve consideration in optimization studies, especially in the shallower lithologies of this dataset.

Analyzing Tables 5.1 and 5.2, the lowest error for a model in one specific formation occurs with the Bourgoyne & Young model and surface measurements in the Lodgepole Limestone formation. The next section optimizes drilling parameters in this situation.

5.1.3 Optimization of Drilling Parameters in the Lodgepole Limestone Formation with B&Y ROP Model and Surface Measurements

With an average percent error of 6.86%, the application of Bourgoyne & Young's model and surface data in the Lodgepole Limestone formation resulted in the following set of model coefficients:

Table 5.4: Bourgoyne & Young model coefficients for Lodgepole Limestone formation with surface data.

Rock Formation	**a1**	**a2**	**a3**	**a4**	**a5**	**a6**	**a7**	**a8**
Lodgepole Limestone	3.21	4.90E-04	1.00E-06	1.00E-06	0.40	0.70	1.32	0.49

The coefficients in Table 5.4 can be employed to predict ROP for different WOB and RPM values in the Lodgepole Limestone formation. This lithology originally contained 720 data points, but 16 of them were deleted in the data filtering process. The modified surface data statistics for the formation is:

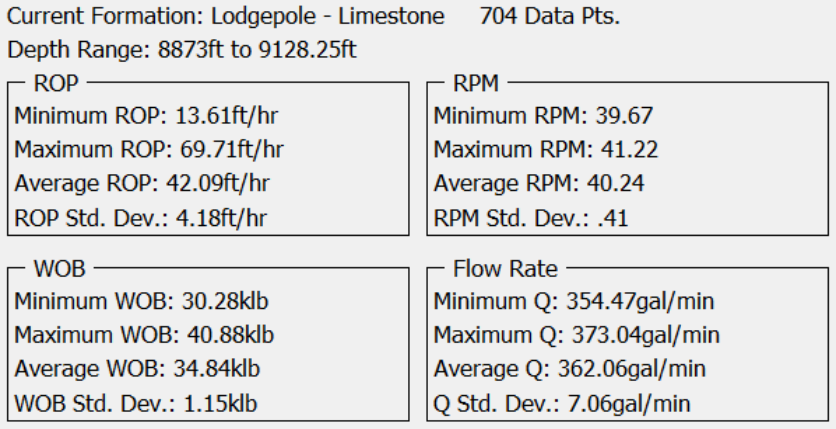

Figure 5.7: Lodgepole Limestone statistics for filtered Marathon surface dataset.

Based on the figure above, depth and flow rate are held at their average values (9000ft and 362gal/min, respectively) and ROP is calculated using the B&Y model and coefficients from Table 5.4 for different WOB and RPM values:

Table 5.5: Prediction of ROP values in ft/hr for different WOB and RPM combinations in the Lodgepole Limestone formation.

LodgePole Limestone	**30 RPM**	**35 RPM**	**40 RPM**	**45 RPM**	**50 RPM**	**55 RPM**	**60 RPM**
WOB = 10klbs	19.91	22.19	24.38	26.49	28.52	30.50	32.43
WOB = 20klbs	26.77	29.84	32.78	35.61	38.35	41.01	43.60
WOB = 30klbs	31.68	35.31	38.78	42.13	45.38	48.52	51.59
WOB = 35klbs	33.75	37.62	41.32	44.89	48.34	51.70	54.96
WOB = 40klbs	35.65	39.73	43.64	47.41	51.06	54.60	58.05
WOB = 50klbs	39.05	43.52	47.80	51.93	55.93	59.81	63.58
WOB = 60klbs	42.05	46.87	51.48	55.93	60.23	64.41	68.47
WOB = 70klbs	44.76	49.89	54.80	59.54	64.12	68.56	72.89

Bourgoyne and Young's model predicts ever-increasing values of ROP with increased WOB and ROP within these bounds. Table 5.5 shows that by doubling the mean WOB (from 35klb to 70klb) and keeping RPM at the average 40 rev/min for the formation, ROP raises to 54.80ft/hr (42.09ft/hr average in formation). Increasing RPM by 50% (60rev/min) and keeping WOB at 35klb, ROP increases to 54.96ft/hr. Proportionally, increases in RPM benefit ROP more than WOB increases in this scenario.

Two more optimization tables are needed to account for varying flow rate. Holding RPM at the average 40rev/min:

Table 5.6: Prediction of ROP values in ft/hr for different WOB and flow rate combinations in the Lodgepole Limestone formation.

LodgePole Limestone	**300 GPM**	**330 GPM**	**360 GPM**	**390 GPM**	**420 GPM**	**450 GPM**	**480 GPM**
WOB = 10klbs	20.81	22.47	24.26	26.19	28.27	30.52	32.95
WOB = 20klbs	27.98	30.21	32.61	35.21	38.01	41.03	44.30
WOB = 30klbs	33.11	35.74	38.59	41.66	44.97	48.55	52.42
WOB = 35klbs	35.27	38.08	41.11	44.38	47.92	51.73	55.85
WOB = 40klbs	37.26	40.22	43.42	46.88	50.61	54.64	58.99
WOB = 50klbs	40.81	44.05	47.56	51.35	55.43	59.85	64.61
WOB = 60klbs	43.95	47.44	51.22	55.30	59.70	64.45	69.58
WOB = 70klbs	46.78	50.50	54.52	58.86	63.55	68.61	74.07

A one third increase in flow rate (360gpm to 480gpm) with WOB at average 35klb results in a ROP of 55.85ft/hr, indicating that increasing flow rate is proportionately the most beneficial to ROP. However, the economics involved in acquiring a bigger pump might not support this notion.

Keeping WOB at the average 35klb and changing RPM and flow rate values:

Table 5.7: Prediction of ROP values in ft/hr for different RPM and flow rate combinations in the Lodgepole Limestone formation.

LodgePole Limestone	300 GPM	330 GPM	360 GPM	390 GPM	420 GPM	450 GPM	480 GPM
30 RPM	28.81	31.10	33.58	36.25	39.14	42.25	45.61
35 RPM	32.11	34.67	37.43	40.40	43.62	47.09	50.84
40 RPM	35.27	38.08	41.11	44.38	47.92	51.73	55.85
45 RPM	38.32	41.37	44.66	48.22	52.05	56.20	60.67
50 RPM	41.27	44.55	48.10	51.93	56.06	60.52	65.34
55 RPM	44.13	47.64	51.43	55.53	59.95	64.72	69.87
60 RPM	46.92	50.65	54.68	59.03	63.73	68.80	74.28

Even though Tables 5.5, 5.6, and 5.7 are useful for ROP prediction of a future well to be drilled through the Lodgepole Limestone formation, more data from other wells in the region is needed to ensure that the coefficients obtained in Table 5.4 are indeed representative of this lithology. The following Eagle Ford optimization example utilizes data from two distinct wells to obtain a more realistic set of model coefficients for each formation.

5.2 Eagle Ford Shale Baker Wells (NOV Data)

Baker A4 and Baker A5 are Eagle Ford horizontal shale wells drilled with PDC bits. Both wells penetrate two rock formations of interest: Lower Eagle Ford and Upper Eagle Ford shales.

5.2.1 Baker A4 Well

5.2.1.1 Data Statistics

The Baker A4 well penetrated the Upper Eagle Ford formation from a measured depth (MD) of 13,196ft to 15,976ft and the Lower Eagle Ford formation from 15,977ft to 19,107ft MD. Parameter statistics for such segment of the well are displayed below:

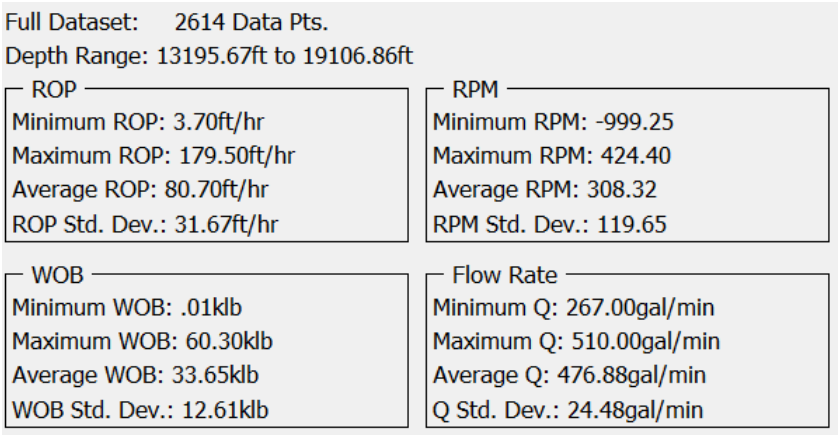

Figure 5.8: Baker A4 well data statistics.

Figure 5.8 shows negative RPM values, which must be removed to ensure proper model calculations. RPM standard deviation is much higher compared to the Marathon dataset in the previous optimization study (Fig 5.2).

5.2.1.2 Modified Data Statistics

Since data points are plentiful for both Eagle Ford formations, all data points with parameter values two standard deviations away from the mean are removed in the data filtering process:

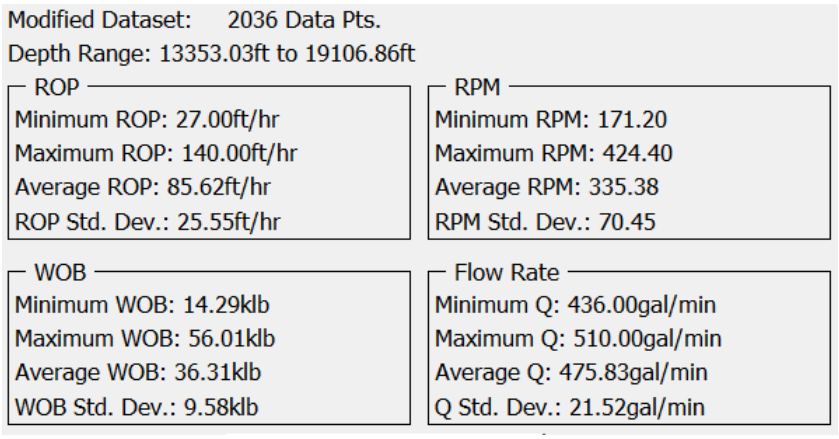

Figure 5.9: Baker A4 well modified dataset statistics.

As seen in Fig. 5.9, 578 data points were deleted from the original dataset. The remaining 2,036 points still display a very high value of RPM standard deviation.

5.2.1.3 ROP Models Average Percent Error

The same model coefficient bounds from Chapter 4 and the Marathon optimization study are employed in computing ROP models for the Baker A4 and Baker A5 wells. Confined compressive strength (CCS) data is not available, and assumed to be 6500psi for both wells. The WWO Roller Bit and Hareland Roller Bit models are not considered again, for being specific to roller cone bits:

Table 5.8: Average percent error for four ROP models with modified Baker A4 well data.

Baker A4 - Rock Formation	Bingham Error	Bourgoyne & Young Error	Hareland Drag Error	Motahhari PDC Error
Upper Eagle Ford	19.52%	26.07%	26.85%	22.57%
Lower Eagle Ford	30.14%	26.70%	32.90%	38.52%
Entire Dataset	25.51%	26.43%	30.26%	31.57%

From the table above, the Bingham model provides the best fit for the entire dataset and for the Upper Eagle Ford formation in the Baker A4 well. Bourgoyne & Young's model is the top performer in the Lower Eagle Ford.

5.2.2 Baker A5 Well

5.2.2.1 Data Statistics

Baker A5 well was drilled through the Upper Eagle Ford formation from 13,024ft to 13,131ft MD and through the Lower Eagle Ford formation from 13,132ft to 19,214ft MD. Data statistics for this portion of the well are presented in Figure 5.10:

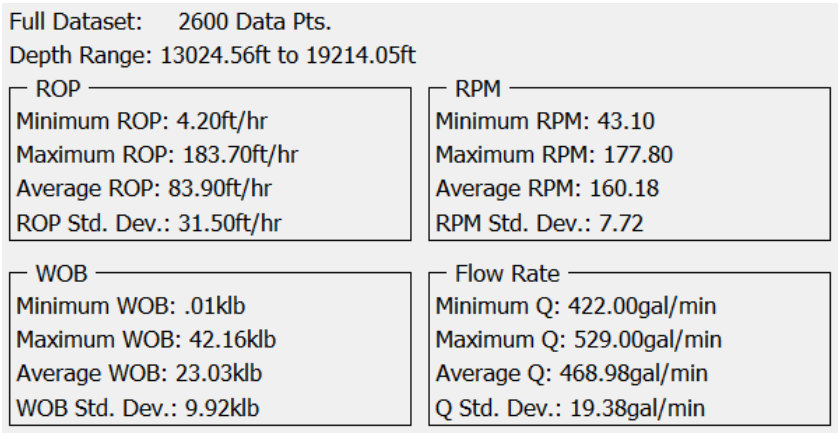

Figure 5.10: Baker A5 well statistics.

RPM standard deviation is only 7.72rev/min compared to 119.65rev/min in Baker A4 well statistics (Fig. 5.8). Other than RPM, average values for the other drilling parameters are similar in both wells.

5.2.2.2 Modified Data Statistics

Removing all Baker A5 well data points with parameter values two standard deviations above or below the mean:

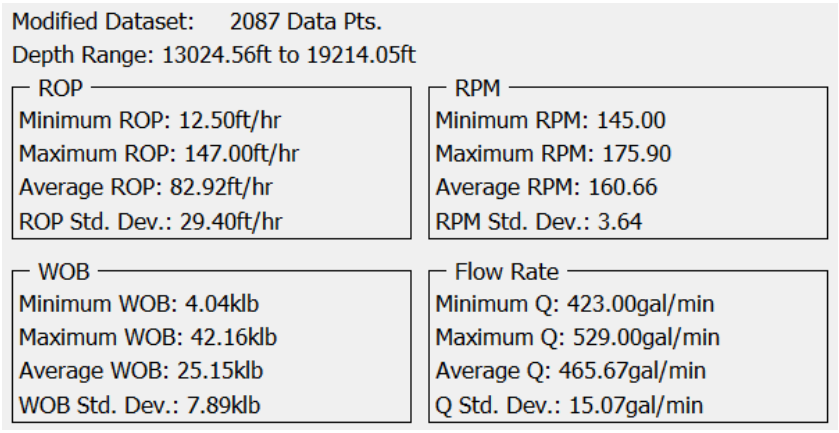

Figure 5.11: Baker A5 well modified dataset statistics.

Modified data statistics are similar for the Baker A4 (Fig. 5.9) and Baker A5 (Fig. 5.11) wells, except for the RPM parameter. RPM maximum, average and standard deviation values are all much higher for the Baker A4 well, indicating a new measurement tool was deployed in Baker A5 measurements or the well was designed differently.

5.2.2.3 ROP Models Average Percent Error

Table 5.9 presents the error of the four ROP models analyses in this well:

Table 5.9: Average percent error for four ROP models with modified Baker A5 well data.

Baker A5 - Rock Formation	Bingham Error	Bourgoyne & Young Error	Hareland Drag Error	Motahhari PDC Error
Upper Eagle Ford	30.46%	51.95%	30.88%	30.44%
Lower Eagle Ford	31.96%	30.42%	39.53%	32.06%
Entire Dataset	31.91%	31.13%	39.24%	32.00%

Motahhari's PDC Bit model beats Bingham's model in the Upper Eagle Ford formation by a very small margin in the Baker A5 well. B&Y has the lowest error in the Lower Eagle Ford formation and overall. Optimization of drilling parameters will consider model performance in both wells, selecting the best ROP model for each Eagle Ford rock formation.

5.2.3 Optimization of Drilling Parameters in the Eagle Ford with Combined Baker A4 and Baker A5 Data

Averaging ROP model errors for Baker A4 (Table 5.8) and Baker A5 (Table 5.9) implementations:

Table 5.10: Average percent error for four ROP models with modified Baker A4 and modified Baker A5 data.

Baker A4/A5 - Rock Formation	Bingham Error	Bourgoyne & Young Error	Hareland Drag Error	Motahhari PDC Error
Upper Eagle Ford	24.99%	39.01%	28.87%	26.51%
Lower Eagle Ford	31.05%	28.56%	36.22%	35.29%
Entire Dataset	28.71%	28.78%	34.75%	31.79%

From Table 5.10, overall performance of Bingham and Bourgoyne & Young models is very similar. Optimization investigations will be conducted separately for each Eagle Ford formation. Bingham's model is the most appropriate for the Upper Eagle Ford, with 24.99% average percent error. The Bourgoyne & Young model will be employed in the Lower Eagle Ford (28.56% error).

5.2.3.1 Upper Eagle Ford Optimization

Combining data for the Upper Eagle Ford formation in both Baker A4 and Baker A5 wells results in average values of ROP = 68.24ft/hr, WOB = 23.50klb and RPM = 267.19rev/min. The Bingham model was selected for this study based on Table 5.10. Flow rate measurements are not necessary because Bingham's model does not include this parameter in its formulation. Bingham model coefficients for each well are shown next:

Table 5.11: Bingham model coefficients for Upper Eagle Ford optimization.

Bingham Model Coefficients	a	b
Baker A4 Well	0.08	0.68
Baker A5 Well	0.12	1.61
Average	0.10	1.15

While the *a* model coefficient has similar values in the two wells, *b* coefficient values diverge considerably. With average coefficient values from Table 5.11, ROP can be predicted for different values of WOB and RPM in the Upper Eagle Ford formation:

Table 5.12: Prediction of ROP values in ft/hr for different WOB and RPM combinations in the Upper Eagle Ford formation.

Upper Eagle Ford	200 RPM	230 RPM	260 RPM	290 RPM	320 RPM	350 RPM	380 RPM
WOB = 10klbs	23.32	26.82	30.32	33.81	37.31	40.81	44.31
WOB = 20klbs	51.75	59.51	67.27	75.04	82.80	90.56	98.32
WOB = 30klbs	82.49	94.87	107.24	119.61	131.99	144.36	156.73
WOB = 40klbs	114.84	132.06	149.29	166.52	183.74	200.97	218.19
WOB = 50klbs	148.43	170.70	192.97	215.23	237.50	259.76	282.03
WOB = 60klbs	183.06	210.52	237.98	265.44	292.90	320.36	347.81
WOB = 70klbs	218.57	251.35	284.14	316.92	349.71	382.49	415.28

It is interesting to note that while WOB step increments influence ROP proportionally throughout this RPM range, increments in RPM have a greater impact on ROP at high WOB values. Comparing this optimization table to the one produced in the Lodgepole Limestone example (Table 5.5), one concludes that ROP is more sensitive to WOB in the Upper Eagle Ford formation. ROP values are almost ten times higher when increasing WOB at constant RPM in Table 5.12. This observation is explained by the high *b* coefficient value (b = 1.15) utilized in this analysis, since *b* is the exponent of the WOB term in Bingham's model.

5.2.3.2 Lower Eagle Ford Optimization

Baker A4 and Baker A5 data for the Lower Eagle Ford shale produce average values of ROP = 85.40ft/hr, WOB = 30.89klb, RPM = 233.27rev/min and Q = 463.48gpm. Table 5.10 shows that the Bourgoyne & Young model is best suited for optimization in the Lower Eagle Ford. B&Y model coefficients for each well are presented in Table 5.13:

Table 5.13: Model coefficients for B&Y model in Lower Eagle Ford shale optimization.

B&Y Model Coefficients	a1	a2	a3	a4	a5	a6	a7	a8
Baker A4	2.53	1.0E-06	1.1E-05	1.0E-06	0.71	0.66	0.79	0.50
Baker A5	3.23	7.0E-06	1.0E-06	1.0E-06	0.47	0.72	1.00	0.49
Average	2.88	4.0E-06	6.0E-06	1.0E-06	0.59	0.69	0.90	0.50

Model coefficient values are comparable for both wells in the table above. Average coefficient values are applied to the B&Y model with constant mean flow rate of 464gpm in order to predict ROP for a range of WOB and RPM values:

Table 5.14: Prediction of ROP values in ft/hr for different WOB and RPM combinations in the Lower Eagle Ford formation.

Lower Eagle Ford	200 RPM	230 RPM	260 RPM	290 RPM	320 RPM	350 RPM	380 RPM
WOB = 10klbs	35.60	39.20	42.66	46.00	49.24	52.38	55.44
WOB = 20klbs	55.09	60.67	66.02	71.19	76.19	81.05	85.78
WOB = 30klbs	70.60	77.75	84.62	91.24	97.65	103.88	109.94
WOB = 40klbs	84.03	92.54	100.71	108.59	116.23	123.64	130.86
WOB = 50klbs	96.11	105.84	115.19	124.20	132.93	141.41	149.67
WOB = 60klbs	107.22	118.07	128.49	138.55	148.29	157.74	166.95
WOB = 70klbs	117.57	129.47	140.90	151.93	162.61	172.98	183.08

Similar to the Upper Eagle Ford optimization (Table 5.12), ROP increases faster with WOB increments than with RPM increases. The ROP dependency on WOB is less accentuated in the table above than in Table 5.12.

For a constant RPM of 233rev/min:

Table 5.15: Prediction of ROP values in ft/hr for different WOB and flow rate combinations in the Lower Eagle Ford formation.

Lower Eagle Ford	400 GPM	430 GPM	460 GPM	490 GPM	520 GPM	550 GPM	580 GPM
WOB = 10klbs	33.50	36.21	39.15	42.32	45.75	49.46	53.46
WOB = 20klbs	51.84	56.04	60.58	65.49	70.79	76.53	82.73
WOB = 30klbs	66.44	71.82	77.64	83.93	90.73	98.09	106.03
WOB = 40klbs	79.07	85.48	92.41	99.90	107.99	116.74	126.21
WOB = 50klbs	90.44	97.77	105.69	114.25	123.51	133.52	144.34
WOB = 60klbs	100.89	109.06	117.90	127.45	137.78	148.95	161.02
WOB = 70klbs	110.63	119.59	129.29	139.76	151.09	163.33	176.57

Once again, WOB proves to be the most influential optimization parameter in Table 5.15.

Table 5.16 is constructed with WOB constant at the average value (31klb) for the Lower Eagle Ford formation:

Table 5.16: Prediction of ROP values in ft/hr for different RPM and flow rate combinations in the Lower Eagle Ford formation.

Lower Eagle Ford	**400 GPM**	**430 GPM**	**460 GPM**	**490 GPM**	**520 GPM**	**550 GPM**	**580 GPM**
200 RPM	60.99	65.94	71.28	77.06	83.30	90.05	97.35
230 RPM	67.17	72.61	78.50	84.86	91.73	99.17	107.20
260 RPM	73.10	79.02	85.43	92.35	99.83	107.92	116.67
290 RPM	78.82	85.21	92.11	99.58	107.64	116.37	125.80
320 RPM	84.36	91.19	98.58	106.57	115.21	124.55	134.64
350 RPM	89.74	97.01	104.87	113.37	122.56	132.49	143.23
380 RPM	94.98	102.68	111.00	119.99	129.71	140.23	151.59

Even with constant WOB, the most influential drilling optimization parameter in this study, Table 5.16 predicts significant ROP increases by raising RPM and flow rate.

Tables 5.14, 5.15 and 5.16 are extremely valuable when drilling another well through the Eagle Ford shale in the same pad as the Baker A4 and Baker A5 wells. These tables quantify the improvement or deterioration in ROP when altering drilling parameters. As an example, if WOB is increased from the average value of 30.89klb to 70klb and flow rate is raised to 580gpm (463.48gpm average), Table 5.15 predicts ROP will increase to 176.57ft/hr in the Lower Eagle Ford formation (85.40ft/hr average). Nevertheless, those predictions must be evaluated carefully. Previously discussed in Chapter 1, Maurer (1962) demonstrated that surpassing a threshold value of WOB is actually detrimental to ROP, since hole-cleaning problems exceed bit weight benefits. Therefore, the ever-increasing ROP trend with increasing WOB, RPM and flow rate, forecast by all optimizations in this chapter, does not account for hole-cleaning problems and other drilling effects that create a plateau for parameter-driven ROP improvements. Additionally, limitations in equipment operating range must be carefully examined.

With these considerations in mind, a field-specific full cost optimization is possible if drilling economics data are available. Specifically, comparing the price of incrementing drilling parameters (e.g. $10 per 1klb increase) to the daily operational well cost in a selected area can help determine if raising a certain parameter is indeed worth the investment. Increasing flow rate from 460gpm to 580gpm in Table 5.16 results in a 30ft/hr raise in ROP at 230RPM, but is the price tag of buying or renting a bigger mud pump justified to save rig time in this case? Similar questions should be posed when acquiring a more powerful motor for higher RPM values or more robust drillpipe for increased WOB. Cost investigations are viable with comprehensive drilling economics data for a field application of choice. The final product of such studies is a single, optimal value for WOB, RPM and flow rate from optimization tables similar to the ones produced in this chapter.

Chapter 6: Conclusions

6.1 Drilling Optimization Study Outcomes

ROPPlotter is extremely useful in data filtering, data visualization and ROP modeling. The program was successfully implemented in optimization of drilling parameters in Chapter 5 of this thesis. Without the aid of this software, computation of model coefficients would have been tedious and time consuming. The best ROP model for each scenario was selected based on model performance. Application of different criteria in determining the appropriate model, such as implementing a bit-specific ROP model to a well drilled with the same bit type, unveils a wide range of promising ROPPlotter implementations. The program facilitates execution of countless industry case studies. Depending on the needs of Wider Windows' sponsors, the data filtering functionality of ROPPlotter can be used to distinguish drilling situations of interest. Slow ROP in a section of the well, sliding drilling and drillstring vibrations are examples of topics that could greatly benefit from utilization of this software.

More complete datasets with multiple wells in the same pad and with regional drilling economics information can lead to extensive optimization studies. Computed values for model coefficients in a lithology are more reliable when averaged out between a greater number of wells drilled through the particular rock formation. Optimal WOB, RPM and flow rate values for a specific field result in cheaper and faster drilling of subsequent wells.

6.2 Extension of ROPPlotter to Torque and Drag and MSE Modeling

The software framework developed for ROPPlotter can be modified for any depth-dependent quantity. Planned program expansion to encompass torque and drag and

mechanical specific energy (MSE) modeling will assist several other projects in the Wider Windows Industrial Affiliate Program.

6.3 The Future of ROP Modeling

In Chapter 5, implementation of ROPPlotter and the Bourgoyne & Young model forecasted ROP in the Lodgepole Limestone formation with less than 7% average error. However, most ROPPlotter applications with models from literature produced 20% to 30% error between model ROP and field ROP (see Chapter 5). For over fifty years, attempts have been made in trying to model ROP with an equation and empirical coefficients. Due to the complexity of drilling and simplifications in each model, not a single model comes close to accurately predicting ROP in every situation. Furthermore, these ROP models are not predictive in nature, but rather a post-processing device: field data from a specific application is needed in order to obtain model coefficients that will be employed in optimizing the next well. Perhaps it is time to move forward and diverge from the classic approach to ROP modeling.

Big data analytics is a new trend in the oil and gas industry. Up to the second drilling measurements are attainable with current technology. Big data and real time optimization of drilling parameters can change the future of ROP modeling. Young (1969) envisioned real time drilling automation, but this concept is still not fully implemented today. Over the last few months, a new Wider Windows project has been developed to apply statistical learning methods to predict ROP. Rather than using a defined equation that greatly simplifies the complex physical interactions between drill bit and formation rock, as many ROP models in literature do, statistical learning relies solely on measurements of surface parameters and their relative contribution to ROP. Early results from this project are very

promising, predicting ROP within 5% error for a 6000ft shale well section after just 500ft of training data.

List of Acronyms

B&Y: Bourgoyne and Young

CCS: Confined compressive strength

ECD: Equivalent circulating density

GDL: Geological Drilling Log

Marathon: Marathon Oil Corporation

MSE: Mechanical Specific Energy

NOV: National Oilwell Varco

NPT: Non-productive time

OB: Overbalance

PDC: Polycrystalline diamond compact

PDM: Positive displacement motor

Q: Flow rate

RMSE: Root-mean-squared error

ROP: Rate of penetration

RPM: Rotations per minute

VBA: Visual Basic for Applications

WOB: Weight-on-bit

WWO: Winters-Warren-Onyia

References

Auwal, I. H., Ningi, H. Z., Suleiman, A. D. I., Yusuf, I., and Ogundele, O. J. (2012). Optimization of drilling parameters in the development plan of an explored area of gulf of Guinea. *Journal of Petroleum and Gas Exploration Research*, v. 2, no. 11, pp. 194-201.

Barros, L. (2015). ROP Modeling Chronology, Sensitive Analyses, and Field Data Comparisons. *M.S Thesis, The University of Texas at Austin*.

Bataee, M., Kamyab, M., and Ashena, R. (2010). Investigation of Various ROP Models and Optimization of Drilling Parameters for PDC and Roller-cone Bits in Shadegan Oil Field. *CPS/SPE International Oil & Gas Conference and Exhibition.* Beijing, China, June 8-10.

Bingham, M. G. (1964). How Rock Properties Are Related to Drilling. *The Oil and Gas Journal*, pp. 94-101.

Bingham, M. G. (1964). How to Interpret Drilling in the Performance Region. *The Oil and Gas Journal*, pp. 173-179.

Bingham, M. G. (1964-1965). A new approach to interpreting Rock Drillability. *The Oil and Gas Journal*.

Bourgoyne, A. T., Jr., and Young, F. S., Jr. (1974). A Multiple Regression Approach to Optimal Drilling and Abnormal Pressure Detection. *Society of Petroleum Engineers Journal*, pp. 371-384.

Bratli, R. K., Hareland, G., Stene, F., Dunsaed, G. W., and Gjelstad, G. (1997). Drilling Optimization Software Verified in the North Sea. *SPE LACPEC Conference*. Rio de Janeiro, Brazil, August 30-September 2.

Cunningham, R. A. (1978). An Empirical Approach For Relating Drilling Parameters. *Journal of Petroleum Technology*, pp. 987-991.

Eckel, J. R. (1967). Microbit Studies of the Effect of Fluid Properties and Hydraulics. *Journal of Petroleum Technology*, pp. 541-546.

Gjelstad, G., Hareland, G., Nikolaisen, K. N., and Bratli, R. K. (1998). The Method of Reducing Drilling Costs More Than 50 Percent. *SPE/ISRM Eurock*. Trondheim, Norway, July 8-10.

Hareland, G., and Hoberock, L. L. (1993). Use of Drilling Parameters To Predict In-Situ Stress Bounds. *SPE/IADC Drilling Conference*. Amsterdam, Netherlands, February 23-25.

Hareland, G., and Rampersad, P. R. (1994). Drag-Bit Model Including Wear. *III Latin American/Caribbean Petroleum Engineering Conference*. Buenos Aires, Argentina, April 27-29.

Hareland, G., Wu, A., Rashidi, B., and James, J. A. (2010). A New Drilling Rate Model for Tricone Bits and Its Application to Predict Rock Compressive Strength. *44th US Rock Mechanics Symposium and 5th U.S.-Canada Rock Mechanics Symposium*. Salt Lake City, UT, USA, June 27-30.

Jorden, J. R., and Shirley, O. J. (1966). Application of Drilling Performance Data to Overpressure Detection. *Journal of Petroleum Technology*, pp. 1387-1394.

Maurer, W. C. (1962). The "Perfect-Cleaning" Theory of Rotary Drilling. *Journal of Petroleum Technology*, pp. 1270-1274.

Motahhari, H. R., Hareland, G., and James, J. A. (2010). Improved Drilling Efficiency Technique Using Integrated PDM and PDC Bit Parameters. *Journal of Canadian Petroleum Technology,* v. 49, no. 10, pp. 45-52.

Nygaard, R., Hareland, G., Budiningsih, Y., Terjesen, H. E., and Stene, F. (2002). Eight Years Experience with a Drilling Optimization Simulator in the North Sea.

IADC/SPE Asia Pacific Drilling Technology. Jakarta, Indonesia, September 9-11.

Rampersad, P. R., Hareland, G., and Boonyapaluk, P. (1994). Drilling Optimization Using Drilling Data and Available Technology. *III Latin American/Caribbean Petroleum Engineering Conference*. Buenos Aires, Argentina, April 27-29.

Rowley, D. S., Howe, R. J., and Deily, P. H. (1961). Laboratory Drilling Performance of the Full-Scale Rock Bit. *Journal of Petroleum Technology*, pp. 71-81.

Walker, B. H., Black, A. D., Klauber, W. P., Little, T., and Khodaverdian, M. (1986). Roller-Bit Penetration Rate Response as a Function of Rock Properties and Well Depth. *61st Annual Technical Conference and Exhibition of the Society of Petroleum Engineers.* New Orleans, LA, USA, October 5-8.

Warren, T. M. (1987). Penetration-Rate Performance of Roller-Cone Bits. *SPE Drilling Engineering*, pp. 9-18.

Winters, W. J., Warren, T. M., and Onyia, E. C. (1987). Roller Bit Model With Rock Ductility and Cone Offset. *62nd Annual Technical Conference and Exhibition of the Society of Petroleum Engineers.* Dallas, TX, USA, September 27-30.

Young, F. S., Jr. (1969). Computerized Drilling Control. *Journal of Petroleum Technology*, pp. 483-496.